

**ENVIRONMENTAL, SYNTHETIC, AND  
MATERIALS APPLICATIONS OF  
MOLYBDENUM TRIOXIDE**

By

**MOHAMED CHEHBOUNI**

Diploma Chemical Engineer  
University of Applied Sciences  
Aachen, Germany  
1999

Submitted to the Faculty of the  
Graduate College of the  
Oklahoma State University  
In partial fulfillment of  
The requirements for  
The Degree of  
DOCTOR OF PHILOSOPHY  
July, 2006

**ENVIRONMENTAL, SYNTHETIC, AND MATERIALS APPLICATIONS  
OF MOLYBDENUM TRIOXIDE**

**Thesis Approved:**

\_\_\_\_\_ **Dr. Allen Apblett** \_\_\_\_\_

**Thesis Adviser**

\_\_\_\_\_ **Dr. K. Darrell Berlin** \_\_\_\_\_

\_\_\_\_\_ **Dr. LeGrande Slaughter** \_\_\_\_\_

\_\_\_\_\_ **Dr. Gary Foutch** \_\_\_\_\_

\_\_\_\_\_ **Dr. A. Gordon Emslie** \_\_\_\_\_

**Dean of the Graduate College**

## **ACKNOWLEDGEMENTS**

I would like to express my sincere appreciation and gratefulness to my thesis advisor, Dr. Allen W. Apblett for his guidance, motivation, financial support, inspiration, and friendship. His valuable advice, criticism, and encouragement have greatly helped me in the materialization of this dissertation. I have benefited much from his broad range of knowledge, his scientific approach and his warm personality. I am sure this will have a positive influence on me for the rest of my scientific career.

My deep appreciation extends to my committee members, Dr. K. Darrell Berlin, Dr. Le. Slaughter, and Dr. Gary Foutch, for their extensive assistance, valuable advice, gracious guidance, constructive comments, willingness to help, and their supports throughout the years.

I am deeply grateful to my colleagues, all former and present members of Dr. Apblett's research group, for their valuable discussions, support, continuous encouragement, and for all the help they extended during the course of my study. Thank you for providing such a pleasant and friendly working environment for the past few years.

I am also thankful to all students, faculty and staff at the Department of Chemistry at Oklahoma State University for their gracious support, kindness and help.

Thanks are also due to my father (in memory), my mom, my brothers and sisters, my relatives, and friends for their moral support, and encouragement throughout the years.

Finally, I am deeply indebted to my wife, Sania Khatib, for her unconditional love, patience, care, and sacrifice. Thank you for your continuous assistance no matter what the need was. My sincere thanks and appreciation extend to my parents -, my brothers- and sisters in law, and to my relative, former roommate and friend Fadi Al-Jorf. Your moral support during this time was invaluable to me.

THANK YOU ALL

## TABLE OF CONTENTS

<b>ACKNOWLEDGEMENTS .....</b>	<b>III</b>
<b>TABLE OF CONTENTS .....</b>	<b>V</b>
<b>LIST OF FIGURES.....</b>	<b>IX</b>

### CHAPTER I

<b>GENERAL INTRODUCTION .....</b>	<b>1</b>
INTRODUCTION .....	1
MOLYBDENUM TRIOXIDE.....	2
The structure of molybdenum trioxide .....	2
Synthesis of molybdenum trioxide .....	4
Properties and applications of molybdenum trioxide .....	5
Chemical intercalation into the molybdenum trioxide host system.....	6
METAL MOLYBDATES .....	7
The structure of the molybdates.....	7
Synthesis of metal molybdates.....	9
Applications of metal molybdates .....	10
PURPOSE AND SCOPE OF THE RESEARCH.....	13
REFERENCES .....	14

### CHAPTER II

<b>REMEDIATION AND RECOVERY OF URANIUM FROM WATER USING     MOLYBDENUM TRIOXIDES .....</b>	<b>23</b>
--	-----------

INTRODUCTION .....	23
EXPERIMENTAL .....	26
Reaction of MoO <sub>3</sub> with uranyl acetate .....	27
Kinetics of MoO <sub>3</sub> reaction with uranyl nitrate at room temperature .....	27
Recovery of uranium and MoO <sub>3</sub> .....	28
RESULTS AND DISCUSSION .....	28
Cyclic process for uranium uptake .....	35
CONCLUSIONS .....	36
REFERENCES .....	37

### **CHAPTER III**

#### **NOVEL ROUTES FOR THE SYNTHESIS OF RARE EARTH MOLYBDATES.. 39**

INTRODUCTION .....	39
EXPERIMENTAL .....	42
Reaction of molybdenum trioxide with gadolinium acetate .....	43
Reaction of MoO <sub>3</sub> with lanthanum acetate .....	43
RESULTS AND DISCUSSION .....	44
Reaction of MoO <sub>3</sub> with gadolinium acetate .....	44
Reaction of MoO <sub>3</sub> with lanthanum acetate .....	47
CONCLUSIONS .....	51
REFERENCES .....	51

### **CHAPTER IV**

#### **SYNTHESIS, CHARACTERIZATION AND APPLICATIONS OF TRANSITION METAL MOLYBDATES..... 54**

INTRODUCTION .....	54
EXPERIMENTAL .....	56
Reaction of molybdenum trioxide with transition metal acetates .....	56

RESULTS AND DISCUSSION .....	57
Reaction of molybdenum trioxide with manganese acetate .....	57
Reaction of molybdenum trioxide with iron salts .....	60
Synthesis of hydrated metal molybdates.....	61
CONCLUSIONS.....	65
REFERENCES .....	66

## CHAPTER V

### REACTION OF ALKALINE EARTH METAL SALTS WITH MOLYBDENUM

<b>TRIOXIDE.....</b>	<b>69</b>
INTRODUCTION .....	69
EXPERIMENTAL.....	71
Reaction of $\text{MoO}_3$ with calcium salts .....	72
Reaction of $\text{MoO}_3$ with strontium salts .....	73
Reaction of $\text{MoO}_3$ with barium acetate .....	74
RESULTS AND DISCUSSION .....	74
CONCLUSIONS.....	81
REFERENCES .....	82

## CHAPTER VI

### REMOVAL OF LEAD FROM WATER USING MOLYBDENUM AND

<b>TUNGSTEN OXIDES.....</b>	<b>85</b>
INTRODUCTION .....	85
EXPERIMENTAL.....	88
Reaction of $\text{MoO}_3$ with lead acetate .....	89
Reaction of lead acetate with tungsten trioxide .....	90
Determination of lead uptake.....	93
RESULTS AND DISCUSSION .....	93
Reaction of $\text{MoO}_3$ with lead acetate .....	93
Reaction of lead acetate with tungsten trioxide .....	95

Kinetics of lead uptake.....	95
CONCLUSIONS.....	97
REFERENCES .....	98

## CHAPTER VII

<b>CONCLUSIONS AND FUTURE DIRECTIONS .....</b>	<b>102</b>
--	------------

CONCLUSIONS.....	102
FUTURE DIRECTIONS .....	103



## LIST OF FIGURES

FIGURE	PAGE
 <b>CHAPTER I</b>	
Figure 1.1. Schematic representation of the orthorhombic $\text{MoO}_3$ structure. ....	3
Figure 1.2. Idealized representation of the layered structure of $\text{MoO}_3$ . ....	4
Figure 1.3. Reaction network of 1-butene on $\text{MoO}_3$ catalyst. ....	5
Figure 1.4. Arrangement in $\text{MnO}_6$ octahedra and $\text{MoO}_4$ tetrahedra in $\text{MnMoO}_4$ . ....	8
Figure 1.5. Polyhedra surrounding the metal atoms in $\text{CoMoO}_4$ . ....	8
 <b>CHAPTER II</b>	
Figure 2.1. Operation of a Permeable Reactive Barrier. ....	25
Figure 2.2. XRD patterns of the product from the reaction between uranyl acetate and $\text{MoO}_3$ as isolated. ....	29
Figure 2.3. XRD pattern of the product from the reaction of $\text{MoO}_3$ and uranyl acetate heated to 600 °C. ....	30
Figure 2.4. Structure of umohoite viewed along the [001] plane and the [100] plane. .	31
Figure 2.5. Layered structure of $\text{MoO}_3$ . ....	31
Figure 2.6. SEM images of molybdenum trioxide and the product from its reaction with uranium acetate. ....	33
Figure 2.7. Change of uranium concentration versus time .....	34
Figure 2.8: Complete cycle of uranium remediation process. ....	36

### CHAPTER III

Figure 3.1. Thermal gravimetric analysis (TGA) of the product from gadolinium acetate and molybdenum trioxide. ....	45
Figure 3.2. The XRD pattern of the product from gadolinium acetate and molybdenum trioxide heated to 800 °C. ....	46
Figure 3.3. The XRD pattern of the product from gadolinium acetate and molybdenum trioxide heated to 1000 °C. ....	46
Figure 3.4. Thermal gravimetric analysis of the product from lanthanum acetate and MoO <sub>3</sub> . ....	48
Figure 3.5. Infrared spectra of the product from MoO <sub>3</sub> and lanthanum acetate at room temperature and after heating to 550 °C. ....	48
Figure 3.6. The XRD pattern of the product from MoO <sub>3</sub> and lanthanum acetate heated to 550 °C. ....	49
Figure 3.7. Carbon 13 NMR of the product from lanthanum acetate and MoO <sub>3</sub> . ....	50

### CHAPTER IV

Figure 4.1. The XRD pattern of the product from manganese (II) acetate and manganese (III) acetate with MoO <sub>3</sub> . ....	58
Figure 4.2. Infrared spectra of the products from MoO <sub>3</sub> with the manganese (II) acetate and manganese (III) acetate respectively ....	59
Figure 4.3. The XRD pattern of the product from iron (II) acetate and iron (III) acetate with MoO <sub>3</sub> . ....	60
Figure 4.4. The XRD pattern and the thermal gravimetric analysis (TGA) of the product from cobalt acetate and MoO <sub>3</sub> . ....	62
Figure 4.5. The XRD pattern of the product from cobalt acetate and MoO <sub>3</sub> heated to 350 °C. ....	62
Figure 4.6. The XRD Pattern of the product from nickel acetate and MoO <sub>3</sub> heated to 500 °C. ....	63
Figure 4.7. The infrared spectrometer of the product from nickel acetate and MoO <sub>3</sub> after heating to 500 °C. ....	64

Figure 4.8. The XRD Pattern of the product from copper (II) acetate and $\text{MoO}_3$ .....	65
--	----

## CHAPTER V

Figure 5.1. Crystal structure of $\text{CaMoO}_4$ at room temperature.....	70
Figure 5.2. The XRD pattern of the product from calcium acetate and $\text{MoO}_3$ .....	75
Figure 5.3. Infrared spectrum of the product from calcium acetate and $\text{MoO}_3$ . ....	76
Figure 5.4. The XRD pattern of the product from calcium nitrate and $\text{MoO}_3$ in $\text{C}_8\text{H}_{19}\text{NO}_5$ - HCl buffer solution. ....	77
Figure 5.5. Infrared spectrum of the product from calcium nitrate and $\text{MoO}_3$ in $\text{C}_8\text{H}_{19}\text{NO}_5$ buffer solution after 72 hours reflux.....	78
Figure 5.6. The XRD pattern of the product from calcium nitrate and $\text{MoO}_3$ in sodium acetate-acetic acid buffer solution.....	79
Figure 5.7. The XRD pattern of the product from strontium acetate and $\text{MoO}_3$ . ....	80
Figure 5.8. Infrared spectrum of the product from strontium acetate and $\text{MoO}_3$ . ....	80
Figure 5.9. The XRD pattern of the product from barium acetate and $\text{MoO}_3$ . ....	81

## CHAPTER VI

Figure 6.1. The XRD pattern of the product from lead acetate and $\text{MoO}_3$ after reflux...	90
Figure 6.2. The XRD pattern of the product from lead acetate and $\text{MoO}_3$ after stirring at room temperature. ....	91
Figure 6.3. Infrared spectrum of the product from lead acetate and $\text{MoO}_3$ after stirring at room temperature. ....	91
Figure 6.4. Infrared spectrum of the lead molybdate from Aldrich.....	92
Figure 6.5. The XRD pattern of the product from lead acetate and $\text{WO}_3$ after heating at reflux. ....	92
Figure 6.6. The XRD pattern of the product from lead acetate and $\text{WO}_3$ after continuously stirring at room temperature. ....	93
Figure 6.7. Plot of $\ln[\text{Pb}]$ versus time .....	96
Figure 6.8. Plot of the rate constant versus mass of $\text{WO}_3$ .....	97

## **CHAPTER I**

### **GENERAL INTRODUCTION**

#### **INTRODUCTION**

Molybdenum is a group VI transition metal lying below chromium and above tungsten in the periodic table. The chemistry of molybdenum is complex due to its ability to form compounds with valence states from 0 to +6. Furthermore, molybdenum compounds can readily disproportionate to mixtures of compounds of different valence states, and they can easily change coordination number.<sup>1</sup> In addition, molybdenum can form complexes with a wide variety of ligands. Thus, molybdenum compounds have versatile applications in many different areas. Due to the anti-wear properties, several molybdenum-containing materials are widely used as lubricants, predominantly in extreme or hostile environmental circumstances.<sup>2</sup> In addition, molybdenum has been identified as a micronutrient vital to plant life, and as a component of numerous important enzyme systems playing a major biochemical role in animal health.<sup>3-5</sup> Moreover, several studies have revealed that molybdenum-deficient diets may be associated with the occurrence of various forms of cancer.<sup>5-8</sup> Additionally, molybdenum has an extremely low or even negligible toxicity.<sup>9</sup> Sax stated that “Molybdenum and its compounds are said to be somewhat toxic, but in spite of their considerable use in industry, industrial poisoning by molybdenum has yet to be reported”.<sup>5,10</sup> A recent listing of the potential carcinogenicity of metal ions have shown that molybdenum compounds

are in the lowest potentially carcinogenic class.<sup>11</sup>

Various molybdates are opaque white and as a result find use as pigments. Moreover, because of their non toxicity, molybdenum compounds act as more attractive corrosion inhibitors and smoke suppressants than many of the much more toxic alternatives.<sup>1,12</sup>

The multiple applications of molybdenum, along with the versatility of its physico-chemical properties, make molybdenum compounds both very interesting and extremely complex. Its oxidation state, ranging from 0 to +6, and coordination numbers (from 4 to 6) gives molybdenum a very diverse chemistry and allows it to form compounds with most inorganic and organic ligands with significant structural, catalytic, magnetic, and electronic properties.<sup>13</sup>

## **MOLYBDENUM TRIOXIDE**

### **The structure of molybdenum trioxide**

Molybdenum trioxide,  $\text{MoO}_3$ , which generally adopts the layered  $\alpha$ -structure, is the ultimate oxidation product of all molybdenum compounds.<sup>2</sup> The structure of  $\text{MoO}_3$  represents a transitional stage between tetrahedral and octahedral coordination.<sup>14</sup> Hence,  $\text{MoO}_3$  can be considered as built up by  $\text{MoO}_4$  tetrahedra, where the molybdenum atoms are surrounded by four close neighbor oxygen atoms at distances 1.94 Å, 1.95 Å, 1.73 Å, and 1.67 Å and two oxygen atoms at considerably longer distance that is 2.25 Å and 2.33 Å, making up a rather distorted octahedron (Figure 1.1).<sup>15,16</sup> The orthorhombic unit cell of  $\text{MoO}_3$  has the following dimensions:  $a_0 = 3.963$  Å,  $b_0 = 13.86$  Å,  $c_0 = 3.696$  Å.<sup>16,17</sup> The structure consists of two-dimensional layered sheets in which  $\text{MoO}_6$  octahedra share

edges to form zig-zag chains, while the rows are mutually connected by corners (Figure 1.2).<sup>14</sup> There are only weak interactions (van der Waals) between the double layer sheets, which is reflected in the inter-layer distance of  $\sim 6 \text{ \AA}$ .<sup>15</sup>

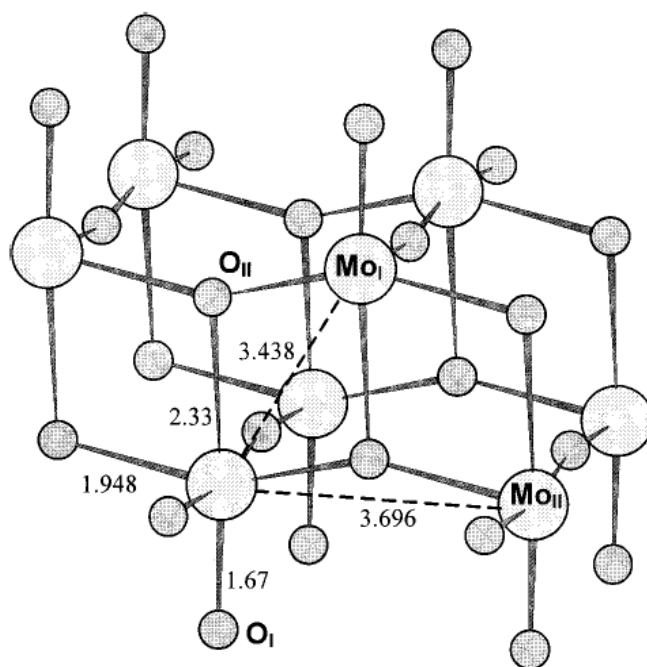


**Figure 1.1.** Schematic representation of the orthorhombic MoO<sub>3</sub> structure. The Mo-O distances within a distorted octahedral coordination and two prominent Mo-Mo distances are indicated.<sup>18</sup>

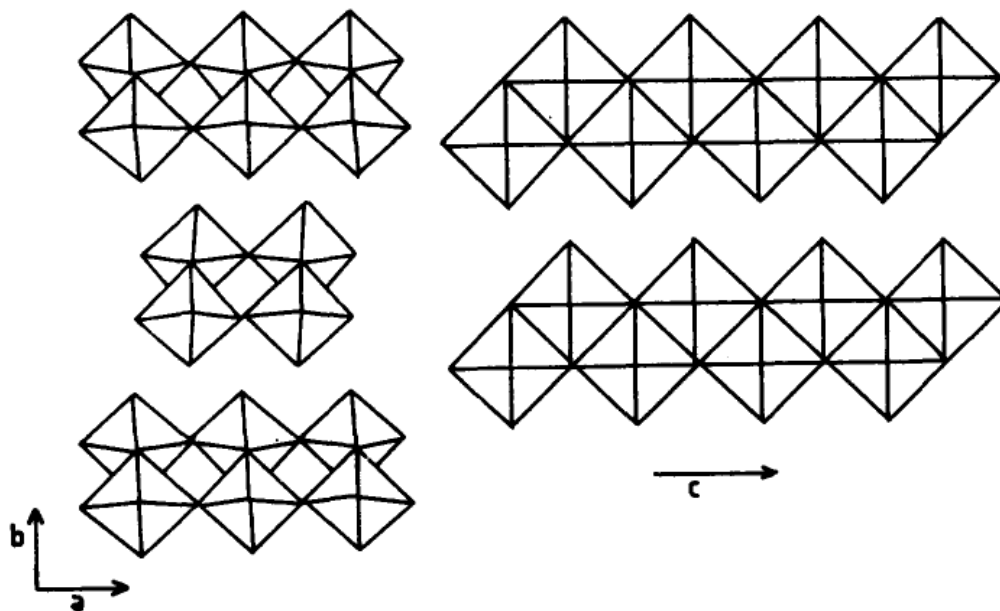


**Figure 1.2.** Idealized representation of the layered structure of  $\text{MoO}_3$ .<sup>19</sup>

### Synthesis of molybdenum trioxide

There are many procedures for the synthesis of pure molybdenum trioxide. Sublimation and wet chemical processing, or a combination of the two are among the most common methods to be found in the literature.<sup>2</sup> In the sublimation process, a final purity of 99.95%  $\text{MoO}_3$  can be obtained when heating the molybdic oxide in air to a temperature above 600 °C. The sublimation method consists of three basic steps, that is the sublimation, the recovery of the sublimed fine  $\text{MoO}_3$  from the furnace, and the densification of the product by the addition of deionised water, followed by carefully drying the product. The latter step is used to increase the apparent density by a factor of seven and therefore allow more economical transport.<sup>2</sup> On the other hand, the wet chemical procedure involves the heating of ammonium molybdate above 400 °C in a

vertical furnace to drive off the ammonia. In this method, the particle size distribution of the oxide is determined by the control of the residence time and temperature.<sup>20</sup>

### Properties and applications of molybdenum trioxide

One of the most remarkable characteristics of molybdenum trioxide is the versatility of its catalytic properties.<sup>21</sup> The main parameters which determine the catalytic behavior of molybdenum oxide are the valence state of molybdenum ions, their local environment, and the type of exposed crystal plane.<sup>21</sup> The role of different crystal planes of MoO<sub>3</sub> in the oxidation of hydrocarbons has been extensively studied and a large experimental exists on MoO<sub>3</sub>.<sup>15,22-26</sup> For instance, a complex reaction network may develop when an olefin is brought in contact with MoO<sub>3</sub> surface. Figure 1.3 illustrates an example of a reaction network of 1-butene on MoO<sub>3</sub> catalyst.

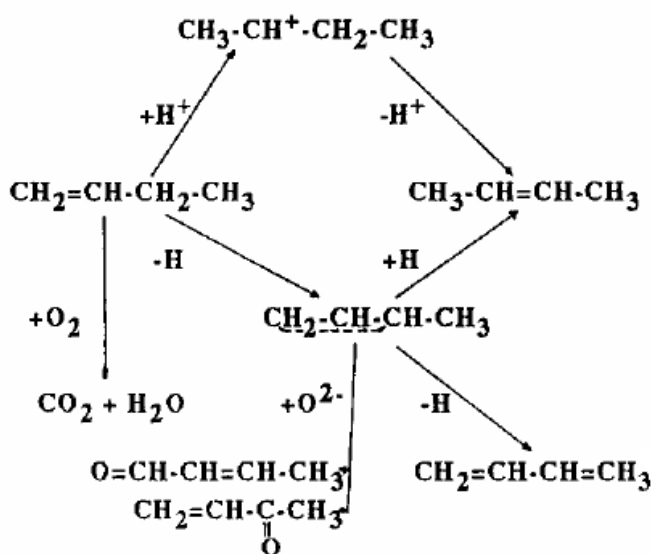


**Figure 1.3.** Reaction network of 1-butene on MoO<sub>3</sub> catalyst.<sup>21,27</sup>



It has been concluded that the MoO<sub>3</sub> surface must contain catalytically active sites accountable for different types of the elementary steps:<sup>21</sup>

- Isomerization of olefins through the formation of carbocations,
- Abstraction of hydrogen resulting in the formation of an allylic group,
- Abstraction of a second hydrogen to form diene,
- Nucleophilic addition of oxygen to the allyl to form aldehydes or ketones, and
- Generation of electrophilic oxygen species resulting in the total oxidation of the molecule.

The influence of the grain morphology of molybdenum trioxide on its catalytic properties, particularly on the reduction of nitric oxide with ammonia, has been investigated.<sup>28,29</sup> Furthermore, molybdenum oxide-based catalysts are employed actively and selectively in a wide range of reactions, such as redox reactions, acid base reactions, hydrogenation and dehydrogenation, selective oxidations, and oxidative conversions.<sup>30</sup> In addition, molybdenum trioxide is widely used as semiconductor material because of its wide variety of magnetic, electrical, thermal, and mechanical properties.<sup>31</sup>

### **Chemical intercalation into the molybdenum trioxide host system**

Intercalation can be described as the encapsulation of mobile guest species such as atoms, molecules, or ions into crystalline lattices containing interconnected systems of empty sites.<sup>32,33</sup> The incorporation of guest species into the host material can have synergistic effects on the new material, and thus enhance the electrical properties and increase the mechanical strength and thermal stability of the new materials.<sup>32</sup> Many methods have been used for the preparation of intercalation compounds. Examples

include redox, coordination, acid-base, and ion-exchange.<sup>34-37</sup> The presence of weak van der Waals forces between the layers of molybdenum trioxide allows the intercalation of a broad range of guest species, such as hydrogen, alkali and alkaline earth metal ions, as well as macromolecules, between the layers of MoO<sub>3</sub>.<sup>16,19,38,39</sup>

## METAL MOLYBDATES

### The structure of the molybdates

Simple molybdates have the general formula M<sup>I</sup><sub>2</sub>MoO<sub>4</sub> or M<sup>II</sup>MoO<sub>4</sub> (where the univalent M is usually an alkali metal and the divalent M is usually a transition metal or an alkaline earth metal). The molybdenum in the formula is in the +6 oxidation state.<sup>40</sup> Furthermore, the structure of most of these molybdates consists of molybdenum in tetrahedral form, although octahedral coordination is also possible.<sup>13</sup> Figure 1.4 shows an example of a common structure type of  $\alpha$ -MnMoO<sub>4</sub> which is monoclinic with tetrahedral coordination around the molybdenum atoms and an octahedral arrangement about the manganese atoms.<sup>41</sup> A different polyhedra arrangement is seen in the monoclinic CoMoO<sub>4</sub> and the isostructural NiMoO<sub>4</sub>.<sup>42,43</sup> The structures have distorted octahedral coordination for both the molybdenum and the other transition metal, resulting in chains of edge-sharing octahedra (Figure 1.5). These chains are further connected by corner-sharing, forming octahedral holes in between. However, structural changes occur when CoMoO<sub>4</sub> and NiMoO<sub>4</sub> are heated to elevated temperatures. For example, NiMoO<sub>4</sub> is converted to a phase that is isostructural with  $\alpha$ -MnMoO<sub>4</sub>.<sup>44</sup>

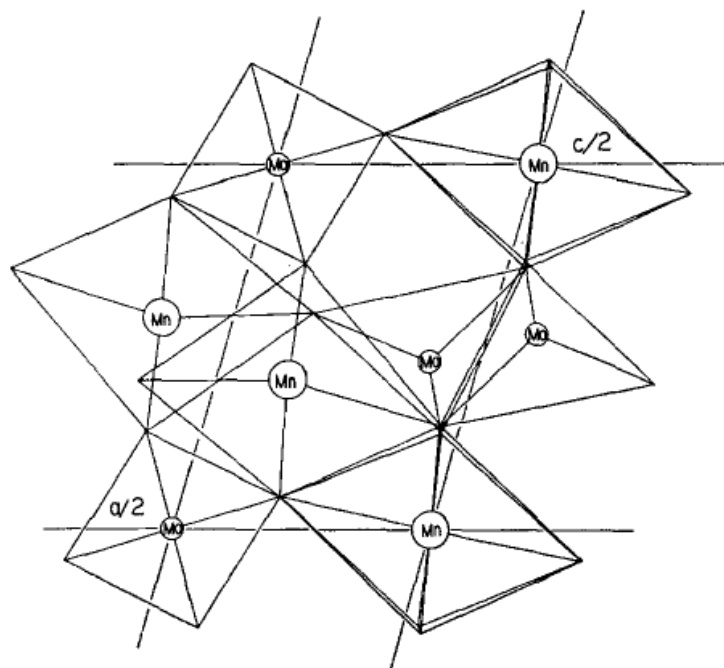


**Figure 1.4.** Arrangement in MnO<sub>6</sub> octahedra and MoO<sub>4</sub> tetrahedra in MnMoO<sub>4</sub>.<sup>41</sup>

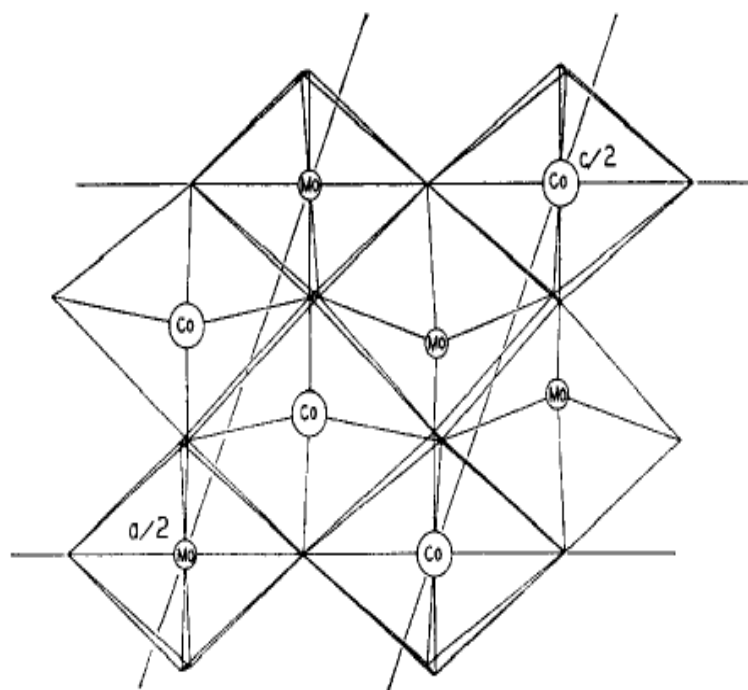


**Figure 1.5.** Polyhedra surrounding the metal atoms in CoMoO<sub>4</sub>.<sup>41</sup>

Interestingly,  $\text{CuMoO}_4$  and  $\text{ZnMoO}_4$  are triclinic. Their structures are more distorted than the previous ones and consists of  $\text{MoO}_4$  in a tetrahedral arrangement along with the octahedral and the square pyramidal coordination for Cu and Zn.<sup>45,46</sup> However, the phases undergo structural changes at high pressures.<sup>44</sup>

### **Synthesis of metal molybdates**

The common synthetic route for metal molybdates is the high temperature solid state reaction of  $\text{MoO}_3$  with the corresponding metal oxide. The main limitation of this method is that deviation from the proper stoichiometry due to sublimation of  $\text{MoO}_3$ . This can lead to the formation of undesired phases. For instance, synthesis of  $\text{AMoO}_4$  (where A the divalent metal) is often accompanied by the formation of  $\text{A}_2\text{MoO}_5$  and other polymolybdates.<sup>47-49</sup> In addition, the high temperature synthesis often results in localized nonstoichiometry to exist due to the differences in original particle sizes and inhomogeneity of the metal oxide and  $\text{MoO}_3$  powders.<sup>50</sup> While the method is conventionally used for the preparation of ceramics, it is not suitable for the synthesis of practical catalysts. The high temperature required for synthesis of metal molybdates leads to materials with low surface areas, and, thus, lower catalytic activity.<sup>51</sup> Therefore, new methods by which metal oxides can be prepared at low temperatures are extremely attractive.

An alternative route to prepare metal molybdates is the precipitation reaction of a soluble metal salt and a soluble molybdate (e.g. sodium or ammonium), taking advantage of the relative insolubility of the metal molybdate.<sup>52</sup> The method works for many metals, since the reaction occurs immediately, and the product is readily isolated. However, for a

number of metal ions, such as transition metal ions, the precipitation is hampered by the lack of overlap of pH ranges in which the metal cation and the molybdate anion are stable.<sup>52</sup> Consequently, it is difficult to obtain the desired stoichiometry. In addition, precipitation reactions typically are not suitable for processing of films or other useful morphologies.

Metal organic deposition (MOD) provides an alternative way to synthesize metal molybdates. It is a non-vacuum, solution based method for depositing thin film.<sup>53,54</sup> In this process, a suitable metallo-organic precursor dissolved in an adequate solvent is coated on a substrate by spin-coating, screen printing, or spray- or dip-coating. The metallo-organic film is then pyrolyzed in air, oxygen, or nitrogen. Hence, the precursors are converted to their constituents, oxides or other compounds.<sup>55</sup> Metal carboxylates are often used as precursors for ceramic oxides due to their air stability, solubility in organic solvents, and their easy decomposition to metal oxides. Unfortunately, the method is environmentally unfriendly and requires the use of organic solvents.

Several metal molybdates crystals are traditionally grown from a high temperature melt by the Szochralski method, where a single crystal rod is rotated and gradually pulled from the melt.<sup>56,57</sup> However, the method faces considerable problems related to oxygen stoichiometry, crack formation, inadequate starting materials, and crucible corrosion.<sup>58,59</sup>

### **Applications of metal molybdates**

Metal molybdates have very interesting catalytic properties. Since molybdenum is in the oxidation state +6 in most of the simple molybdates, and can hence be reduced,

the compounds can behave as oxidizing agents. For instance  $\text{MnMoO}_4$  and  $\text{CuMoO}_4$  are used as catalysts in the oxidation of propene and similar alkenes.<sup>60,61</sup>

Bismuth molybdate [ $\text{Bi}_2(\text{MoO}_4)_3$ ] catalyst is used for the oxidation of olefins. The bismuth ions activate the olefin molecules by abstraction of hydrogen and formation of the allyl species, while the molybdate sublattice is responsible for the nucleophilic addition of oxygen.<sup>27,62</sup> Also, the synthesis of acrylonitrile by the ammoxidation of propene using bismuth molybdate catalyst is considered an important point in the history of modern petrochemistry since it is an important intermediate for the production of elastomers, fibers, and water-soluble polymers.<sup>63</sup> In addition, the hydrodesulfurization of petroleum using molybdenum based catalysts is considered one of the largest heterogeneous catalytic processes since the world production of more than two and a half billion tons of crude oil occurs each year.<sup>64</sup> Most commercial processes use molybdates as catalysts to produce formaldehyde from methanol.<sup>2</sup>

Nickel and cobalt molybdate are extensively used as selective oxidation catalysts in a variety of reactions, such as the ammoxidation of propylene, the oxidation of 1-butene to maleic anhydride, and the oxidative dehydrogenation of propane.<sup>65-69</sup> Moreover, nickel molybdate catalysts are widely used in the hydrodenitrogenation of petroleum distillates, where the C-N bonds in organic compounds undergo hydrogenolysis to give ammonia and the corresponding hydrocarbon. They are also used in the hydrotreating reaction to remove sulfur, nitrogen, oxygen, and metals from petroleum distillates.<sup>70</sup> Moreover, nickel and cobalt molybdate catalysts have also found their way in the water-gas shift reaction, steam reforming, cracking of n-butane, oxidative coupling of methane, and other important hydrogenation and reactions.<sup>71,72</sup>

Lead molybdates are widely used in acousto-optical and high voltage measurements devices. In addition, lead molybdate compounds have received growing attention due to their significant applications as optic modulators, deflectors, and ionic conductors.<sup>73-75</sup> Moreover, lead molybdate is found to be a potential candidate to be used as a scintillator for nuclear instrumental applications.<sup>76</sup> Industrial processes based on supported and unsupported ferric molybdate catalysts for the selective oxidation of methanol to formaldehyde and as Harshaw catalysts present numerous advantages over the traditional routes.<sup>77-80</sup> Low feed concentrations of methanol are needed to achieve large yields of formaldehyde using ferric-molybdenum oxide catalysts. Hence, the risk of fire or explosion is diminished since the process uses low concentrations of methanol and work at lower temperature.<sup>80</sup>

Molybdates have been commercially used as non-toxic, anti-corrosion agents and as anodic or passivating inhibitors due to their ability to protect both ferrous and non-ferrous metals and their low-toxicity.<sup>5,81-84</sup> When a coating film containing molybdate pigments (e.g.  $\text{CaMoO}_4$  or  $\text{ZnMoO}_4$ ) is exposed to water, a small amount of molybdate ions is released into the coating film.<sup>85</sup> When the released ions come into contact with the metal substrate, they react to form a protective, passive oxide layer on the metal preventing subsequent corrosion of the metal substrate.<sup>5,85</sup> Calcium and zinc molybdates have also been used as smoke suppressants and flame retardants in the formulation of halogenated polymers such as PVC, polyolefins, and other plastics.<sup>1</sup>

Alkaline earth molybdates have been commonly used in electro-optics, microwave ceramics, additives to steel, and for smelting of ferromolybdenum.<sup>86-90</sup> Due to its attractive luminescence properties, calcium molybdate has been proposed for use as

a potential disperse element in an electronically tunable laser serving as an acousto-optic filter, and as an efficient mixed hole ion conductor.<sup>91-94</sup>

Lanthanide molybdates have been increasingly used in optics and electronics. Gadolinium molybdate [ $\text{Gd}_2(\text{MoO}_4)_3$ ] is the first material where both ferroelectricity and ferroelasticity were observed together.<sup>95-97</sup> Consequently, gadolinium molybdate has been widely used in memory cells, low-speed mechanical positioning systems, and as an efficient laser medium for laser-diode pumping.<sup>98,99</sup> Gadolinium molybdate, doped with neodymium, has been used for multicolor generation, self-frequency doubling, and self-frequency mixing.<sup>99</sup> On the other hand, lanthanum molybdenum oxide ( $\text{La}_2\text{Mo}_2\text{O}_9$ ) exhibits good ionic conductivity.<sup>100-105</sup> Hence, lanthanum molybdate has been used as a solid electrolyte material for several electrochemical applications. Examples include, components for fuel cells, oxygen sensors, dense ceramics for oxygen separation membranes, oxygen pumps, and oxygen permeable membrane catalysts.<sup>106</sup> In addition, lanthanum molybdate has also been employed for the selective oxidation of hydrocarbons to organic oxygenated compounds.<sup>107</sup>

## **PURPOSE AND SCOPE OF THE RESEARCH**

The overall objective of this thesis is to investigate the effectiveness of molybdenum trioxide for applications in the removal of uranium and other heavy metals from aqueous solutions. First, the method was tested for uranium removal, and the results obtained were applied to many other heavy metals. A cyclic process was developed (Chapter II) whereby  $\text{MoO}_3$  adsorbed uranium from aqueous solutions, and then molybdenum oxide and uranium were separated. The rate of the metal uptake was



also studied (Chapter II and VI). In addition, a successful environmentally friendly method (Chapter III to V) to synthesize useful metal molybdates directly from molybdenum trioxide and an aqueous solution of the corresponding metal salts was introduced. A comparison was made between molybdenum trioxide and tungsten oxide in the removal of lead from aqueous solutions (Chapter VI). Finally, an investigation was conducted into the pH dependence of the formation of the molybdates using different metal salts (Chapter V).

## REFERENCES

- [1] Kennelly, W. J. *Proceedings of the International Conference on Fire Safety* **2000**, 29, 185-192.
- [2] Braithwaite, E. R.; Haber, J. *Molybdenum: An Outline of its Chemistry and Uses*; Elsevier: Amsterdam ; New York, 1994.
- [3] Anderson, A. J. *J. Australian Inst. Agr. Sci.* **1942**, 8, 73-5.
- [4] Richert, D. A.; Westerfeld, W. W. *Journal of Biological Chemistry* **1953**, 203, 915-23.
- [5] Vukasovich, M. S.; Farr, J. P. G. *Polyhedron* **1986**, 5, 551-9.
- [6] Burrell, R. J.; Roach, W. A.; Shadwell, A. *Journal of the National Cancer Institute* **1966**, 36, 201-9.
- [7] Luo, X. M. *Zhonghua liu xing bing xue za zhi = Zhonghua liuxingbingxue zazhi* **1982**, 3, 91-6.
- [8] Nemenko, B. A.; Moldakulova, M. M.; Zorina, S. N. *Voprosy onkologii* **1976**, 22, 75-6.

- [9] Ashmead, H. *Journal of Applied Nutrition* **1972**, 24, 8-17.
- [10] Sax, N. I. *Dangerous Properties of Industrial Materials. 5th Ed*; Van Nostrand Reinhold: New York, 1979.
- [11] Sigel, H.; Editor *Metal Ions in Biological Systems, Vol. 10: Carcinogenicity and Metal Ions*, Dekker: New York, 1980.
- [12] Cepero, A.; Kudelin, Y. I.; Timonir, V. A. *Revista de Ciencias Quimicas* **1982**, 13, 93-109.
- [13] Moini, A. Ph.D. Dissertation, Department of Chemistry, Texas A&M University, 1986.
- [14] Itoh, M.; Hayakawa, K.; Oishi, S. *Journal of Physics: Condensed Matter* **2001**, 13, 6853-6864.
- [15] Papakondylis, A.; Sautet, P. *Journal of Physical Chemistry* **1996**, 100, 10681-10688.
- [16] Kihlberg, L. *Arkiv foer Kemi* **1963**, 21, 357-64.
- [17] Hsu, Z. Y.; Zeng, H. C. *Journal of Physical Chemistry B* **2000**, 104, 11891-11898.
- [18] Ressler, T.; Timpe, O.; Neisius, T.; Find, J.; Mestl, G.; Dieterle, M.; Schlögl, R. *Journal of Catalysis* **2000**, 191, 75-85.
- [19] Chippindale, A. M.; Dickens, P. G.; Powell, A. V. *Progress in Solid State Chemistry* **1991**, 21, 133-98.
- [20] Ma, E. *Bull Chem. Soc. Japan* **1964**, 37, 171-5.

- [21] Haber, J.; Lalik, E. *Catalysis Today* **1997**, 33, 119-137.
- [22] Bruckman, K.; Grabowski, R.; Haber, J.; Mazurkiewicz, A.; Sloczynski, J.; Wiltowski, T. *J. Catal.* **1987**, 104, 71-9.
- [23] Bruckman, K.; Haber, J.; Wiltowski, T. *Journal of Catalysis* **1987**, 106, 188-201.
- [24] Haber, J.; Serwicka, E. *Polyhedron* **1986**, 5, 107-9.
- [25] Vedrine, J. C.; Coudurier, G.; Forissier, M.; Volta, J. C. *Materials Chemistry and Physics* **1985**, 13, 365-78.
- [26] Silvestre, J. *Journal of the American Chemical Society* **1987**, 109, 594-5.
- [27] Haber, J. *Studies in Surface Science and Catalysis* **1992**, 72, 279-304.
- [28] Klimisch, R. L.; Larson, J. G.; General Motors Corporation. *The Catalytic Chemistry of Nitrogen Oxides: [Proceedings of the Symposium held in Warren, Michigan, October 7-8, 1974]*; Plenum Press: New York, 1975.
- [29] Baiker, A.; Dollenmeier, P.; Reller, A. *Journal of Catalysis* **1987**, 103, 394-8.
- [30] Hermann, K.; Witko, M.; Michalak, A. *Catalysis Today* **1999**, 50, 567-577.
- [31] Hanna, A. A.; Khilla, M. A. *Thermochimica Acta* **1983**, 65, 311-20.
- [32] Molla, S. R. M.Sc. Dissertation, Department of Chemistry, University of Prince Edward Island (Canada), 2006.
- [33] Whittingham, M. S.; Jacobson, A. J. *Intercalation Chemistry*; Academic Press: New York, 1982.

- [34] Besenhard, J. O.; Heydecke, J.; Wudy, E.; Fritz, H. P.; Foag, W. *Solid State Ionics* **1983**, 8, 61-71.
- [35] Guliants, V. V.; Benziger, J. B.; Sundaresan, S. *Chemistry of Materials* **1994**, 6, 353-6.
- [36] Johnson, J. W.; Jacobson, A. J.; Rich, S. M.; Brody, J. F. *Journal of the American Chemical Society* **1981**, 103, 5246-7.
- [37] Sienko, M. J.; Plane, R. A. *Chemistry: Principles and Applications. 3rd Ed*, 1979.
- [38] Hoang-Van, C.; Zegaoui, O. *Applied Catalysis, A: General* **1995**, 130, 89-103.
- [39] Sian, T. S.; Reddy, G. B.; Shivaprasad, S. M. *Japanese Journal of Applied Physics, Part 1: Regular Papers, Short Notes & Review Papers* **2004**, 43, 6248-6251.
- [40] Cotton, F. A.; Wilkinson, G. *Advanced Inorganic Chemistry: A Comprehensive Text*; 5th ed.; Wiley: New York, 1988.
- [41] Abrahams, S. C.; Reddy, J. M. *Journal of Chemical Physics* **1965**, 43, 2533-43.
- [42] Smith, G. W. *Acta Cryst.* **1962**, 15, 1054-7.
- [43] Smith, G. W.; Ibers, J. A. *Acta Cryst.* **1965**, 19, 269-75.
- [44] Sleight, A. W.; Chamberland, B. L. *Inorganic Chemistry* **1968**, 7, 1672-5.
- [45] Abrahams, S. C. *Journal of Chemical Physics* **1967**, 46, 2052-63.
- [46] Abrahams, S. C.; Bernstein, J. L.; Jamieson, P. B. *Journal of Chemical Physics* **1968**, 48, 2619-29.

- [47] Machida, N.; Chusho, M.; Minami, T. *Journal of Non-Crystalline Solids* **1988**, *101*, 70-4.
- [48] Znasik, P.; Jamnicky, M. *Journal of Non-Crystalline Solids* **1992**, *146*, 74-80.
- [49] He, C.; Lin, Y.; Su, W.; Shen, B.; Li, Z.; Gu, W.; Rong, X. *Guisuanyan Xuebao* **1981**, *9*, 285-94.
- [50] Zeng, H. C. *Journal of Materials Research* **1996**, *11*, 703-15.
- [51] Wachs, I. E.; Editor *Characterization of catalytic materials*, Butterworth-Heinemann: Boston, Greenwich, 1992.
- [52] Killeffer, D. H.; Linz, A. *Molybdenum Compounds*, 1952.
- [53] Mantese, J. V.; Micheli, A. L.; Hamdi, A. H.; Vest, R. W. *MRS Bulletin* **1989**, *14*, 48-53.
- [54] Vest, R. W. *Ceram. Films Coat.* **1993**, 303-47.
- [55] Apblett, A. W.; Chehbouni, M.; Reinhardt, L. E. *Ceramic Transactions* **2006**, *174*, 39-46.
- [56] Brown, S.; Marshall, A.; Hirst, P. *Materials Science & Engineering, A: Structural Materials: Properties, Microstructure and Processing* **1993**, *A173*, 23-7.
- [57] Laudise, R. A. *The Growth of Single Crystals*; Prentice-Hall: Englewood Cliffs, N.J., 1970.
- [58] Blistanov, A. A.; Galagan, B. I.; Denker, B. I.; Ivleva, L. I.; Osiko, V. V.; Polozkov, N. M.; Sverchkov, Y. E. *Kvantovaya Elektronika (Moscow)* **1989**, *16*, 1152-4.

- [59] Flournoy, P. A.; Brixner, L. H. *Journal of the Electrochemical Society* **1965**, *112*, 779-81.
- [60] Maggiore, R.; Galvagno, S.; Bart, J. C. J.; Giannetto, A.; Toscano, G. *Zeitschrift fuer Physikalische Chemie (Muenchen, Germany)* **1982**, *132*, 85-91.
- [61] Veleva, S.; Trifiro, F. *Reaction Kinetics and Catalysis Letters* **1976**, *4*, 19-24.
- [62] Grzybowska, B.; Haber, J.; Janas, J. *J. Catal.* **1977**, *49*, 150-63.
- [63] Callahan, J. L.; Grasselli, R. K.; Milberger, E. C.; Strecker, H. A. *Industrial & Engineering Chemistry Product Research and Development* **1970**, *9*, 134-42.
- [64] Knoezinger, H. *Proc. - Int. Congr. Catal., 9th* **1988**, *5*, 20-53.
- [65] Brito, J. L.; Barbosa, A. L. *Journal of Catalysis* **1997**, *171*, 467-475.
- [66] Madeley, R. A.; Wanke, S. E. *Applied Catalysis* **1988**, *39*, 295-314.
- [67] Mazzocchia, C.; Aboumrar, C.; Diagne, C.; Tempesti, E.; Herrmann, J. M.; Thomas, G. *Catalysis Letters* **1991**, *10*, 181-91.
- [68] Yoon, Y. S.; Ueda, W.; Moro-oka, Y. *Topics in Catalysis* **1996**, *3*, 265-275.
- [69] Zou, J.; Schrader, G. L. *Journal of Catalysis* **1996**, *161*, 667-686.
- [70] Braithwaite, E. *Chemistry & Industry (London, United Kingdom)* **1978**, 405-12.
- [71] Li, J. L.; Dai, W. L.; Dong, Y.; Deng, J. F. *Materials Letters* **2000**, *44*, 233-236.
- [72] Madeira, L. M.; Portela, M. F.; Mazzocchia, C. *Catalysis Reviews - Science and Engineering* **2004**, *46*, 53-110.

- [73] Bonner, W. A.; Zydzik, G. J. *Journal of Crystal Growth* **1970**, 7, 65-8.
- [74] Satoh, T.; Ohhara, A.; Fujii, N.; Namikata, T. *Journal of Crystal Growth* **1974**, 24-25, 441-4.
- [75] Takano, S.; Esashi, S.; Mori, K.; Namikata, T. *Journal of Crystal Growth* **1974**, 24-25, 437-40.
- [76] Spassky, D. A.; Ivanov, S. N.; Kolobanov, V. N.; Mikhailin, V. V.; Zemskov, V. N.; Zadneprovski, B. I.; Potkin, L. I. *Radiation Measurements* **2004**, 38, 607-610.
- [77] Kim, T. H.; Ramachandra, B.; Choi, J. S.; Saidutta, M. B.; Choo, K. Y.; Song, S.-D.; Rhee, Y.-W. *Catalysis Letters* **2004**, 98, 161-165.
- [78] Roy, A.; Ghose, J. *Journal of Solid State Chemistry* **1998**, 140, 56-61.
- [79] Soares, A. P. V.; Portela, M. F. *Catalysis Reviews - Science and Engineering* **2005**, 47, 125-174.
- [80] Belhekar, A. A.; Ayyappan, S.; Ramaswamy, A. V. *Journal of Chemical Technology and Biotechnology* **1994**, 59, 395-402.
- [81] Foley, R. T. *Corrosion (Houston, TX, United States)* **1964**, 20, 267t-268t.
- [82] Choudhury, A. K.; Shome, S. C. *Journal of Scientific & Industrial Research* **1958**, 17A, 30-4.
- [83] Choudhury, A. K.; Shome, S. C. *Journal of Scientific & Industrial Research* **1959**, 18A, 568-70.
- [84] Killeffer, D. H. *Paint, Oil and Chemical Review* **1954**, 117, 24-5.
- [85] Simpson, C. *Chemtech* **1997**, 27, 40-42.

- [86] Abdel-Rehim, A. M. *Journal of Thermal Analysis* **1997**, 48, 177-202.
- [87] Abdel-Rehim, A. M. *Journal of Thermal Analysis and Calorimetry* **1999**, 57, 415-431.
- [88] Abdel-Rehim, A. M. *Journal of Thermal Analysis and Calorimetry* **2004**, 76, 557-569.
- [89] Dinesh, R.; Fujiwara, T.; Watanabe, T.; Byrappa, K.; Yoshimura, M. *Journal of Materials Science* **2006**, 41, 1541-1546.
- [90] Zhang, Y.; Holzwarth, N. A. W.; Williams, R. T. *Physical Review B: Condensed Matter and Materials Physics* **1998**, 57, 12738-12750.
- [91] Barbosa, L. B.; Ardila, D. R.; Cusatis, C.; Andreeta, J. P. *Journal of Crystal Growth* **2002**, 235, 327-332.
- [92] Cho, W.-S.; Yashima, M.; Kakihana, M.; Kudo, A.; Sakata, T.; Yoshimura, M. *Journal of the American Ceramic Society* **1997**, 80, 765-769.
- [93] Petrov, A.; Kofstad, P. *Journal of Solid State Chemistry* **1979**, 30, 83-8.
- [94] Yang, P.; Yao, G.-Q.; Lin, J.-H. *Inorganic Chemistry Communications* **2004**, 7, 389-391.
- [95] Alexeyev, A. N.; Roshchupkin, D. V. *Applied Physics Letters* **1996**, 68, 159-60.
- [96] Petzelt, J.; Smutny, F.; Katkanant, V.; Ullman, F. G.; Hardy, J. R.; Volkov, A. A.; Kozlov, G. V.; Lebedev, S. P. *Physical Review B: Condensed Matter and Materials Physics* **1984**, 30, 5172-82.
- [97] Takashige, M.; Hamazaki, S.; Fukurai, N.; Shimizu, F.; Kojima, S. *Ferroelectrics* **1997**, 203, 221-225.



- [98] Kim, S. I.; Kim, J.; Kim, S. C.; Yun, S. I.; Kwon, T. Y. *Materials Letters* **1995**, 25, 195-8.
- [99] Nishioka, H.; Odajima, W.; Tateno, M.; Ueda, K.; Kaminskii, A. A.; Butashin, A. V.; Bagayev, S. N.; Pavlyuk, A. A. *Applied Physics Letters* **1997**, 70, 1366-1368.
- [100] Collado, J. A.; Aranda, M. A. G.; Cabeza, A.; Olivera-Pastor, P.; Bruque, S. *Journal of Solid State Chemistry* **2002**, 167, 80-85.
- [101] Fournier, J. P.; Fournier, J.; Kohlmuller, R. *Bulletin de la Societe Chimique de France* **1970**, 4277-83.
- [102] Goutenoire, F.; Isnard, O.; Retoux, R.; Lacorre, P. *Chemistry of Materials* **2000**, 12, 2575-2580.
- [103] Goutenoire, F.; Isnard, O.; Suard, E.; Bohnke, O.; Laligant, Y.; Retoux, R.; Lacorre, P. *Journal of Materials Chemistry* **2001**, 11, 119-124.
- [104] Lacorre, P.; Goutenoire, F.; Bohnke, O.; Retoux, R.; Laligant, Y. *Nature (London)* **2000**, 404, 856-858.
- [105] Wang, X. P.; Fang, Q. F. *Solid State Ionics* **2002**, 146, 185-193.
- [106] Minh, N. Q. *Proceedings - Electrochemical Society* **1995**, 95-1, 138-45.
- [107] Kuang, W.; Fan, Y.; Yao, K.; Chen, Y. *Journal of Solid State Chemistry* **1998**, 140, 354-360.

## **CHAPTER II**

### **REMEDIATION AND RECOVERY OF URANIUM FROM WATER USING MOLYBDENUM TRIOXIDES**

#### **INTRODUCTION**

Uranium is one of the most important heavy metals due to its chemical toxicity and radioactivity.<sup>1</sup> Uranium contamination of groundwater and surface water is a widespread environmental concern.<sup>2,3</sup> The latter occurs naturally in the earth's crust, in surface, and in ground water. When bedrock, consisting mainly of granitoids and granites, comes in contact with soft, slightly alkaline bicarbonate waters under oxidizing conditions, uranium will solubilize over a wide pH range. These conditions are widely seen throughout the world. For instance, in Finland, concentrations of up to 12,000 ppb are found in wells drilled in bedrock.<sup>4</sup> In private wells in Canada, concentrations of up to 700 ppb were observed.<sup>5</sup> Moreover, in the United States, in some uranium mine tailings disposal sites near Tuba City, AZ, uranium concentrations were found as high as 20 times the maximum concentration allowed for ground water in the United States.<sup>6</sup> In addition, in the Simpsonville-Greenville area of South Carolina, high amounts of uranium (30 to 9900 ppb) were found in 31 drinking water wells. The contamination with uranium is believed to be due to veins of pegmatite that occur in the area. Besides entering drinking water from naturally occurring deposits, contamination of uranium can also occur in the

water supply as a result of human activity, such as uranium mining, mill tailing, and even agriculture.<sup>7,8</sup> Phosphate fertilizers often contain uranium at an average concentration of 150 ppm, hence they are an important contributor of uranium to groundwater.<sup>9</sup> Depleted uranium ammunition used in several military conflicts has also contributed to drinking water contamination.

The major health effect of uranium is chemical kidney toxicity, rather than a radiation hazard as proven by animal testing and studies of exposed people.<sup>10</sup> It has been demonstrated that the uranium contamination causes functional as well as histological damage to the proximal tubules of the kidney.<sup>11</sup> Despite the fact that little is known about the effects of long term environmental uranium exposure in humans, there has been an association of uranium exposure with increased urinary glucose, alkaline phosphatase, and  $\beta$ -microglobulin excretion, as well as increased urinary albumin levels.<sup>12,13</sup> As a result of such studies, the World Health organization has proposed a guideline value of 2 ppb of uranium in drinking water, while the US EPA has specified a limit of 30 ppb. Therefore, ground water remediation measures are essential to lower the uranium concentration under the suitable limit designed by the Environmental and Protection Agency.<sup>14</sup>

A variety of methods have been used for removing uranium from ground water. For instance, modification of pH or chemical treatment (often with alum) or a combination of the two is effective in removing uranium from water.<sup>15</sup> In addition, it has been shown that activated carbon, iron powder, magnetite, and ion exchange technology can adsorb uranium. Notably, ion exchange resins that are widely used for waste water and ground water treatment are capable of absorbing more than 90% of the uranium from drinking water. In addition to treatment of well water, there is also a strong need for

prevention of the spread of uranium contamination from concentrated sources such as uranium mine tailings.<sup>6</sup> Unfortunately, commonly used above-ground water treatment processes are not effective and do not provide an adequate solution to the problem.

Permeable reactive barriers (PRBs) are a cost effective, promising method to control uranium contamination in seepage water (Figure 2.1).<sup>16</sup> The barriers previously used for uranium consisted of zero-valent iron, ferric oxyhydroxide, or bone char phosphate. When iron metal was used, uranium concentrations were lowered by more than 99.9% after the contaminated groundwater had traveled 1.5 ft. into the permeable reactive barrier.<sup>16</sup>

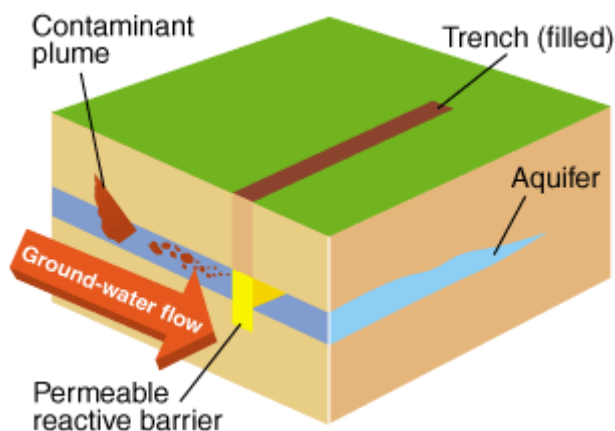


**Figure 2.1.** Operation of a Permeable Reactive Barrier.<sup>16</sup>

Molybdenum hydrogen bronze (also called molybdenum blue),  $\text{HMo}_2\text{O}_6$ , has been investigated for application in removal of uranium from aqueous solutions and possible use in a cyclic process for uranium recovery.<sup>17</sup> It was shown that the oxidation of the blue reagent occurred during the adsorption process causing the reagent to change color from blue to yellow. Using the above method, the uptake of uranium was found to

be 122% by weight which exceeded the capacity of protons present (the proton concentration in the bronze was 3.46 mEq/g while the uranium absorption was 5.14 mEq/g). The reaction of molybdenum bronze and uranium acetate revealed the formation of the mineral irrignite,  $\text{UMo}_2\text{O}_9 \cdot 3\text{H}_2\text{O}$ . The oxidation of the Mo (V) centers in the bronze was found to be due to the reaction of molecular oxygen as the layered structure was disassembled by the reaction with uranyl ions. This result suggested that prior reduction of  $\text{MoO}_3$  to  $\text{HMo}_2\text{O}_6$  was unnecessary for uranium adsorption. Hence, the investigation to use  $\text{MoO}_3$  as a reagent to absorb uranium from water was prompted.

## EXPERIMENTAL

All reagents were commercial products (ACS reagent grade or higher) and were used without further purification. Bulk pyrolyses at various temperatures were performed in air in a digitally-controlled muffle furnace using approximately 1 g samples, a ramp of 10 °C/min, and a hold time for 4 hours. The X-ray powder diffraction (XRD) patterns were recorded on a Bruker AXS D-8 Advanced X-ray powder diffractometer using copper  $\text{K}_\alpha$  radiation. Crystalline phases were identified using a search/match program and the PDF-2 database of the International Center for Diffraction Data. Scanning Electron Microscopy (SEM) photographs were recorded using a JEOL Scanning Electron Microscope. Colorimetry was performed on a Spectronic 200 digital spectrophotometer using 1 cm cylindrical cuvettes. The uranium concentrations in the treated solutions were measured at a wavelength  $\lambda = 415 \text{ nm}$  (after 5 ml solutions) after treatment with concentrated nitric acid (1 ml) to ensure no speciation of metals would interfere with the

measurements. The calibration curve was constructed from 5 standards in the range of 0.01 to 0.1 M uranyl acetate and was found to be linear in accord with Beer's law.

### **Reaction of MoO<sub>3</sub> with Uranyl Acetate**

MoO<sub>3</sub> (1.00 g, 6.95 mmol) was added to a 100 ml of 0.100 M uranyl acetate solution (10.0 mmol). The mixture was refluxed for 7 days. Upon cooling, a yellow solid was isolated by filtration through a fine sintered glass filter and dried in vacuum at room temperature over night. The yield of the yellow product was 3.23 g. Thermal gravimetric analysis showed a weight loss of 9.24% at 600 °C. Powder XRD of the product indicated the formation of the mineral Umohoite [UMoO<sub>6</sub> · 2(H<sub>2</sub>O), ICDD # 43-0355]. Upon heating the product to 600 °C, a dehydrated form of the mineral (UMoO<sub>6</sub>) was observed by XRD analysis. The infrared spectrum of the isolated product (DRIFTS, solid diluted in KBr, cm<sup>-1</sup>) contained the following peaks: 3582 w, 3513 vs, br, 3195 w, 2928 w, 1630 s, 1611 s, 1402 s, 918 vs, 889 vs, 859 vs, 821 vs, 724 m, 642 m, 541 m. The overall yield was 2.97 g.

### **Kinetics of MoO<sub>3</sub> reaction with uranyl nitrate at room temperature**

Uranyl acetate (8.48 g, 20.0 mmol) was dissolved in 200 ml of 0.100 M aqueous solution of acetic acid. After that, MoO<sub>3</sub> (2.00 g, 14.0 mmol) was added to the solution, and the mixture was stirred magnetically. Aliquots (5.0 ml) of the reaction were withdrawn at regular intervals, and uranium was quantified by colorimetry.

### **Recovery of Uranium and MoO<sub>3</sub>**

Uranium and MoO<sub>3</sub> were recovered from the umohoite product by treatment with a strong base. Thus, 1.00 g of the product was reacted with a 100 ml of a 15% solution of ammonium hydroxide. The mixture was separated by filtration through a 20  $\mu$ m nylon membrane filter. The solid product was washed with distilled water and dried in vacuum over night at room temperature to yield 0.70 g. Thermal gravimetric analysis showed water content of 9.32%. The filtrate was evaporated, and the solid obtained was analyzed by infrared spectroscopy, thermal gravimetric analysis, and X-ray powder diffraction.

### **RESULTS AND DISCUSSION**

Molybdenum trioxide was allowed to react with an aqueous solution of uranyl acetate for an extended period of time in order to determine the maximum uptake of uranium. It was found that MoO<sub>3</sub> absorbed 165% by weight of uranium. This equates 6.94 millimoles of uranium per gram of MoO<sub>3</sub> and exceeded the 122% by weight observed when using HMo<sub>2</sub>O<sub>6</sub>.<sup>18</sup> The color of the product obtained was yellow, which is a characteristic of hexavalent uranium, implying that the difference in uranium uptake is due to varying ratios of uranium to molybdenum in the product rather than to differences in uranium oxidation states. An X-ray powder diffraction analysis (Figure 2.2) of the solid product from the uranium uptake and molybdenum oxides showed that the product mainly consisted of the mineral umohoite UMoO<sub>6</sub>·2H<sub>2</sub>O. In addition to umohoite, several unidentified peaks were obtained, the strongest of which was at  $2\theta = 15^\circ$ . It is believed that the latter corresponds to a more hydrated form of UMoO<sub>6</sub> than umohoite. Supporting this hypothesis, the thermal gravimetric analysis showed a water content of

9.24%, or approximately 2.43 molar equivalent of water per  $\text{UMoO}_6$  formula unit. Furthermore, the X-ray powder diffraction of the product between uranyl acetate and molybdenum oxide taken before drying showed considerably more intense peaks of the more likely hydrated phase than the dried sample. Moreover, as the product from uranyl acetate and  $\text{MoO}_3$  was heated to  $600\text{ }^\circ\text{C}$ , a phase-pure dehydrated form of umohoite ( $\text{UMoO}_6$ ) was obtained (Figure 2.3), eliminating the possibility of the presence of a crystalline phase with a different ratio of uranium to molybdenum other than one to one.

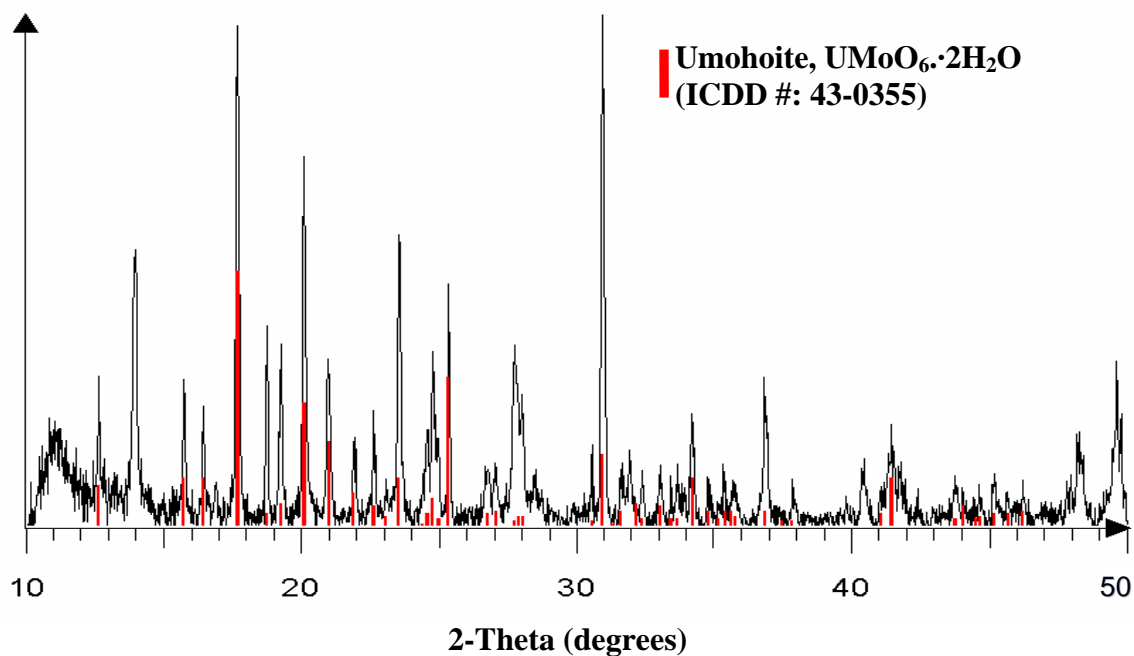


**Figure 2.2.** XRD patterns of the product from the reaction between uranyl acetate and  $\text{MoO}_3$  as isolated.



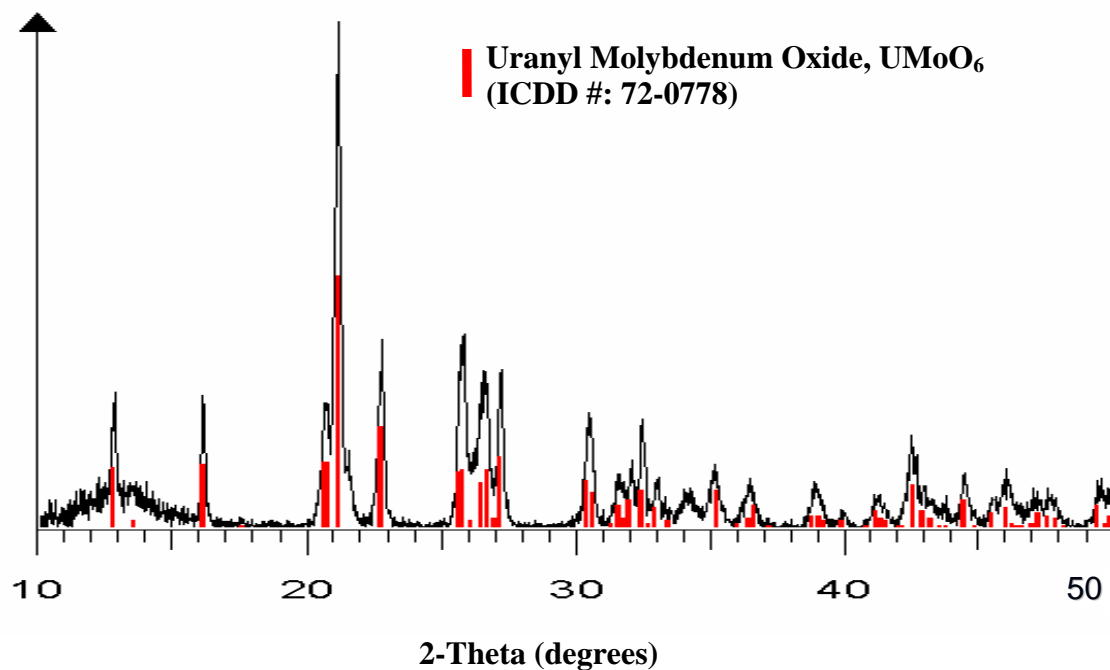


**Figure 2.3.** XRD pattern of the product from the reaction of MoO<sub>3</sub> and uranyl acetate heated to 600 °C.

The structure of umohoite (Figure 2.4) formed from the reaction of MoO<sub>3</sub> with uranyl ions, appears to preserve part of the structure of MoO<sub>3</sub> (Figure 2.5). The latter compound is composed of distorted MoO<sub>6</sub> octahedra interconnected through corners linking along the [100] plane to form infinite chains that edge-share along the [001] plane to form double-layer sheets parallel to the [010] plane.<sup>19</sup> The sheets are stacked together via van der Waals forces to give the final layered structure.

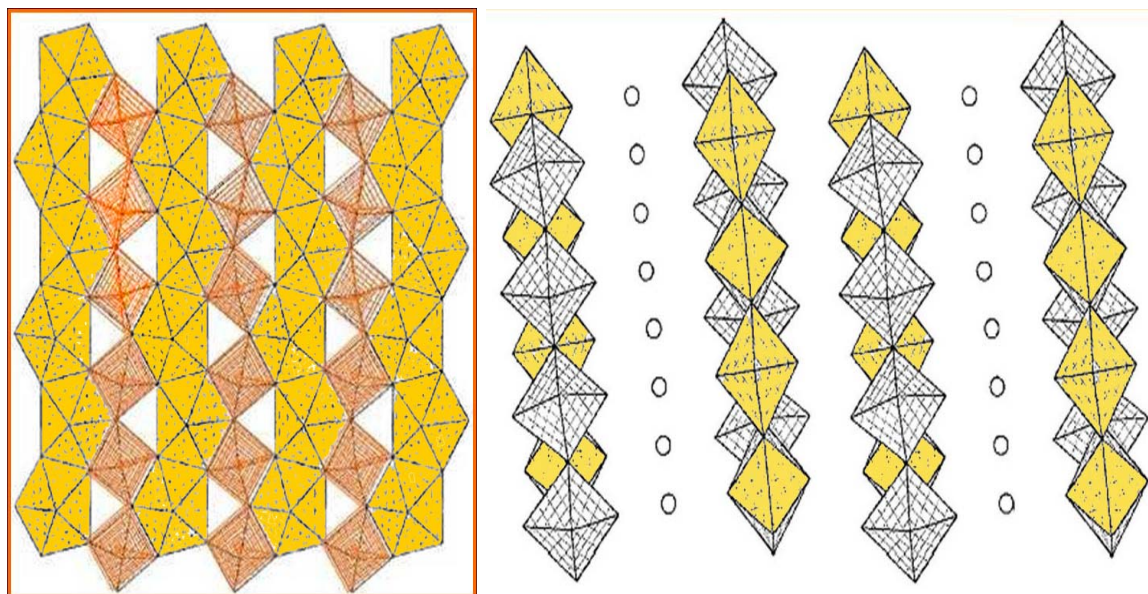


**Figure 2.4.** Structure of umohoite viewed along the [001] plane (left) and the [100] plane (right). Lighter shaded octahedra are  $\text{MoO}_6$  while yellow shaded decahedra are  $\text{UO}_7$ . Circles are water.<sup>20</sup>

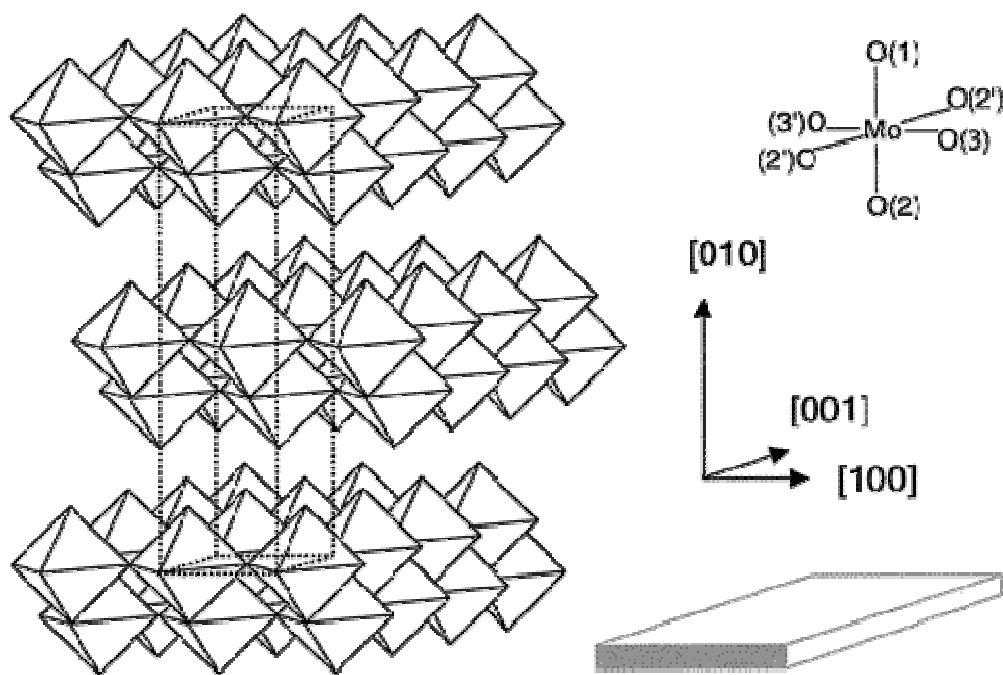


**Figure 2.5.** Layered structure of  $\text{MoO}_3$ .<sup>19</sup>

The structure of umohoite contains  $U^{+6}$  ions which are strongly bonded to two oxygen atoms, resulting in nearly linear uranyl ions  $(UO_2)^{2+}$ . Each uranyl ion is coordinated by five additional oxygen atoms in the form of pentagonal bipyramids to form  $UO_7$  decahedra. Each  $Mo^{+6}$  cation is bonded to five oxygen atoms and one  $H_2O$  group to form a highly distorted octahedron. The  $H_2O$  groups are the sixth ligand of the distorted octahedra, which explains the need of high temperatures (600 °C) to dehydrate the product. The chains of uranyl oxide decahedra share edges with molybdenum oxide octahedra (Figure 2.4). The interlayer at  $z = 0$  contains the second  $H_2O$  groups, whereas the interlayer at  $z = 0.5$  is unoccupied.<sup>20</sup> The structural changes from  $MoO_3$  to the umohoite structure imply that the mechanism of the reaction might involve the intercalation of the chains of  $UO_7$  decahedra between the edge-shared chains of  $MoO_6$  octahedra to give a new layered structure. However, SEM images of the  $MoO_3$  and the product with uranyl acetate (Figure 2.6) showed that the new particles (Figure 2.6, right) are much smaller than the  $MoO_3$  reagent used (Figure 2.6, left). The latter particles are square plates and rectangles. This result suggests an alternative mechanism, in which the molybdenum trioxide particles completely dissolve in a dissolution/precipitation process and generate new particles with different morphology. Similar morphological rearrangements were also seen in the reaction of  $HMo_2O_6$  with uranyl acetate.<sup>17</sup> Unfortunately, the experiments performed so far can not confirm the mechanism. Additional investigation with large single crystals of molybdenum trioxide is needed to further elucidate the mechanism.

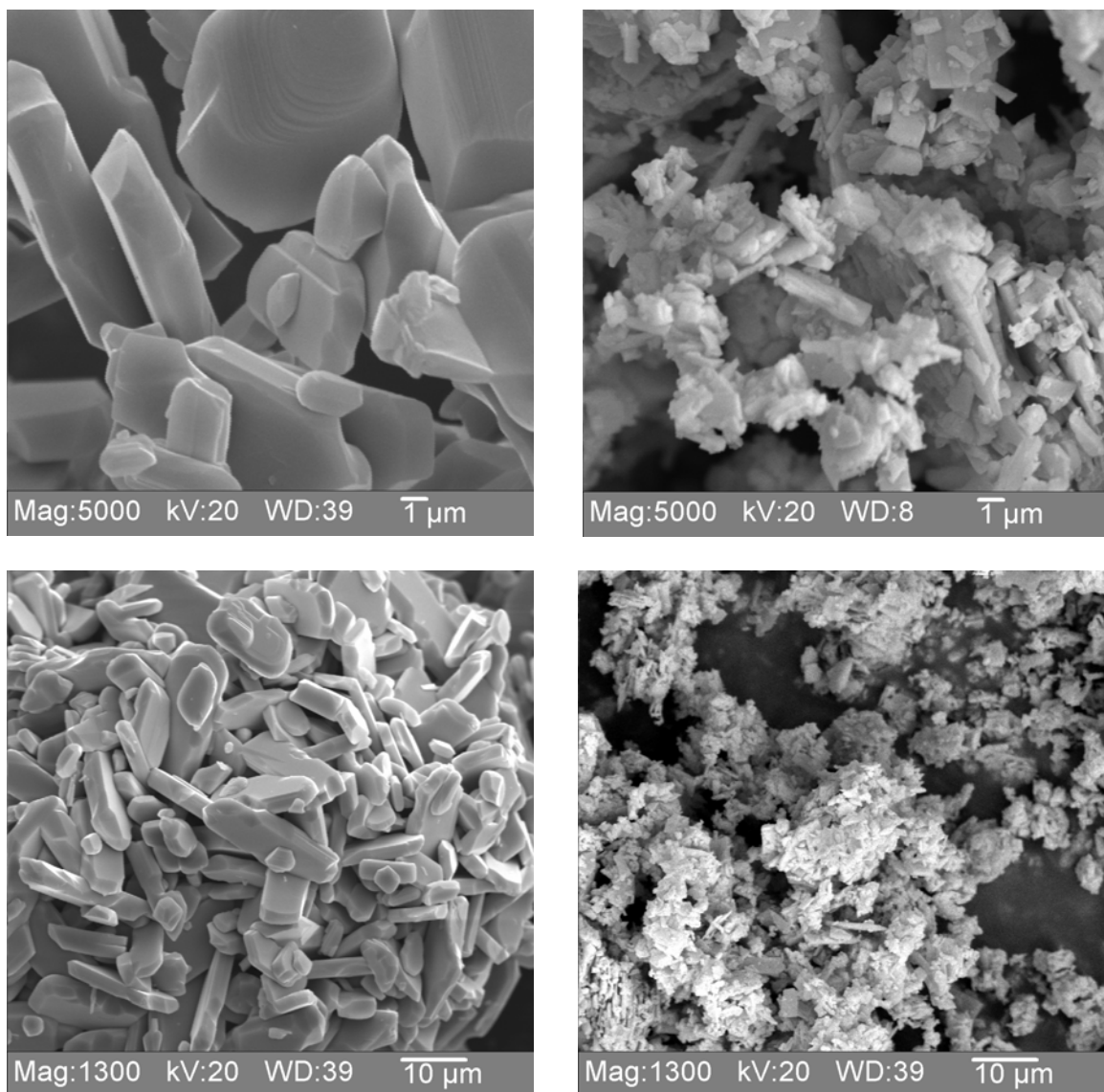


**Figure 2.6.** SEM images of molybdenum trioxide (left) and the product from its reaction with uranium acetate (right).

Due to the importance of the rate of reaction of MoO<sub>3</sub> in the purification of drinking water or in the construction of permeable reactive barriers that must take place under ambient temperature, the rate of the absorption of uranium from aqueous uranyl acetate was investigated. The results are shown in Figure 2.7.

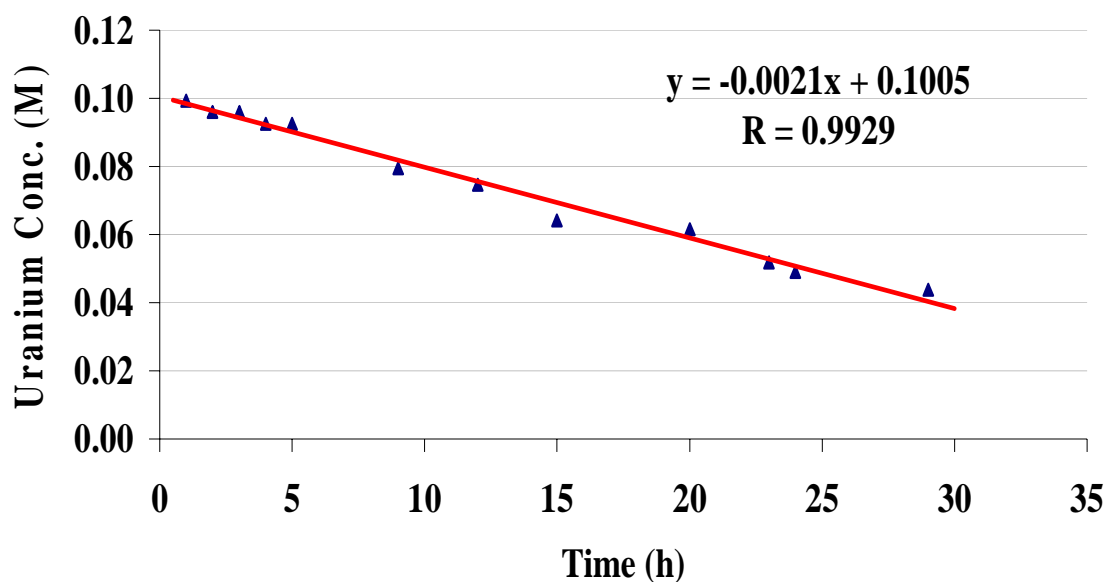


**Figure 2.7.** Change of uranium concentration versus time.

The uranyl acetate solution was acidified with acetic acid to prevent hydrolysis of the uranyl ions and a 43% excess of uranyl acetate to  $\text{MoO}_3$  was used. The reaction was found to be zero order with a rate constant of 0.42 mmol/hour. The result is consistent with the dissolution/precipitation mechanism since it would cause smaller particles of  $\text{MoO}_3$  to be formed during the reaction. The resulting increase in specific surface area could offset the diminishment of the amount of  $\text{MoO}_3$  present and possibly lead to the observed zero order kinetics of the reaction. The initial surface area of  $\text{MoO}_3$  was 0.712  $\text{m}^2/\text{g}$ , therefore, the rate constant for uranium uptake is 0.295 mmol U/hr. $\text{m}^2$   $\text{MoO}_3$ .

### **Cyclic process for uranium uptake**

The umohoite product obtained from the reaction of  $\text{MoO}_3$  and uranyl acetate was treated with a 15% solution of ammonium hydroxide. After stirring the reaction for 12 hours at room temperature, the reaction mixture was separated by filtration.

The X-ray powder diffraction of the residue corresponded to ammonium uranate  $[(\text{NH}_4)_2\text{U}_3(\text{OH})_2\text{O}_9 \cdot 2\text{H}_2\text{O}]$ , ICDD # 43-0366], which has application in the nuclear power industry. The ammonium uranate can be further converted to the orthorhombic phase of  $\text{U}_3\text{O}_8$  upon heating to 600 °C (ICDD #: 47-1493). Figure 2.8 illustrates the complete cycle of uranium remediation process. The recovery of uranium was 98.9 % by weight. The X-ray powder diffraction of the evaporated filtrate corresponded to ammonium molybdate  $[(\text{NH}_4)_6\text{Mo}_7\text{O}_{24} \cdot 4\text{H}_2\text{O}]$ , ICDD #: 27-1013]. The  $\text{MoO}_3$  could be recovered upon heating of the ammonium molybdate product to 540 °C as determined by thermal gravimetric analysis and X-ray powder diffraction analysis. Hence, a complete cycle for uranium concentration can be developed in which the only reagents consumed are ammonium hydroxide. Potentially, the ammonia could be recovered and reused to yield a process with no waste products.

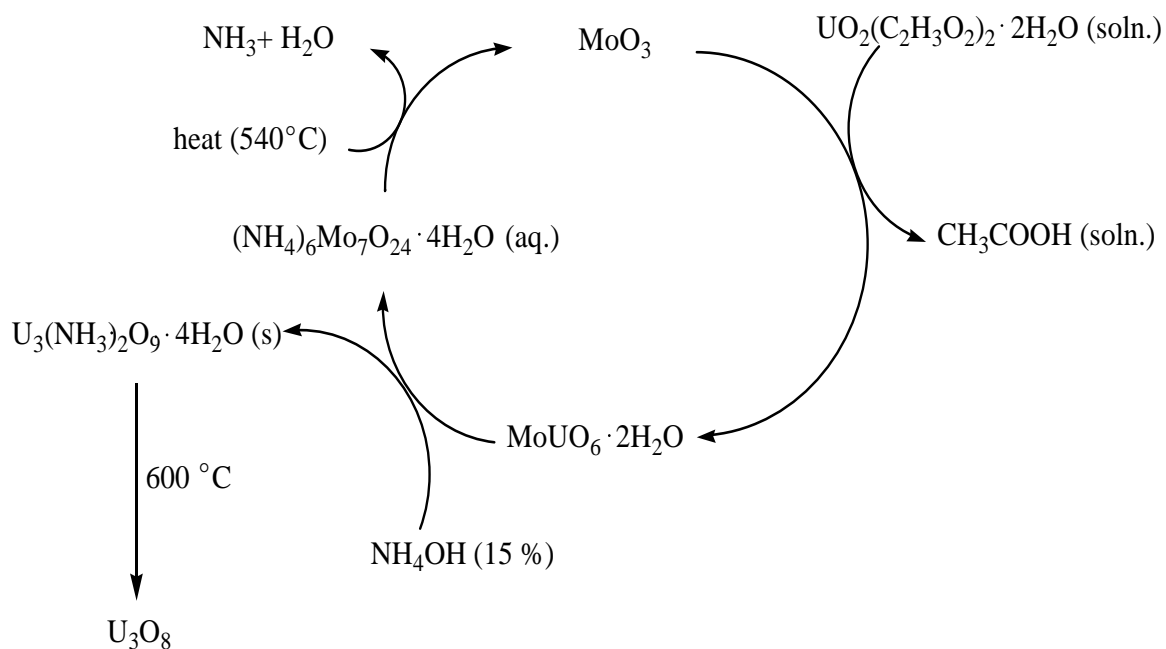


**Figure 2.8:** Complete cycle of uranium remediation process.

## CONCLUSIONS

In conclusion, it was shown that molybdenum trioxide has an extremely high capacity to absorb uranium from water. It was found that  $\text{MoO}_3$  could absorb up to 165% by weight of uranium via a chemical reaction that produces an insoluble uranium molybdenum oxide mineral called umohoite,  $\text{UMoO}_2 \cdot 2\text{H}_2\text{O}$ . The rate of reaction between molybdenum trioxide and a slight excess (43 mole %) of 0.100 M uranyl acetate was found to be zero order with a rate constant of 0.42 mmol/hr. A cyclic process was developed, in which  $\text{MoO}_3$  adsorbed uranium from aqueous solutions and then the uranium and molybdenum trioxide were separated by treatment with aqueous ammonia. Solid ammonium uranate was isolated by filtration and the aqueous ammonium molybdate was converted back to  $\text{MoO}_3$  by heating. The recovery of uranium from the separation was 98.9%. Hence,  $\text{MoO}_3$  has considerable promise for application in

environmental remediation and for construction of reactive barriers for the prevention of the spread of contaminant plumes.

## REFERENCES

- [1] Parab, H.; Joshi, S.; Shenoy, N.; Verma, R.; Lali, A.; Sudersanan, M. *Bioresource Technology* **2005**, 96, 1241-8.
- [2] Gregory, K. B.; Lovley, D. R. *Environmental Science and Technology* **2005**, 39, 8943-8947.
- [3] Morrison, S. J.; Metzler, D. R.; Dwyer, B. P. *Journal of Contaminant Hydrology* **2002**, 56, 99-116.
- [4] Salonen, L. *IAHS Publication* **1994**, 222, 71-84.
- [5] M. A. Moss; R. F. McCurdy; K. C. Dooley; M. L. Givner; L. C. Dymond; J. M. Slayer, a. M. M. C. In *International Chemical Toxicology and Clinical Chemistry of Metals*; Savory, S. S. B. a. J., Ed.; Academic Press: London, 1983, p 149-152.
- [6] Abdelouas, A.; Lutze, W.; Nuttall, E. *Journal of Contaminant Hydrology* **1998**, 34, 343-361.
- [7] Cothorn, C. R.; Lappenbusch, W. L. *Health Physics* **1983**, 45, 89-99.
- [8] Dreesen, D. R.; Williams, J. M.; Marple, M. L.; Gladney, E. S.; Perrin, D. R. *Environmental Science and Technology* **1982**, 16, 702-9.
- [9] Spalding, R. F.; Sackett, W. M. *Science (Washington, DC, United States)* **1972**, 175, 629-31.



- [10] Taylor, D. M.; Taylor, S. K. *Reviews on Environmental Health* **1997**, *12*, 147-157.
- [11] Haley, D. P. *Laboratory Investigation* **1982**, *46*, 196-208.
- [12] Mao, Y.; Desmeules, M.; Schaubel, D.; Berube, D.; Dyck, R.; Brule, D.; Thomas, B. *Environmental Research* **1995**, *71*, 135-140.
- [13] Zamora, M. L.; Tracy, B. L.; Zielinski, J. M.; Meyerhof, D. P.; Moss, M. A. *Toxicological Sciences* **1998**, *43*, 68-77.
- [14] Simon, F.-G.; Biermann, V.; Segebade, C.; Hedrich, M. *Science of the Total Environment* **2004**, *326*, 249-56.
- [15] White, S. K.; Bondietti, E. A. *Journal-American Water Works Association* **1983**, *75*, 374-80.
- [16] [www-ssrl.slac.stanford.edu/fuller\\_fig1v2.gif](http://www-ssrl.slac.stanford.edu/fuller_fig1v2.gif)
- [17] Kiran, B. P.; Apblett, A. W.; Chehbouni, M. *Ceramic Transactions* **2003**, *143*, 385-394.
- [18] Bollapragada, P. K. S., 1975- Ph.D. Dissertation, Department of Chemistry, Oklahoma State University, 2003.
- [19] Hsu, Z. Y.; Zeng, H. C. *Journal of Physical Chemistry B* **2000**, *104*, 11891-11898.
- [20] Krivovichev, S. V.; Burns, P. C. *Canadian Mineralogist* **2000**, *38*, 717-726.

## CHAPTER III

### NOVEL ROUTES FOR THE SYNTHESIS OF RARE EARTH MOLYBDATES

#### INTRODUCTION

In recent years, rare earth molybdates  $\text{Ln}_2(\text{MoO}_4)_3$  (where Ln represents the respective rare earth element) have attracted significant attention.<sup>1</sup> Gadolinium molybdate  $\text{Gd}_2(\text{MoO}_4)_3$  (GMO) is typical and the most investigated representative of the rare-earth molybdates. GMO displays very interesting electronic and optical properties. Below its Curie point ( $T_c$ ), the crystal state of GMO can be switched from one orientation domain to the other by applying either an electric field (ferroelectricity) or a mechanical stress (ferroelasticity).<sup>2,3</sup> GMO is the first crystal where both ferroelectricity and ferroelasticity phenomena were observed.<sup>4</sup> Due to this unusual behavior, GMO has several unique and potentially useful properties.<sup>5</sup> Consequently, GMO is of fundamental interest in memory cells, and low-speed mechanical positioning systems.<sup>6</sup> Furthermore,  $\text{Gd}_2(\text{MoO}_4)_3$  is used as an efficient laser medium for laser-diode pumping.<sup>5</sup> If doped with neodymium, GMO can be used for multicolor generation, self-frequency doubling, and self-frequency mixing.<sup>6</sup>

The direct synthesis of  $\text{Gd}_2(\text{MoO}_4)_3$  from metathesis or precipitation reaction between an aqueous gadolinium salt and aqueous sodium molybdate fails due to

preferential formation of  $\text{NaGd}(\text{MoO}_4)_2$ .<sup>7</sup> GMO can be prepared at high temperature from a mixture of the corresponding oxides. However, the main drawback of such an approach is inhomogeneity of the product and incompatibility with processing into thin films or thin electronic circuits.<sup>4</sup> Metal organic deposition (MOD) provides an alternative method to synthesize the desired oxides. It is a non-vacuum, solution based method for depositing thin film.<sup>8,9</sup> In the MOD process, a suitable metalloorganic precursor dissolved in an appropriate solvent is coated on a substrate by spin-coating, screen printing, or spray- or dip-coating. The soft metallo-organic film is then pyrolyzed in air, oxygen, nitrogen or other suitable atmospheres to convert the precursors to their constituent elements, oxides, or other compounds.<sup>7</sup> Shrinkage generally occurs only in the vertical dimension so that conformal coverage of a substrate may be realized. Metal carboxylates with long, slightly branched alkyl chains (e.g. 2-ethylhexanoate or neodecanoate) are often used as precursors for ceramic oxides since they are usually air-stable, soluble in organic solvents, and decompose readily to the metal oxides.

The need for environmental friendly processes places strict requirements on precursors for ceramic materials. In particular, the avoidance of organic solvents imposes the development of water-soluble, or even solventless preceramic compounds. A novel method for preparing gadolinium molybdates and lanthanum molybdates directly from the acetate of the corresponding rare earth metal and molybdenum trioxide is reported herein.

Oxide ion conductors have been increasingly studied because of their important fields of application.<sup>10</sup> A new kind of ion conductor has been recently reported which displays good ion conductivity at moderate temperatures.<sup>10-15</sup> Lanthanum molybdenum

oxide ( $\text{La}_2\text{Mo}_2\text{O}_9$ ) exhibits good ionic conductivity at intermediate temperatures, and thus it is of interest as a solid electrolyte material for numerous electrochemical applications, such as a component of fuel cells, oxygen sensors, dense ceramics for oxygen separation membranes, oxygen pumps, and oxygen-permeable membrane catalysts.<sup>16</sup> Furthermore, lanthanum molybdate is also used for selective oxidation of hydrocarbons to organic oxygenated compounds.<sup>17</sup> The reason for the good ionic conductivity of this material is because its structure includes about 10 % vacant intrinsic oxygen sites.<sup>18</sup> In the case of traditional oxide ion conductors, such as  $\text{AO}_2$  fluorite type, the substitution of tetravalent cations by tri- or divalent cations usually generates the ionic vacancies. However, the structure of  $\text{La}_2\text{Mo}_2\text{O}_9$  allows accommodation of excess of oxygen without the need of substitution. As a result, the high conductivity has been explained by the easy migration of oxygen ions via vacant sites.<sup>10,13,14,18,19</sup> The conduction properties can also be attributed to the lone pair substitution concept.<sup>20</sup> The crystal structure of  $\text{La}_2\text{Mo}_2\text{O}_9$  is similar to that of  $\text{SnWO}_4$  which can be rewritten as  $\text{Sn}_2\text{W}_2\text{O}_8\text{L}_2$ , where L is the lone pair of  $\text{Sn}^{+2}$ .<sup>19,21</sup> In the case of  $\text{La}_2\text{Mo}_2\text{O}_9$ , tungsten is substituted by molybdenum and  $\text{La}^{+3}$  replaces  $\text{Sn}^{+2}$ . Consequently, the lone pair site can remain either as a vacant site or be occupied by oxide anions because of the high valance of  $\text{La}^{+3}$ . Thus, the structural formula can be rewritten as  $\text{La}_2\text{Mo}_2\text{O}_{8+1}\square$  (where  $\square$  is a vacancy).<sup>19</sup> Therefore, the high conductivity can be explained by the migration of the extra oxide anions through the vacancies.

$\text{La}_2\text{Mo}_2\text{O}_9$  has previously been prepared by the conventional solid state reactions (SS) of  $\text{La}_2\text{O}_3$  and  $\text{MoO}_3$ .<sup>22</sup> The freeze-drying (FD) method, in which the precursors were prepared from solutions obtained by dissolving  $\text{La}_2\text{O}_3$  with diluted nitric acid, and

dissolving  $\text{MoO}_3$  with diluted ammonia is also known.<sup>19</sup> In addition, lanthanum molybdate was also prepared by direct ball milling synthesis of the a mixture of the metal oxides to generate solid solutions.<sup>23</sup> Unfortunately, the synthesis or ceramic compounds using solid state reactions do not always produce homogeneous products with controlled stoichiometry. Moreover, environmental concern is growing about the use or organic solvents for preparing ceramic products. Therefore, a direct environmental friendly method to synthesize lanthanum molybdenum oxide from lanthanum acetate and molybdenum oxide is investigated.

## EXPERIMENTAL

All reagents were commercial products purchased from Aldrich or Strem Chemical and were used without further purification. Thermogravimetric studies were performed using 23-30 mg samples under a 100 ml/min flow of dry air in a Seiko ExStar 6500 TGA/DTA instrument. Bulk pyrolyses at various temperatures were performed in ambient air in a temperature programmable muffle furnace using 1-2 g samples, at a temperature change of 5 °C/min and a hold time of 6-12 hours. The X-ray powder diffraction patterns were obtained using copper  $K_\alpha$  radiation on a Bruker D8 Advance diffractometer. Crystalline phases were identified using the PDF-2 database of the International Center of Diffraction Data (ICDD).<sup>24</sup> Infrared spectra were recorded by diffuse reflectance infrared Fourier transform spectroscopy (DRIFTS) on a Nicolet infrared spectrometer. Samples were diluted with potassium bromide and loaded in a diffuse reflectance cell for collection of the data. A total of 128 scans were collected

with a resolution of  $4\text{ cm}^{-1}$  and were averaged. Elemental analyses for carbon and hydrogen were performed by Desert Analytics.

### **Reaction of molybdenum trioxide with gadolinium acetate**

$\text{MoO}_3$  (2.16 g, 15.0 mmol) was added to a solution of gadolinium acetate (4.06 g, 10.0 mmol) in water (100 ml). The mixture was heated at reflux for 7 days. Upon cooling, a white solid was isolated by filtration through a fine sintered glass filter. After drying in vacuum at room temperature, the yield of  $\text{Gd}_2\text{Mo}_3\text{O}_{12} \cdot 2.2\text{H}_2\text{O}$  was found to be 4.37 g which corresponds to a yield of 96.0%, based on  $\text{MoO}_3$ . Thermal gravimetric analysis indicated a water content of 9.01% (Figure 3.1). Infrared spectrum (DRIFTS, solid diluted in KBr,  $\text{cm}^{-1}$ ): 3538 vs, br, 3351 vs, br, 2319 w, 1633 vs, 1549 w, 1429 w, 1364 w, 940 m, 878m 756 m, br, 593 w. The solid obtained was heated to  $800\text{ }^\circ\text{C}$  to yield the monoclinic phase of gadolinium molybdate ( $\text{Gd}_2(\text{MoO}_4)_3$ , Figure 3.2). The monoclinic phase was then converted to the ferroelectric orthorhombic gadolinium molybdate when the product was heated further to  $1000\text{ }^\circ\text{C}$  (Figure 3.3).

### **Reaction of $\text{MoO}_3$ with lanthanum acetate**

$\text{MoO}_3$  (4.32 g, 30.0 mmol) was allowed to react with a solution of lanthanum acetate (11.38 g, 36.0 mmol) in water (300 ml) at reflux for 7 days. Upon cooling, a white solid was isolated by filtration and dried in vacuum at room temperature overnight. The weight of the product obtained was 11.06 g. Thermal gravimetric analysis indicated a weight loss of 19.3 % at  $550\text{ }^\circ\text{C}$  (Figure 3.4). Infrared spectra (DRIFTS, solid diluted in KBr,  $\text{cm}^{-1}$ ) was taken of the sample at room temperature and after heating to  $550\text{ }^\circ\text{C}$

(Figure 3.5). The powder X-ray diffraction patterns of the product from molybdenum trioxide and lanthanum acetate were recorded at room temperature and after heating to 550 °C (Figure 3.6).

## RESULTS AND DISCUSSION

### Reaction of MoO<sub>3</sub> with gadolinium acetate

Previously, reactions of molybdenum trioxide with metal glyconates were used to generate mixed metal carboxylates that served as a single-source precursors for metal molybdates salts.<sup>25</sup> Therefore, the reaction of gadolinium acetate with molybdenum trioxide was investigated as a possible route for synthesis of gadolinium molybdate. A mixture of a stoichiometric amount of molybdenum trioxide (molar ratio Gd: Mo = 2:3) and a 0.1 M solution of gadolinium acetate in water was heated at reflux for seven days. At this point, all of the gadolinium had been absorbed from solution to yield a white solid that was isolated by filtration and was then dried in a vacuum at room temperature. The infrared spectrum of the material indicated that it was a hydrate, and its water content was determined to be 9.01% gravimetrically (Figure 3.1) upon heating to 600 °C. Thus, the formula of the product was Gd<sub>2</sub>(MoO<sub>4</sub>)<sub>3</sub>·2.2 H<sub>2</sub>O. An XRD analysis showed that the product was crystalline, but a match to known gadolinium or molybdenum compounds could not be found. However, upon heating to 600 °C, the solid was converted primarily to the tetragonal phase of Gd<sub>2</sub>Mo<sub>3</sub>O<sub>12</sub> that is based on defect scheelite structure.<sup>26</sup> This is a metastable phase previously prepared by calcining the precipitate formed by reaction of gadolinium nitrate with ammonium paramolybdate at 520 °C.<sup>26</sup> Interestingly, this material has ionic conductivity and is active in methanol oxidation. The XRD pattern of

the gadolinium acetate/molybdenum trioxide product calcined at 600 °C showed that the scheelite-based phase was present along with traces of monoclinic  $\text{Gd}_2(\text{MoO}_4)_3$ . Heating the product to 800 °C completed the transformation of the tetragonal phase to the monoclinic one (Figure 3.2). Further heating to 1000 °C produced the orthorhombic ferroelectric phase of  $\text{Gd}_2(\text{MoO}_4)_3$  (Figure 3.3).

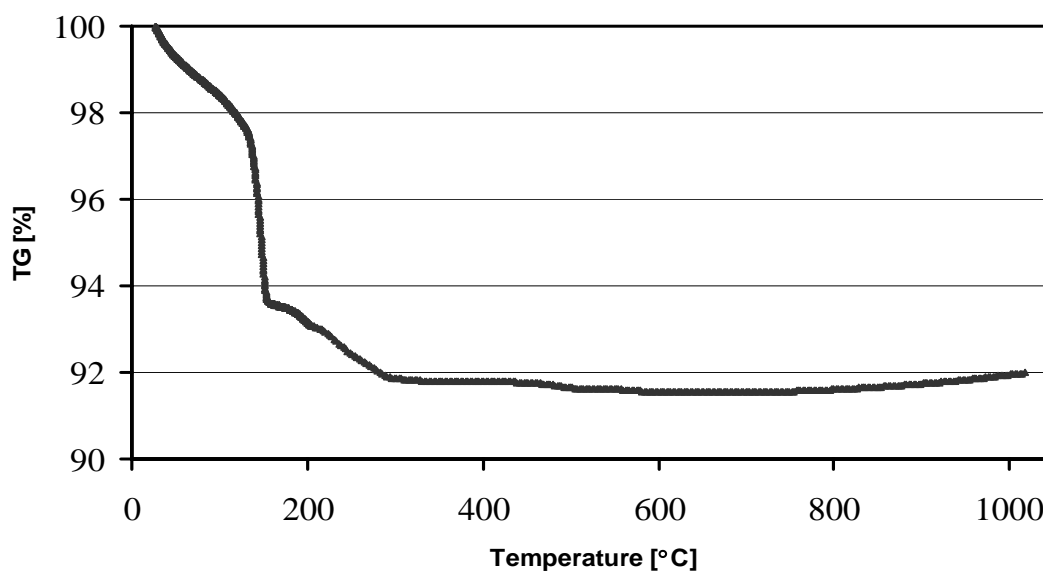


**Figure 3.1.** Thermal gravimetric analysis (TGA) of the product from gadolinium acetate and molybdenum trioxide.



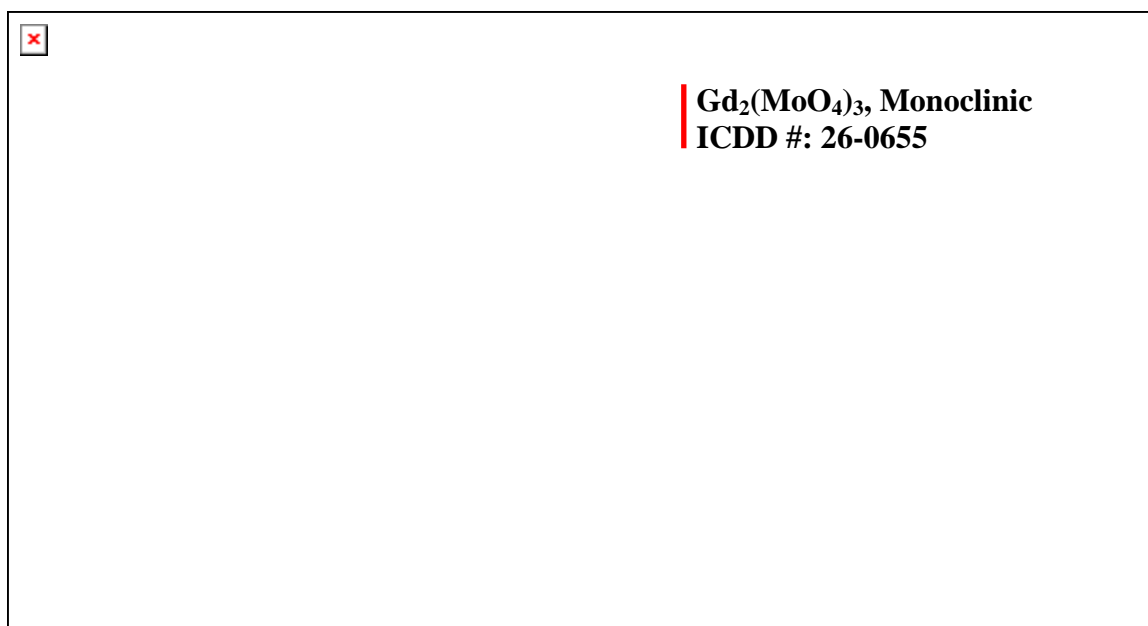
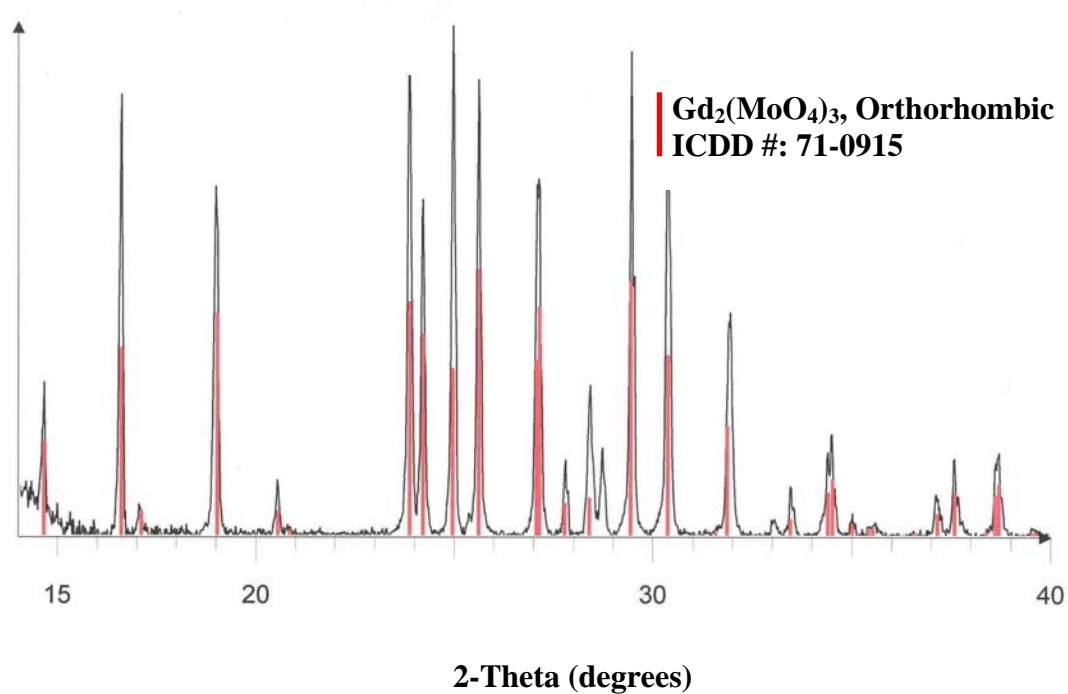


Figure 3.2. The XRD pattern of the product from gadolinium acetate and molybdenum trioxide heated to 800 °C.



**Figure 3.3.** The XRD pattern of the product from gadolinium acetate and molybdenum trioxide heated to 1000 °C.

### **Reaction of MoO<sub>3</sub> with lanthanum acetate**

The same technique used to synthesize gadolinium molybdate was applied to the synthesis of the fast ion conductor lanthanum molybdate. A mixture of a stoichiometric amount of molybdenum trioxide and a solution of lanthanum acetate in water was heated at reflux for seven days. After the lanthanum had been absorbed from the solution, a white solid was obtained, which was isolated by filtration and dried in a vacuum at room temperature. The results of the thermal gravimetric analysis are shown in Figure 3.4. The total weight loss was 19.3%, and it occurred in two steps up to 550 °C. The infrared spectrum of the product at room temperature (Figure 3.5, top) showed a broad peak at 879 cm<sup>-1</sup> which corresponds to molybdenum oxide stretches. The small and sharp peak shown at 1346 cm<sup>-1</sup> can be assigned to the C-O stretching frequency. The IR spectrum indicates the presence of the acetate group in the product. The evidence of having the acetate in the product is the three sharp peaks at 1423, 1466 and 1500 cm<sup>-1</sup>, which correspond to the symmetrical and asymmetrical carboxylate stretching. In addition, the presence of a sharp peak at 1650 cm<sup>-1</sup>, can also be assigned to the stretching vibration of carboxylate ions (COO<sup>-</sup>). There was also a broad peak at 3444 cm<sup>-1</sup> attributable to the O-H stretching of water. The infrared spectrum also shows the disappearance of the acetate peaks as the product was heated to 550 °C (Figure 3.5, bottom). There were only two major peaks to be seen, one broad signal at 879 cm<sup>-1</sup> which corresponds to the Mo-O stretching and a small broad one at 3443 cm<sup>-1</sup>.

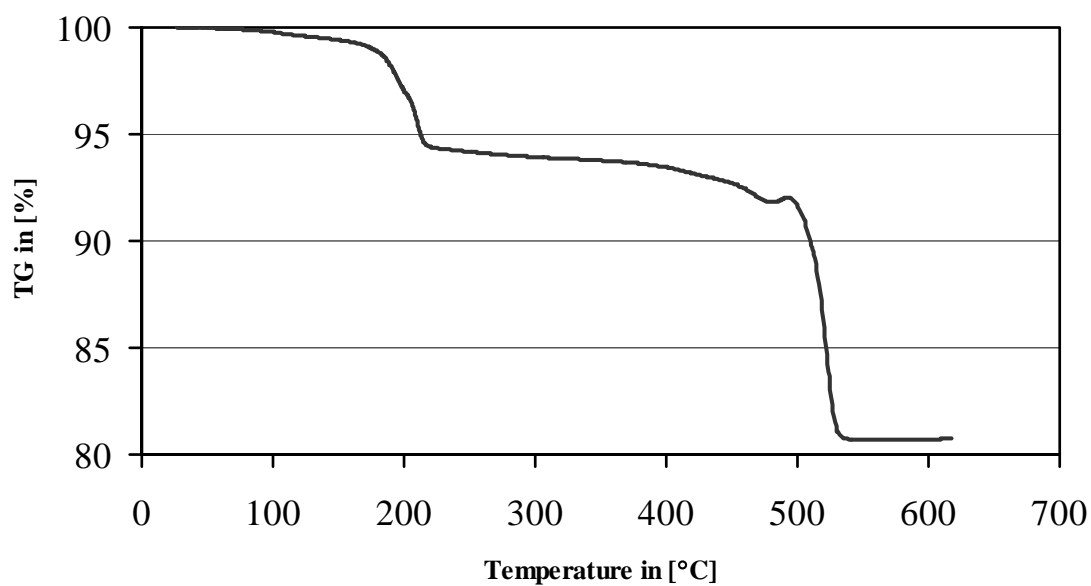


**Figure 3.4.** Thermal gravimetric analysis of the product from lanthanum acetate and  $\text{MoO}_3$ .

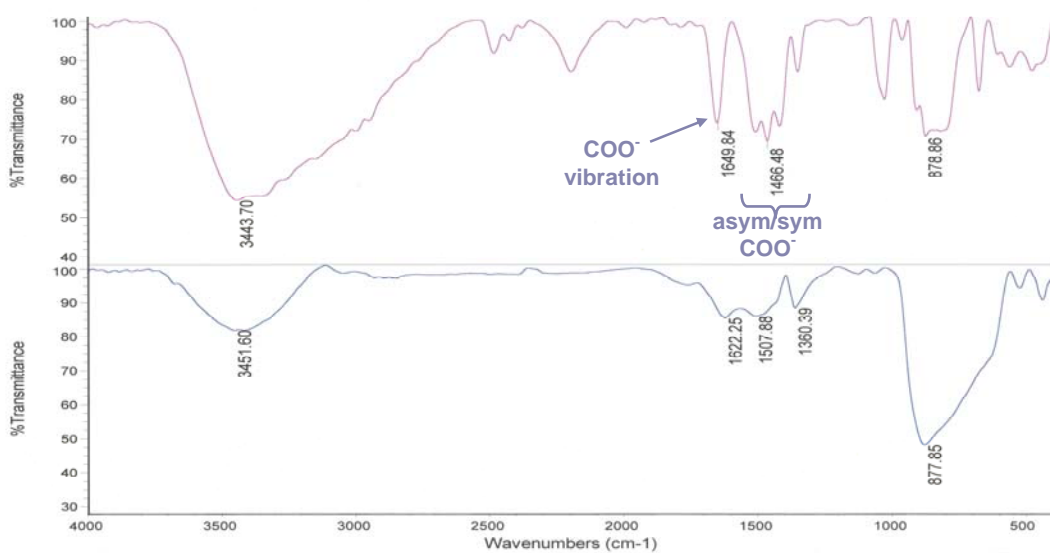


**Figure 3.5.** Infrared spectra of the product from  $\text{MoO}_3$  and lanthanum acetate at room temperature (top) and after heating to 550 °C (bottom).

The results from the infrared spectrum are in agreement with the thermal gravimetric analysis data, which explained the loss of weight at higher temperature. The

powder X-ray pattern of the product at room temperature showed a crystalline phase. However, no matching to a known phase was found. After heating to product to 550 °C, the X-ray patterns of the solid showed a matching with the cubic phase of lanthanum molybdenum oxide,  $\text{La}_2\text{Mo}_2\text{O}_9$  (Figure 3.6).

From the molecular weight of the lanthanum molybdate, the weight loss obtained by the thermal gravimetric analysis and the information from the infrared spectrum showing the presence of acetate at room temperature, the identity of the white solid at room temperature can be  $\text{La}_2\text{Mo}_2\text{O}_8(\text{CH}_3\text{CO}_2)_2 \cdot 2\text{H}_2\text{O}$ . The solid state carbon-13 NMR analyses showed two sets of peaks, one set at 191 ppm and 188.5 ppm, and the other one at 28.5 ppm and 25.6 ppm, implying the presence of two acetate groups (Figure 3.7). To our knowledge, this is the first synthesis of a mixed molybdate acetate salt. Fortunately, the product is obtained with the appropriate stoichiometry for a  $\text{La}_2\text{Mo}_2\text{O}_9$  precursor. The experimental yield was 98.3%, based on  $\text{MoO}_3$ . The reaction was performed two more time to check the reproducibility and the same results were obtained.

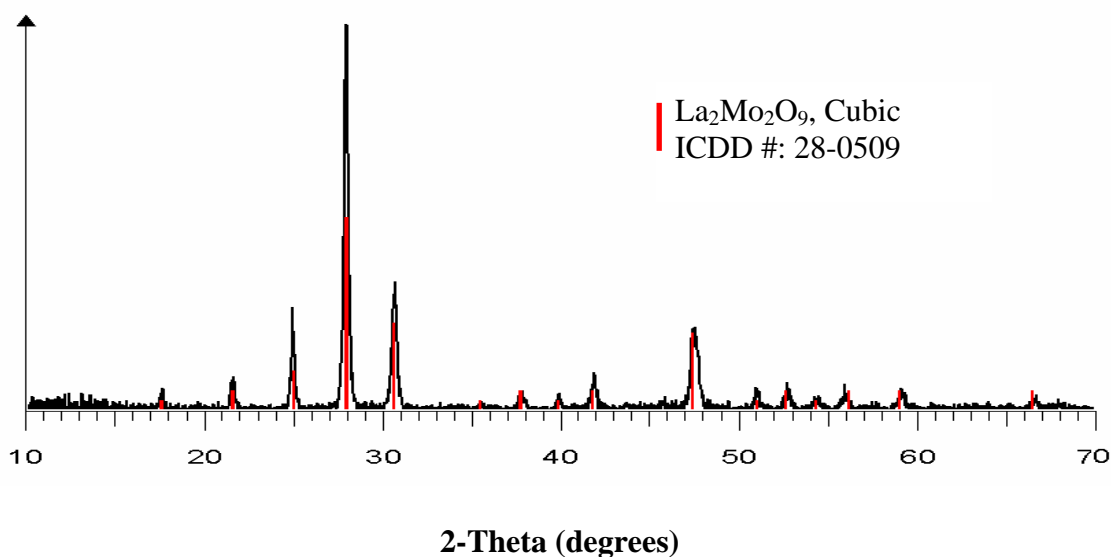


**Figure 3.6.** The XRD pattern of the product from  $\text{MoO}_3$  and lanthanum acetate heated to 550 °C.

The reaction with lanthanum acetate and molybdenum trioxide formed a mixed molybdate acetate salt at room temperature, while the reaction with gadolinium acetate with  $\text{MoO}_3$  formed a hydrated form of metal molybdate using different stoichiometry. To verify whether the mixed molybdate salt formed from lanthanum acetate was due to the lanthanum or to the stoichiometry of the metal salt, the reaction of gadolinium acetate with  $\text{MoO}_3$  on a 1.2 to 1 stoichiometry was carried out. In addition, the reactions of other lanthanides with  $\text{MoO}_3$  on a 1.2 to 1.0 stoichiometry were also explored. Only the reaction of cerium acetate with  $\text{MoO}_3$  produced the mixed metal oxide acetate. However, as  $\text{Ln}(\text{CH}_3\text{CO}_2)_3$  (where  $\text{Ln} = \text{Pr, Nd, Sm, Eu, Gd, Er, Lu}$ ) was reacted with  $\text{MoO}_3$ , the product obtained after reflux was a hydrous form of the lanthanide molybdate. The XRD pattern of the products and the infrared spectroscopy showed enormous similarities. From the thermal gravimetric data, the infrared spectroscopy and the powder X-ray pattern of the products, the structure formula can be written as  $\text{Ln}_4\text{Mo}_4\text{O}_{16}(\text{OH})_4(\text{H}_2\text{O})$ .

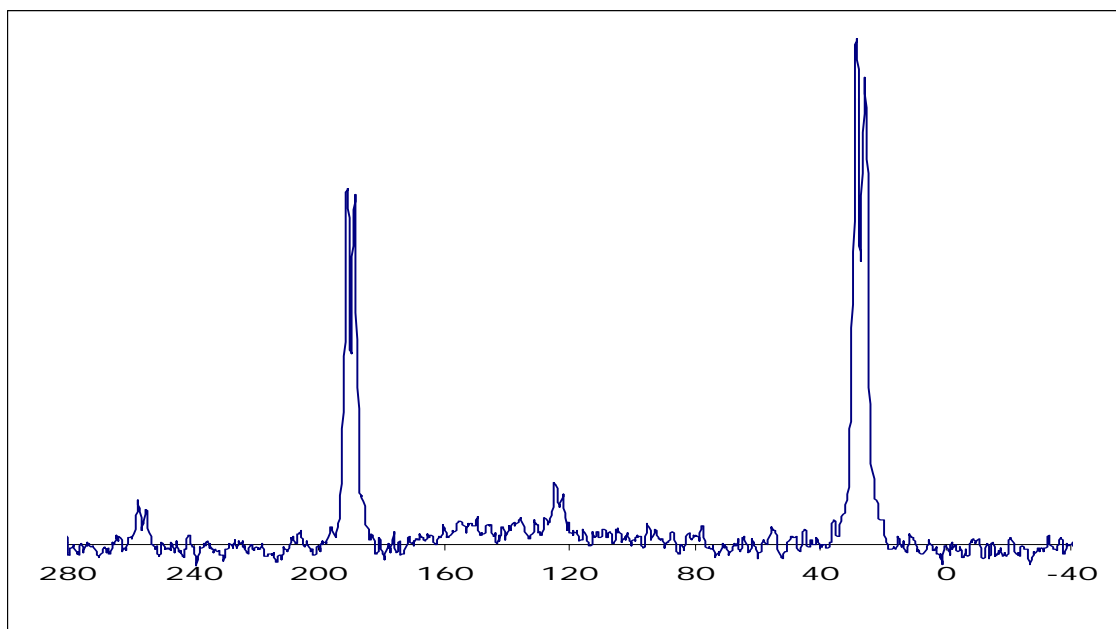


**Figure 3.7.** Carbon-13 NMR of the product from lanthanum acetate and  $\text{MoO}_3$ .

## CONCLUSIONS

The reaction of molybdenum trioxide with gadolinium acetate provides a convenient approach to the synthesis of ferroelectric gadolinium molybdate through a series of intermediates. At room temperature, a hydrous mixed metal oxide was formed that converted to the monoclinic  $\text{Gd}_2(\text{MoO}_4)_3$  at 800 °C which further transformed to the orthorhombic ferroelectric  $\text{Gd}_2(\text{MoO}_4)_3$  at 1000 °C. On the other hand, the reaction with lanthanum acetate with molybdenum trioxide yielded a mixed metal molybdate acetate that was converted to the cubic form of  $\text{La}_2\text{Mo}_2\text{O}_9$  (an oxide conductor) upon heating to 550 °C.

## REFERENCES

- [1] Xue, D.; Betzler, K.; Hesse, H.; Lammers, D. *Journal of Physics and Chemistry of Solids* **2002**, 63, 359-361.
- [2] Alexeyev, A. N.; Roshchupkin, D. V. *Applied Physics Letters* **1996**, 68, 159-60.
- [3] Petzelt, J.; Smutny, F.; Katkanant, V.; Ullman, F. G.; Hardy, J. R.; Volkov, A. A.; Kozlov, G. V.; Lebedev, S. P. *Physical Review B: Condensed Matter and Materials Physics* **1984**, 30, 5172-82.
- [4] Takashige, M.; Hamazaki, S.; Fukurai, N.; Shimizu, F.; Kojima, S. *Ferroelectrics* **1997**, 203, 221-225.
- [5] Kim, S. I.; Kim, J.; Kim, S. C.; Yun, S. I.; Kwon, T. Y. *Materials Letters* **1995**, 25, 195-8.
- [6] Nishioka, H.; Odajima, W.; Tateno, M.; Ueda, K.; Kaminskii, A. A.; Butashin, A. V.; Bagayev, S. N.; Pavlyuk, A. A. *Applied Physics Letters* **1997**, 70, 1366-1368.

- [7] Apblett, A. W.; Chehbouni, M.; Reinhardt, L. E. *Ceramic Transactions* **2006**, *174*, 39-46.
- [8] Vest, R. W. *Ceram. Films Coat.* **1993**, 303-47.
- [9] Mantese, J. V.; Micheli, A. L.; Hamdi, A. H.; Vest, R. W. *MRS Bulletin* **1989**, *14*, 48-53.
- [10] Goutenoire, F.; Isnard, O.; Retoux, R.; Lacorre, P. *Chemistry of Materials* **2000**, *12*, 2575-2580.
- [11] Collado, J. A.; Aranda, M. A. G.; Cabeza, A.; Olivera-Pastor, P.; Bruque, S. *Journal of Solid State Chemistry* **2002**, *167*, 80-85.
- [12] Fournier, J. P.; Fournier, J.; Kohlmuller, R. *Bulletin de la Societe Chimique de France* **1970**, 4277-83.
- [13] Goutenoire, F.; Isnard, O.; Suard, E.; Bohnke, O.; Laligant, Y.; Retoux, R.; Lacorre, P. *Journal of Materials Chemistry* **2001**, *11*, 119-124.
- [14] Lacorre, P.; Goutenoire, F.; Bohnke, O.; Retoux, R.; Laligant, Y. *Nature (London)* **2000**, *404*, 856-858.
- [15] Wang, X. P.; Fang, Q. F. *Solid State Ionics* **2002**, *146*, 185-193.
- [16] Minh, N. Q. *Proceedings - Electrochemical Society* **1995**, *95-1*, 138-45.
- [17] Kuang, W.; Fan, Y.; Yao, K.; Chen, Y. *Journal of Solid State Chemistry* **1998**, *140*, 354-360.
- [18] Marrero-Lopez, D.; Ruiz-Morales, J. C.; Perez-Coll, D.; Nunez, P.; Abrantes, J. C. C.; Frade, J. R. *Journal of Solid State Electrochemistry* **2004**, *8*, 638-643.

- [19] Marrero-Lopez, D.; Ruiz-Morales, J. C.; Nunez, P.; Abrantes, J. C. C.; Frade, J. R. *Journal of Solid State Chemistry* **2004**, *177*, 2378-2386.
- [20] Lacorre, P. *Solid State Sciences* **2000**, *2*, 755-758.
- [21] Arulraj, A.; Goutenoire, F.; Tabellout, M.; Bohnke, O.; Lacorre, P. *Chemistry of Materials* **2002**, *14*, 2492-2498.
- [22] Rocha, R. A.; Muccillo, E. N. S. *Chemistry of Materials* **2003**, *15*, 4268-4272.
- [23] Lacorre, P.; Retoux, R. *Journal of Solid State Chemistry* **1997**, *132*, 443-446.
- [24] Standards., J. C. o. P. D. *Powder Diffraction File: Inorganic Volume.*; JCPDS.: Swarthmore, PA. 1997
- [25] Walker, E. H.; Georgieva, G. D.; Holt, E. M.; Reinhardt, L. E.; Apblett, A. W. *Ceramic Transactions* **1999**, *100*, 87-94.
- [26] Huang, Q.; Xu, J.; Li, W. *Solid State Ionics* **1989**, *32-33*, 244-9.



## **CHAPTER IV**

### **SYNTHESIS, CHARACTERIZATION AND APPLICATIONS OF TRANSITION METAL MOLYBDATES**

#### **INTRODUCTION**

Mixed metal oxides play a significant role in many areas of chemistry, physics and material sciences.<sup>1</sup> The combination of two metals in an oxide can lead to the production of materials with superior performance in industrial applications. Molybdenum is known to form stable oxides in combination with a large series of metals.<sup>1-3</sup> Transition metal molybdates are an important class of compounds from both the fundamental and the technological point of view. First row transition metal molybdates, in particular, have been the topic of many investigations because of their structural, electronic, and catalytic properties.<sup>4,5</sup> Nickel and cobalt molybdates are widely used by industry as selective oxidation catalysts, in reactions that include the ammoxidation of propylene, the oxidation of 1-butene to maleic anhydride, the oxidative dehydrogenation of propane. They also serve as precursors in the synthesis of hydrodesulfurization (HDS) catalysts with the active catalyst being generated by sulfidation with  $\text{H}_2\text{S}$ .<sup>6-10</sup> A large number of papers and patents can be found in the literature regarding these applications. In addition, nickel molybdate catalysts are used in

other processes, such as the hydrodenitrogenation of petroleum distillates, the water-gas shift reaction, steam reforming, hydrogenolysis, cracking of n-butane, oxidative coupling of methane, and other useful hydrogenation and hydrotreating reactions.<sup>11,12</sup>  $\text{Fe}_2(\text{MoO}_4)_3$  is widely used for selective oxidation of methanol to formaldehyde and as the commercial Harshaw catalyst.<sup>13-15</sup> Transition metal molybdates have also been utilized as cathode materials for lithium rechargeable batteries.<sup>16</sup> Typically, mixed metal molybdates are used as “hosts” for lithium insertion. Another application of transition metal molybdates is as corrosion inhibitors due to their ability to protect both ferrous and nonferrous metals and their very low toxicity.<sup>17,18</sup> Molybdates are increasingly replacing the traditional more-toxic inhibitors, such as chromate, nitrate, phosphate and borate.<sup>18</sup> Recently, the US Navy has patented numerous molybdate pigments as corrosion inhibitive coating systems for steel and aluminum.<sup>19</sup>

Transition metal molybdates are conventionally prepared by solid state reactions of  $\text{MoO}_3$  and the corresponding transition metal oxides. However, deviation from the proper stoichiometry often occurs and leads to the formation of unwanted subphases. For instance, synthesis of  $\text{AMoO}_4$  (A = divalent transition metal) is often complicated by the formation of  $\text{A}_2\text{MoO}_5$  and other polymolybdates.<sup>20,21</sup> In addition, during the high temperature treatment, the localized nonstoichiometry may still exist due to the difference in original particle sizes and inhomogeneity of the transition metal oxides and  $\text{MoO}_3$  powders. The precipitation reactions between aqueous sodium molybdate and aqueous transition metal salts lead to the formation of sodium metal molybdates as undesired phases.<sup>22</sup> Precipitation by treatment of aqueous solutions of  $\text{A}^{2+}$  salts with ammonium

heptamolybdate leads to the formation of hydrated precursors of general formula  $\text{AMoO}_4 \cdot n\text{H}_2\text{O}$ .<sup>6</sup>

The objective of the present work is to explore the effectiveness of molybdenum trioxide to provide an alternative method for synthesis of metal molybdates using environmental friendly techniques where water is the solvent, and to apply similar reactions to removal of heavy metals from water.

## **EXPERIMENTAL**

All reagents were commercial products purchased from Aldrich or Strem Chemicals and were used without further purification. Thermogravimetric analyses were performed using a Seiko EXSTAR 6500 TG/DTA 6200 instrument under flowing of air (100 ml/min). Infrared spectra were collected using a Nicolet Magna-IR 750 spectrometer, and the data were collected by diffuse reflectance of a ground powder diluted with potassium bromide. The X-ray powder diffraction patterns were obtained using a Bruker AXS D8 advance diffractometer with copper  $\text{K}\alpha$  radiation with a wavelength of 1.5418 Å. All of the XRD patterns were collected at ambient temperature, and the crystalline phases were identified using the search/match PDF-2 database of the International Center of Diffraction Data (ICDD).<sup>23</sup>

### **Reaction of molybdenum trioxide with transition metal acetates**

The  $\text{MoO}_3$  (2.16 g, 12.0 mmol) was added to a stoichiometric solution of the corresponding transition metal acetate (10.0 mmol) in water (100 ml). The mixture was heated at reflux for 72 hours. Upon cooling, a solid was isolated by filtration through a

fine sintered-glass filter. After drying in vacuum at room temperature, the yield of the corresponding metal molybdates was calculated based on  $\text{MoO}_3$ . Infrared spectra (DRIFTS, solid diluted in KBr), X-ray powder diffraction, and thermal gravimetric analysis of the products from molybdenum oxide and the corresponding transition metal acetate were recorded. The same procedure using the same stoichiometry was applied to trivalent transition metals.

In the case of cadmium acetate, the white product obtained was identified by the X-ray diffraction powder as a phase pure cadmium molybdate ( $\text{CdMoO}_4$ , ICDD #: 07-0209). The weight of the isolated product was 2.63 g corresponding to a 96.5 % yield. On the other hand, the reaction of cadmium nitrate with  $\text{MoO}_3$  did not produce the desired cadmium molybdate. The XRD pattern of the product showed only matching with the molybdenum trioxide starting material. The effect of the metal salt and the pH on the formation of metal molybdate will be discussed in chapter 5.

## **RESULTS AND DISCUSSION**

### **Reaction of molybdenum trioxide with manganese acetate**

The light brown product obtained from the reaction of manganese (II) acetate and  $\text{MoO}_3$  was identified by the X-ray powder diffraction as the triclinic phase of manganese molybdenum oxide monohydrate,  $\text{MnMoO}_4 \cdot \text{H}_2\text{O}$  (ICDD #: 78-0220, Figure 4.1, bottom). The structure consists of molybdate tetrahedra and Mn (II) octahedra where the tetrahedron shares four corners with four different octahedra.<sup>4</sup> The water molecule is coordinated to the manganese. The oxidation state of the manganese in the manganese molybdate product is + 2. The weight of the product was 2.2 g, which correspond to a

94.5% yield based on  $\text{MoO}_3$ . Furthermore, the result from the thermal gravimetric analysis showed a weight loss of 7.53% at 350 °C, which corresponds to the loss of one water molecule. Heating the hydrate to 350 °C yielded anhydrous  $\text{MnMoO}_4$ .  $\text{MnMoO}_4 \cdot \text{H}_2\text{O}$  was also obtained when manganese (III) acetate (12.0 mmol) was reacted with  $\text{MoO}_3$  (10.0 mmol) reflecting the instability of aqueous  $\text{Mn}^{3+}$  (Figure 4.1, top).

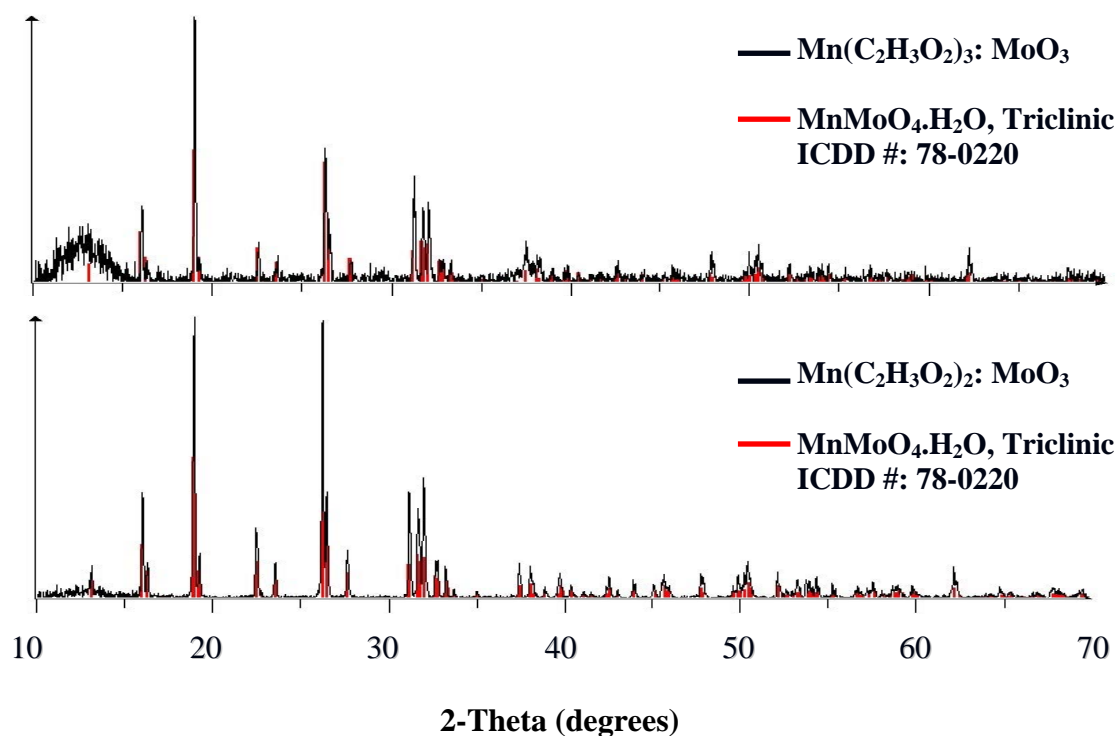


**Figure 4.1.** The XRD pattern of the product from manganese (II) acetate (bottom) and manganese (III) acetate (top) with  $\text{MoO}_3$ .

However, the intensity of the X-ray reflections from the Mn (III)-derived powder was significantly lower than of the Mn (II) product. This suggests that an amorphous Mn(III) compound may be present. The color of the solid from manganese III acetate was dark brown, while that of Mn (II) product was light brown. Also the yield of the solid in the Mn (III) reaction was only 1.34 g. which corresponds to 57.5% based on  $\text{MoO}_3$ . The infrared spectra of both products (Figure 4.2) showed a band around 1620

$\text{cm}^{-1}$  which corresponds to the water bend. There are a number of intense adsorption bands in the region between  $700\text{ cm}^{-1}$  and  $940\text{ cm}^{-1}$ . The bands near  $850\text{ cm}^{-1}$  and  $940\text{ cm}^{-1}$  represent asymmetric and symmetric  $\text{MoO}_4$  stretching, while the rest should result from the octahedral  $\text{MnO}_6$  groups.<sup>24,25</sup> The manganese III derived product has stronger bands due to Mn-O stretching vibrations.

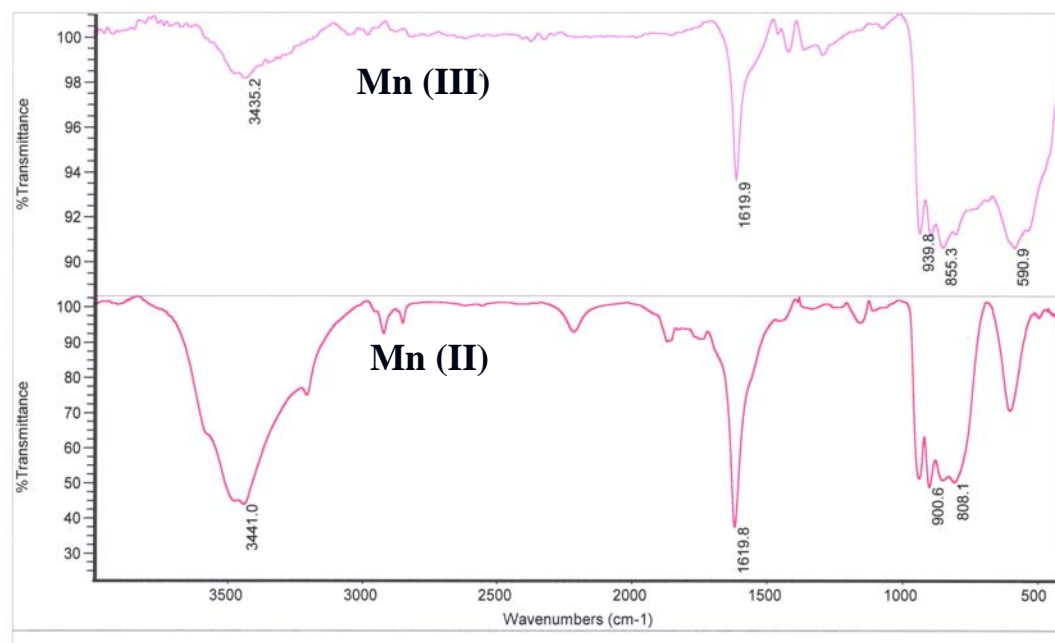


**Figure 4.2.** Infrared spectra of the products from  $\text{MoO}_3$  with the manganese (II) acetate (bottom) and manganese (III) acetate (top) respectively.

The formation of  $\text{MnMoO}_4 \cdot \text{H}_2\text{O}$  in the Mn III reaction is likely due to the disproportionation of manganese (III) to manganese (II) and (IV). The manganese (II) forms the crystalline phase of manganese molybdenum oxide while the manganese (IV) oxide is amorphous. The difference in color of the two products and the low yield of the solid in the manganese (III) reaction support this theory. The thermal gravimetric

analysis of the product from manganese (III) and  $\text{MoO}_3$  showed water content of 12.9 % at 350 °C.

### Reaction of molybdenum trioxide with iron salts

Iron (III) nitrate was reacted with 1.5 molar equivalents molybdenum trioxide to form the monoclinic phase of iron (III) molybdate  $[\text{Fe}_2(\text{MoO}_4)_3]$  identified by the powder X-ray diffraction (Figure 4.3, top). The same product was obtained by the reaction of iron (II) acetate with  $\text{MoO}_3$  (Figure 4.3., bottom).

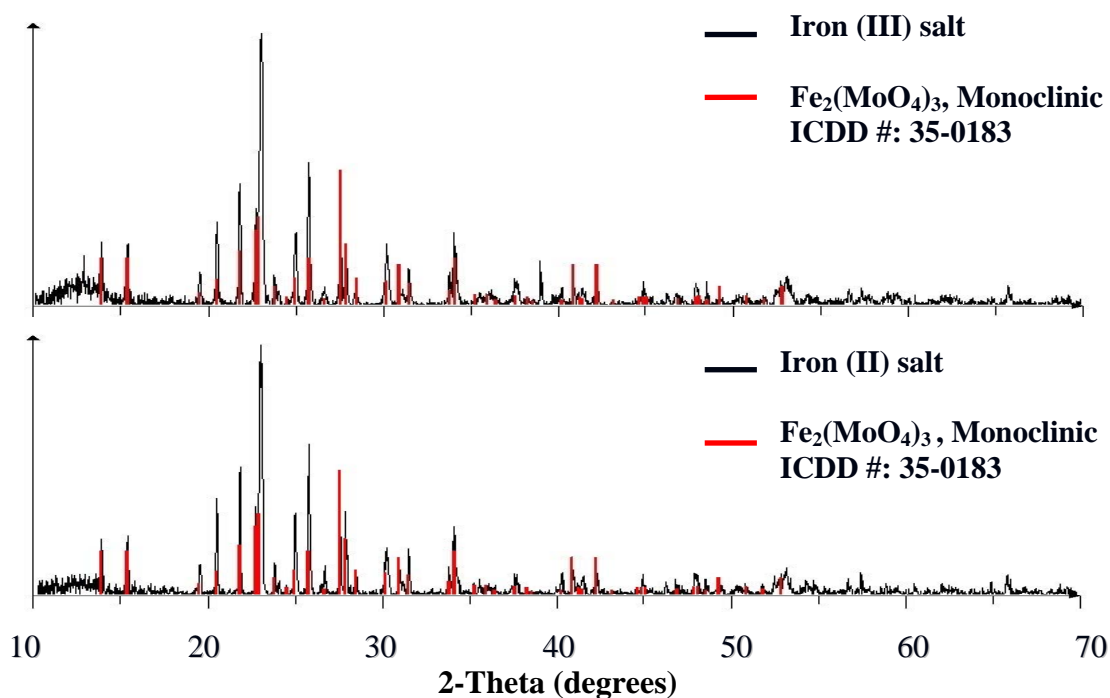


**Figure 4.3.** The XRD pattern of the product from iron (II) acetate (bottom) and iron (III) acetate (top) with  $\text{MoO}_3$ .

Ferrous ions are very prone to oxidation by oxygen in aqueous solutions.<sup>6</sup> This explains the formation of iron (III) molybdate from iron (II) salt. In fact, it was

previously reported that iron (II) molybdate could be prepared under an inert gas atmosphere to prevent the oxidative decomposition of  $\text{FeMoO}_4$  to  $\text{Fe}_2(\text{MoO}_4)_3$ .<sup>26</sup>

### **Synthesis of hydrated metal molybdates**

Hydrated metal molybdates with the form  $\text{AMoO}_4 \cdot n\text{H}_2\text{O}$  (where A = Co, Ni, Cu, and n = the degree of hydration) were synthesized from reactions of their metal salts with molybdenum trioxide. In the case of cobalt, the XRD pattern of the product from cobalt acetate and  $\text{MoO}_3$  did not give any matching to a known phase (Figure 4.4). No XRD data seem to be available in the literature for the hydrated cobalt molybdate. The thermal gravimetric analysis of the product showed a loss of weight of 6.1% at 350 °C. The powder X-ray diffraction of the solid product heated to 350 °C showed the formation of the monoclinic phase of cobalt molybdate,  $\text{CoMoO}_4$  (ICDD #: 21-0868, Figure 4.5). From the thermal gravimetric analysis and the X-ray data, the 6.1% weight loss would correspond to a hydration of n = 0.8. Thus, the likely formula of the product from cobalt acetate and  $\text{MoO}_3$  would be  $\text{CoMoO}_4 \cdot 0.8 \text{H}_2\text{O}$ . The yield of the brown product was 95.9% based on  $\text{MoO}_3$ . The infrared spectra of the product from cobalt acetate and  $\text{MoO}_3$  heated to 350 °C revealed two sharp peaks at 743  $\text{cm}^{-1}$  and 958  $\text{cm}^{-1}$  which correspond to the  $\text{MoO}_4$  tetrahedra (a useful precursor for the hydrosulfurization (HDS) catalysts).<sup>6</sup>



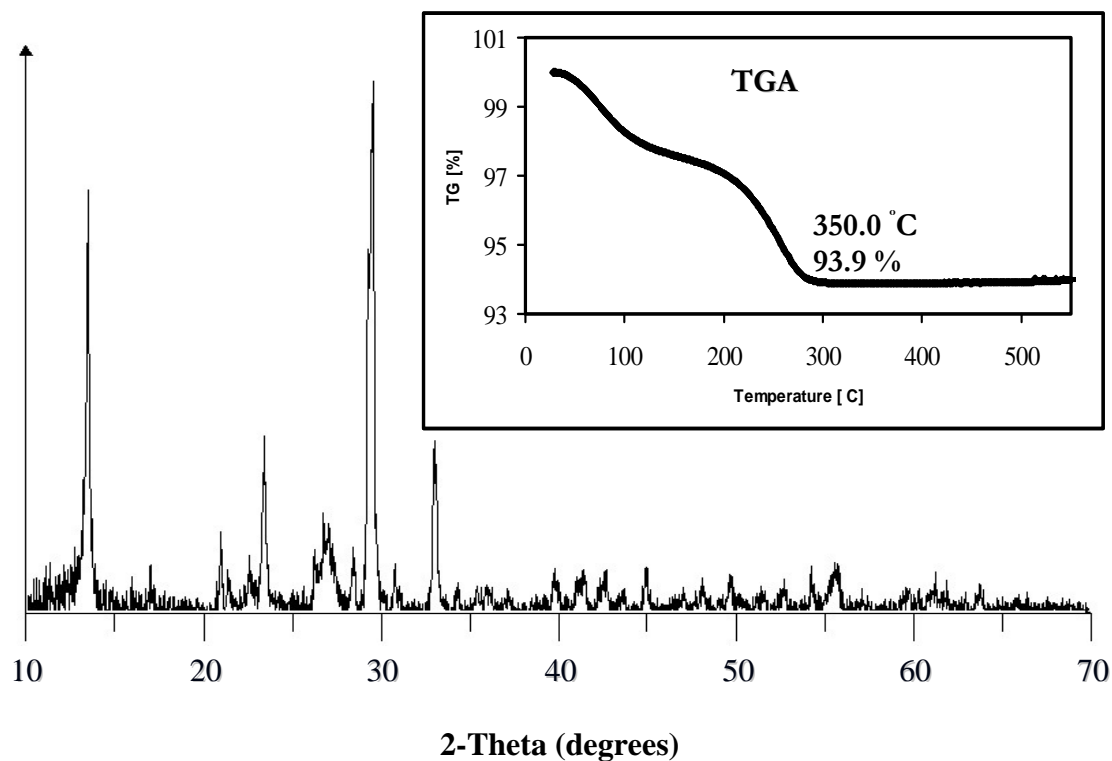


**Figure 4.4.** The XRD pattern and the thermal gravimetric analysis (TGA) of the product from cobalt acetate and  $\text{MoO}_3$ .

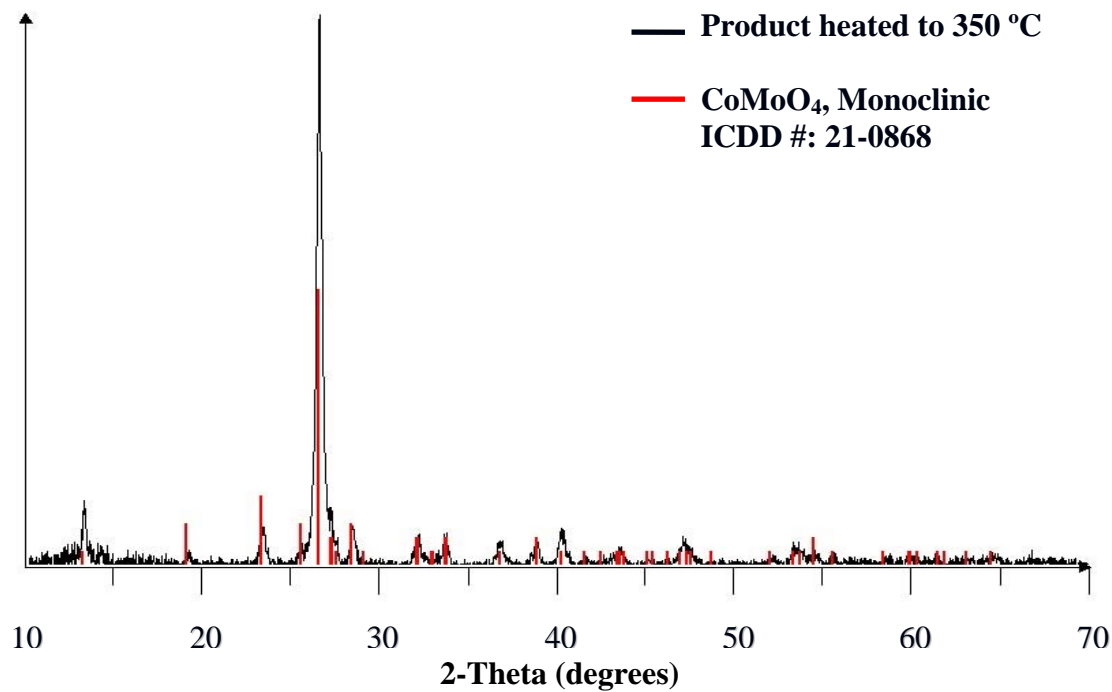


**Figure 4.5.** The XRD pattern of the product from cobalt acetate and molybdenum trioxide heated to 350 °C.

In the case of nickel, the solid product from nickel acetate and  $\text{MoO}_3$  at room temperature showed a higher hydration ( $n = 1.2$ ) as compared to cobalt. The value of the hydration was calculated using the data from the thermal gravimetric analysis which showed a loss of weight of 9.1% at 500 °C and from the X-ray powder diffraction (taken at 500 °C) which identified the product as the monoclinic phase of  $\text{NiMoO}_4$  (Figure 4.6). The yield of the solid product was 96.6% based on  $\text{MoO}_3$ . Moreover, two strong peaks characteristics of  $\text{MoO}_4$  tetrahedra at  $606\text{ cm}^{-1}$  and  $969\text{ cm}^{-1}$  were observed in the infrared spectra of the product produced by heating to 500 °C (Figure 4.7). The  $\beta$ -phases of Ni and Co are isostructural with Mo present in tetrahedral coordination and the second metal in octahedral coordination.<sup>6</sup>

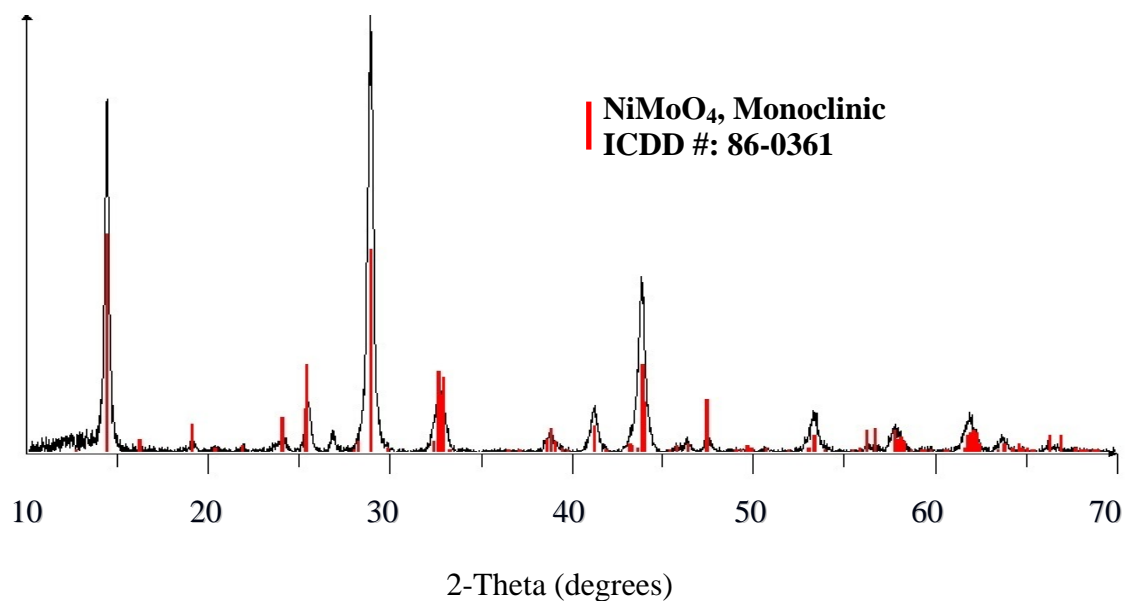


**Figure 4.6.** The XRD pattern of the product from nickel acetate and molybdenum trioxide heated to 500 °C.

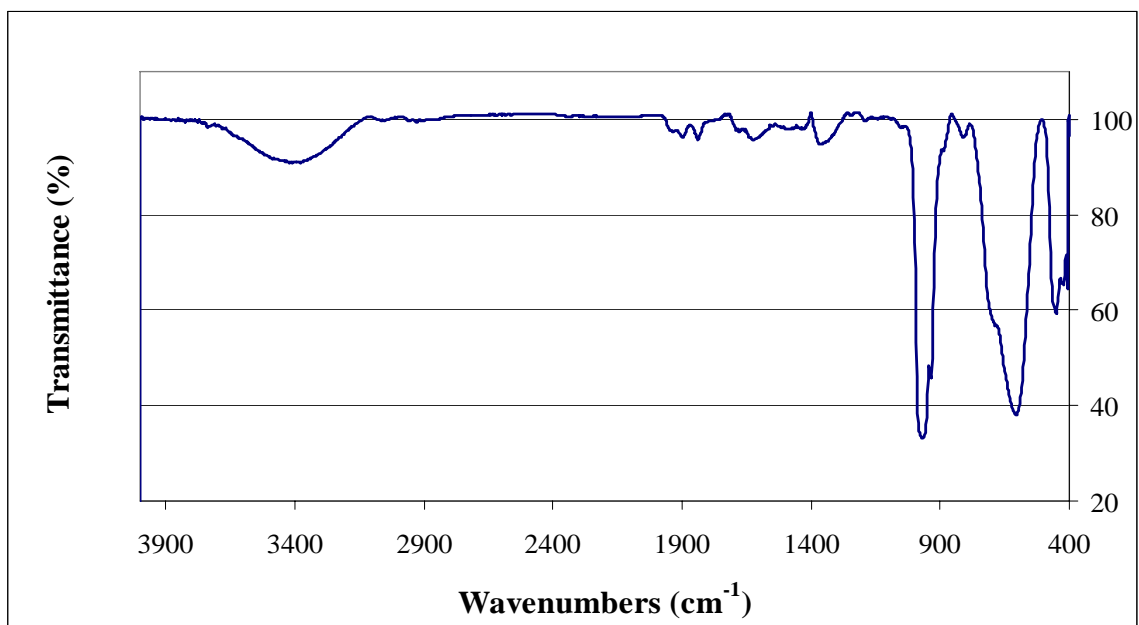


**Figure 4.7.** The infrared spectrometer of the product from nickel acetate and  $\text{MoO}_3$  after heating to 500 °C.

The reaction of copper (II) acetate and  $\text{MoO}_3$  formed a green solid, identified by the X-ray powder diffraction as the mineral lindgrenite,  $\text{Cu}_3(\text{MoO}_4)_2(\text{OH})_2$  (ICDD#: 36-0405, Figure 4.8). It is a hydroxyl copper molybdate found in Chuquicamata, Chile. The structure consists of Cu  $\text{O}_6$  octahedra ( $\text{O} = \text{O}$  or  $\text{OH}$ ) which share edges with  $\text{MoO}_4$  tetrahedra.<sup>27</sup>

In order to apply the reflux method in removing heavy metals from water, the same stoichiometric mixture of molybdenum trioxide (10.0 mmol) and the corresponding metal acetate (12.0 mmol) was used, and the mixture was stirred at room temperature for 7 days. The same products obtained by reflux were also formed using the above method. This implies that molybdenum trioxide is able not only to form useful metal molybdates, but also to remove heavy metals from water.

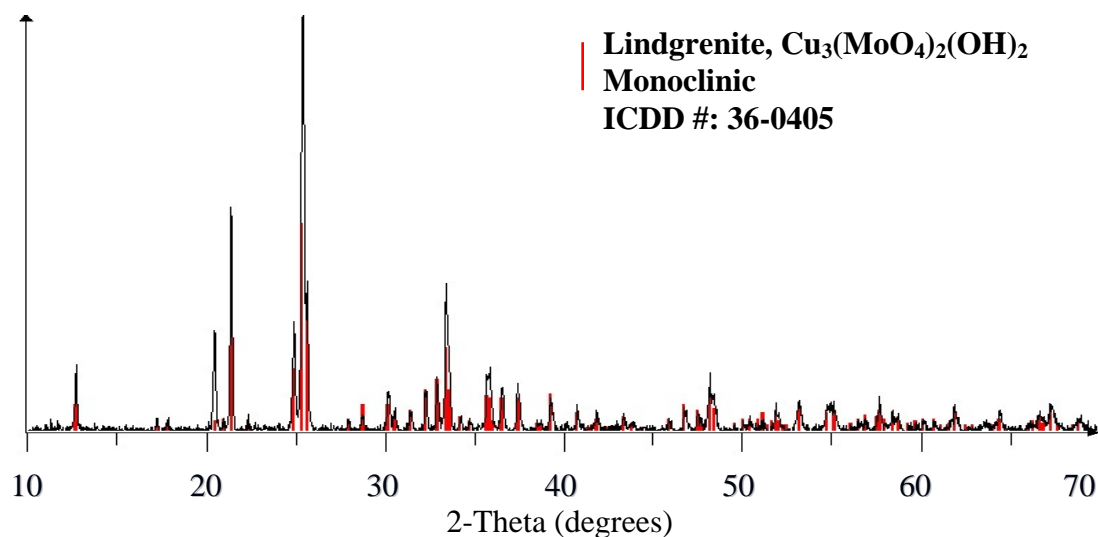


**Figure 4.8.** The XRD pattern of the product from copper (II) acetate and  $\text{MoO}_3$ .

## CONCLUSIONS

It has been shown that  $\text{MoO}_3$  is a very valuable reagent for the synthesis of transition metal molybdates. The reaction involves reflux of a stoichiometric ratio of molybdenum trioxide with the corresponding transition metal salts. The product obtained was the hydrated form of the transition metal molybdates. After heating the solids to higher temperature, the dehydrated form of the metal molybdates was obtained. The synthesis of the metal molybdates was also achieved by stirring the metal salts dissolved in water with  $\text{MoO}_3$ , implying the potential of heavy metal remediation using this method.

## REFERENCES

- [1] Rodriguez, J. A.; Hanson, J. C.; Chaturvedi, S.; Maiti, A.; Brito, J. L. *Journal of Chemical Physics* **2000**, *112*, 935-945.
- [2] Wyckoff, R. W. G. *Crystal Structures*; 2<sup>nd</sup> ed.; Interscience Publishers: New York, 1963.
- [3] Wells, A. F. *Structural Inorganic Chemistry*; 5th ed.; Clarendon Press: Oxford University Press: Oxford [Oxfordshire], New York, 1984.
- [4] Clearfield, A.; Moini, A.; Rudolf, P. R. *Inorganic Chemistry* **1985**, *24*, 4606-9.
- [5] Van Uitert, L. G.; Sherwood, R. C.; Williams, H. J.; Rubin, J. J.; Bonner, W. A. *Physics and Chemistry of Solids* **1964**, *25*, 1447-51.
- [6] Brito, J. L.; Barbosa, A. L. *Journal of Catalysis* **1997**, *171*, 467-475.
- [7] Mazzocchia, C.; Aboumrad, C.; Diagne, C.; Tempesti, E.; Herrmann, J. M.; Thomas, G. *Catalysis Letters* **1991**, *10*, 181-91.
- [8] Zou, J.; Schrader, G. L. *Journal of Catalysis* **1996**, *161*, 667-686.
- [9] Yoon, Y. S.; Ueda, W.; Moro-oka, Y. *Topics in Catalysis* **1996**, *3*, 265-275.
- [10] Madeley, R. A.; Wanke, S. E. *Applied Catalysis* **1988**, *39*, 295-314.
- [11] Li, J. L.; Dai, W. L.; Dong, Y.; Deng, J. F. *Materials Letters* **2000**, *44*, 233-236.

- [12] Madeira, L. M.; Portela, M. F.; Mazzocchia, C. *Catalysis Reviews - Science and Engineering* **2004**, 46, 53-110.
- [13] Kim, T. H.; Ramachandra, B.; Choi, J. S.; Saidutta, M. B.; Choo, K. Y.; Song, S.-D.; Rhee, Y.-W. *Catalysis Letters* **2004**, 98, 161-165.
- [14] Roy, A.; Ghose, J. *Journal of Solid State Chemistry* **1998**, 140, 56-61.
- [15] Soares, A. P. V.; Portela, M. F. *Catalysis Reviews - Science and Engineering* **2005**, 47, 125-174.
- [16] Leyzerovich, N. N.; Bramnik, K. G.; Buhrmester, T.; Ehrenberg, H.; Fuess, H. *Journal of Power Sources* **2004**, 127, 76-84.
- [17] Foley, R. T. *Corrosion (Houston, TX, United States)* **1964**, 20, 267t-268t.
- [18] Vukasovich, M. S.; Farr, J. P. G. *Polyhedron* **1986**, 5, 551-9.
- [19] Simpson, C. *ACS Symposium Series* **1998**, 689, 356-365.
- [20] Machida, N.; Chusho, M.; Minami, T. *Journal of Non-Crystalline Solids* **1988**, 101, 70-4.
- [21] Znasik, P.; Jamnicky, M. *Journal of Non-Crystalline Solids* **1992**, 146, 74-80.
- [22] Clearfield, A.; Gopal, R.; Saldarriaga-Molina, C. H. *Inorganic Chemistry* **1977**, 16, 628-31.

- [23] Standards., J. C. O. P. D. *Powder Diffraction File: Inorganic Volume.*; JCPDS.: Swarthmore, Pa.
- [24] Nakamoto, K. *Infrared Spectra of Inorganic and Coordination Compounds. 2nd ed*, Wiley: New York, 1970.
- [25] Saleem, S. S.; Aruldas, G.; Bist, H. D. *Journal of Solid State Chemistry* **1983**, 48, 77-85.
- [26] Trifiro, F.; DeVecchi, V.; Pasquon, I. *Journal of Catalysis* **1969**, 15, 8-16.
- [27] Hawthorne, F. C.; Eby, R. K. *Neues Jahrbuch fuer Mineralogie, Monatshefte* **1985**, 234-40.

## CHAPTER V

### REACTION OF ALKALINE EARTH METAL SALTS WITH MOLYBDENUM TRIOXIDE

#### INTRODUCTION

Alkaline earth molybdates in the form  $\text{AMoO}_4$  (where  $A = \text{Ca, Sr, and Ba}$ ) have recently attracted great attention due to their significant usage in electro-optics, microwave ceramics, and their interesting luminescence, and structural properties.<sup>1,2</sup> Furthermore,  $\text{AMoO}_4$  single crystals are promising host materials for the incorporation of optically active hexavalent ions, such as  $\text{Mn}^{+6}$ , in tetrahedral oxo-coordination.<sup>3</sup> Molybdates in combination with cations with large ionic radii, such as the alkaline earth metals (except the magnesium), adopt the scheelite type structure ( $\text{CaWO}_4$ ).<sup>4</sup> In the scheelite structure, the alkaline earth metal cations are each surrounded with eight oxygen atoms in the form of a bisdiphenoid polyhedron, whereas, the molybdenum ions are surrounded by four oxygen atoms forming a tetrahedral unit.<sup>5-7</sup> The structure can be regarded as a cubic closed packed arrangement of  $\text{A}^{2+}$  and  $\text{MoO}_4^{2-}$  ions. The oxygens are coordinated to two  $A$  cations and one  $\text{Mo}$  cation.<sup>6</sup> A typical three dimensional representation of  $\text{AMoO}_4$  unit cell is shown in Figure 5.1 (where  $A = \text{Ca}$  in this case).



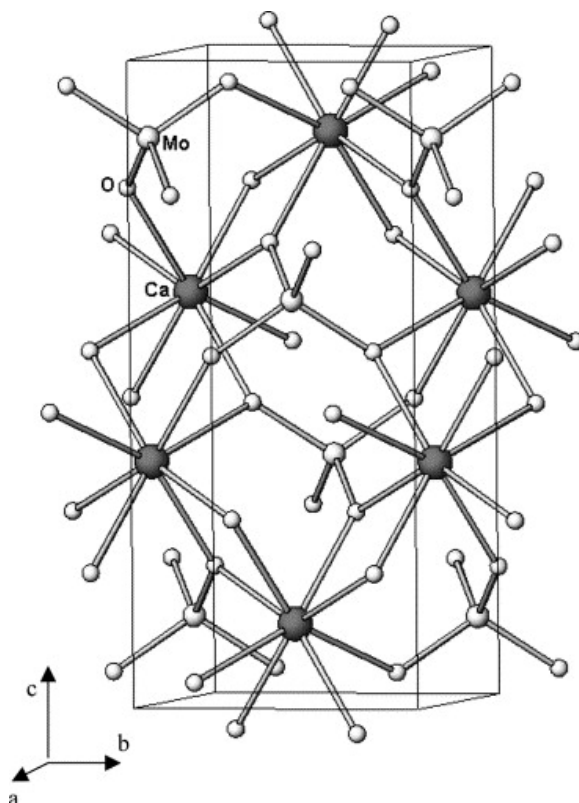


**Figure 5.1.** Crystal structure of  $\text{CaMoO}_4$  at room temperature (25 °C).<sup>4</sup>

Powellite, (calcium molybdate,  $\text{CaMoO}_4$ ) is an important industrial product used as an additive to steel and for the smelting of ferromolybdenum.<sup>8</sup> The reason for its use is the fact that calcium molybdate is cheaper than ferromolybdenum. In the latter application, smelting of steel, calcium molybdate is reduced by iron, and molybdenum is alloyed with steel to form a solid solution, whereas calcium oxide remains in the slag.<sup>9,10</sup> In addition,  $\text{CaMoO}_4$  has been of practical interest due to its attractive luminescence properties.<sup>11,12</sup> Crystals of  $\text{CaMoO}_4$  have been proposed as a potential dispersive elements in electronically tunable lasers serving as an acousto-optic filter and as an efficient mixed electron-hole ion conductor.<sup>13,14</sup> Powellite is a naturally occurring

mineral which can also be made synthetically. The molybdates of calcium and strontium are also used as corrosion-inhibiting paint pigments.<sup>15</sup>

Most previous approaches for the preparation of  $\text{AMoO}_4$  powders require high temperatures and harsh reaction conditions.<sup>16</sup> An example is the Czochralski method. This technique has significant problems related to oxygen stoichiometry, crack formation, inadequate starting materials, and crucible corrosion.<sup>17,18</sup> Alternatively, different techniques, such as the conventional solid state high temperature (heat and beat) reaction, the hydrothermal method, and the co-precipitation method have also been used to synthesize alkaline earth metal molybdates.<sup>1,19-21</sup> However,  $\text{AMoO}_4$  powders prepared by these processes have relatively large grain size and inhomogeneous morphology and composition.<sup>16</sup> In addition, the chemical vapor depositions and physical vapor depositions methods used for alkaline earth molybdate synthesis have critical problems. These processes consume an enormous amount of energy and materials, which can hardly be recovered or recycled. As a result, they are regarded as environmental unfriendly.<sup>1</sup>

We report the successful, environmentally-friendly synthesis of alkaline earth molybdates directly from an aqueous solution of metal acetates and molybdenum trioxide. In addition, an investigation into the pH dependence of the formation of the molybdates using different metal salts was conducted.

## EXPERIMENTAL

All reagents were commercial products (ACS Reagent grade or higher) and were used without further purification. Bulk pyrolyses at various temperatures were performed in air in a digitally-controlled muffle furnace using approximately 1 g samples, a ramp of

10 °C/min, and a hold time for 4 hours. The X-ray powder diffraction (XRD) patterns were recorded on a Bruker AXS D-8 Advance X-ray powder diffractometer using copper  $K_{\alpha}$  radiation. Crystalline phases were identified using a search/match program and the PDF-2 database of the International Center for Diffraction Data. Scanning Electron Microscopy (SEM) photographs were recorded using a JEOL Scanning Electron Microscope. Colorimetry was performed with a Spectronic 200 digital spectrophotometer using 1 cm cylindrical cuvettes. The pH of the reaction was measured using a pH meter type with an ISFET electrode.

### **Reaction of $\text{MoO}_3$ with calcium salts**

In order to study the influence of the salt and the pH dependence on the synthesis of calcium molybdate products, the reactions of calcium acetate, calcium nitrate and calcium chloride with  $\text{MoO}_3$  were carried out in water. In addition, two different buffer solutions [2,2-bis(hydroxymethyl) -2,2'2''-nitrilotriethanol ( $\text{C}_8\text{H}_{19}\text{NO}_5$ )-HCl], and [sodium acetate (2M)-acetic acid ( $\text{CH}_3\text{CO}_2\text{Na}$ - $\text{CH}_3\text{CO}_2\text{H}$ )] were tested with the reaction of calcium nitrate and  $\text{MoO}_3$ . Consequently, 1.44 g of  $\text{MoO}_3$  (10.0 mmol) was added to a solution of calcium salt (12.0 mmol) in water (100 ml). The mixture was heated at reflux for 72 hours. Upon cooling, the solid obtained was isolated by filtration through a fine sintered glass filter and dried in vacuum at room temperature. The product gained for each reaction was then characterized using X-ray powder diffraction, and the infrared spectroscopy. The pH of the solution at the start and after completion was checked.

From the powder X-ray diffraction pattern and the infrared spectroscopy of the characterized products, only the reaction with calcium acetate produced the desired

calcium molybdate product. Hence, calcium acetate was selected as the calcium source to be used with two different buffer solutions. Thus, 5.23 g of 2,2-bis(hydroxymethyl)-2,2'2''-nitrilotriethanol ( $\text{C}_8\text{H}_{19}\text{NO}_5$ , 25.0 mmol) was dissolved in water (100 ml). Subsequently, HCl solution (80.0 ml, 0.1 N) was added to adjust the pH to the desired value ( $\sim 6.8$ ). Calcium nitrate (2.83 g, 12.0 mmol) was dissolved in this solution, and  $\text{MoO}_3$  (1.44 g, 10.0 mmol) was added. The mixture was heated at reflux for 72 hours. The same reaction was carried out using 100 ml of sodium acetate (2M)-acetic acid buffer solution.

### **Reaction of $\text{MoO}_3$ with strontium salts**

The reaction of strontium acetate with  $\text{MoO}_3$  was carried out using the same stoichiometry as in the case of calcium acetate. Hence,  $\text{MoO}_3$  (1.44 g, 10.0 mmol) was added to a strontium acetate solution (2.47 g, 12 mmol) in water (100 ml). Then 2.44 g of white solid was gained after the product was filtrated and dried in vacuum overnight at room temperature. The powder X-ray diffraction of the solid showed a match with the tetragonal phase of strontium molybdenum oxide ( $\text{SrMoO}_4$ , ICDD #: 08-0482) (Figure 5.7). Additionally, Figure 5.8 shows the infrared spectrum of the white product. The pH of the reaction at the start was 5.90 and 3.59 after completion. In addition, the reaction of strontium nitrate with  $\text{MoO}_3$  was also carried out using the same stoichiometry and the product obtained was characterized.

### Reaction of MoO<sub>3</sub> with barium acetate

In a similar approach, the reaction of barium acetate with MoO<sub>3</sub> was carried out under reflux for 72 hours. Consequently, barium acetate (3.05 g, 12.0 mmol) was reacted with MoO<sub>3</sub> (1.44 g, 10.0 mmol) in water (100 ml). The pH of the solution at the start was 5.80, whereas the pH after filtration of the product was 3.65. The weight of the white product obtained after reflux was 2.93 g. The powder X-ray diffraction of the product indicated the formation of the tetragonal phase of barium molybdenum oxide (BaMoO<sub>4</sub>, ICDD # 21-0193) (Figure 5.9). In contrast, the reaction with barium nitrate and MoO<sub>3</sub> did not produce the barium molybdate product. The pH of both at the start and after completion of the reaction were measured.

## RESULTS AND DISCUSSION

The X-ray powder diffraction of the solid obtained by the reaction of calcium acetate and MoO<sub>3</sub> at reflux for 72 hours showed the formation of the phase-pure tetragonal calcium molybdate (CaMoO<sub>4</sub>, ICDD #: 22-0351) (Figure 5.2). The weight of the product was 2.0 grams which corresponded to a yield of 100 % based on MoO<sub>3</sub>, implying that the reaction went to completion. The infrared spectrum of the product on Figure 5.3 displayed a very broad adsorption band at 860 cm<sup>-1</sup>. This band has been reported to correspond to Mo-O stretching vibration in the MoO<sub>4</sub><sup>2-</sup> (tetrahedron).<sup>22,23</sup> The absence of the MoO<sub>3</sub> peaks in the spectrum are in agreement with the XRD data and confirmed the purity of the powellite mineral produced. However, the absorption band around 3400 cm<sup>-1</sup> is probably due to water molecules absorbed from air by the sample since the characterization was performed at room temperature. The pH of the mixture at

the start of the reaction was 5.46. After completion of the reaction, the pH of the filtrate, checked after filtration of the solid product, was 3.80. The decrease in the pH during the reaction is due to protons released as water molecules are converted to oxide. The pH decrease was not as large as predicted by stoichiometry due to buffering by acetate ions.

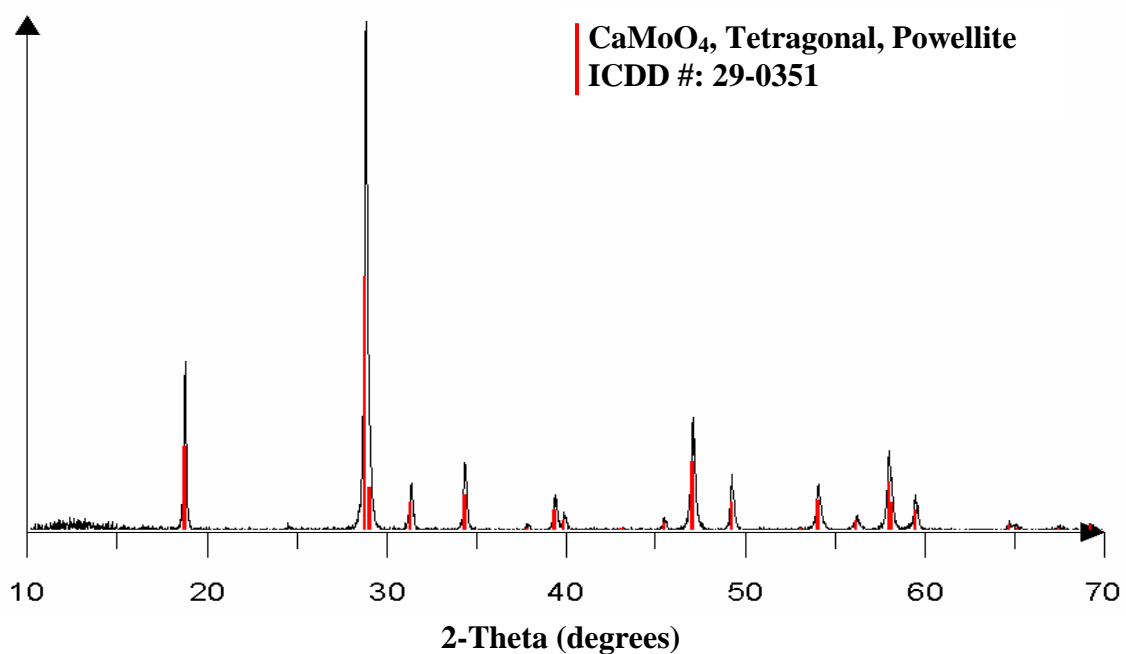


**Figure 5.2.** The XRD pattern of the product from calcium acetate and MoO<sub>3</sub>.

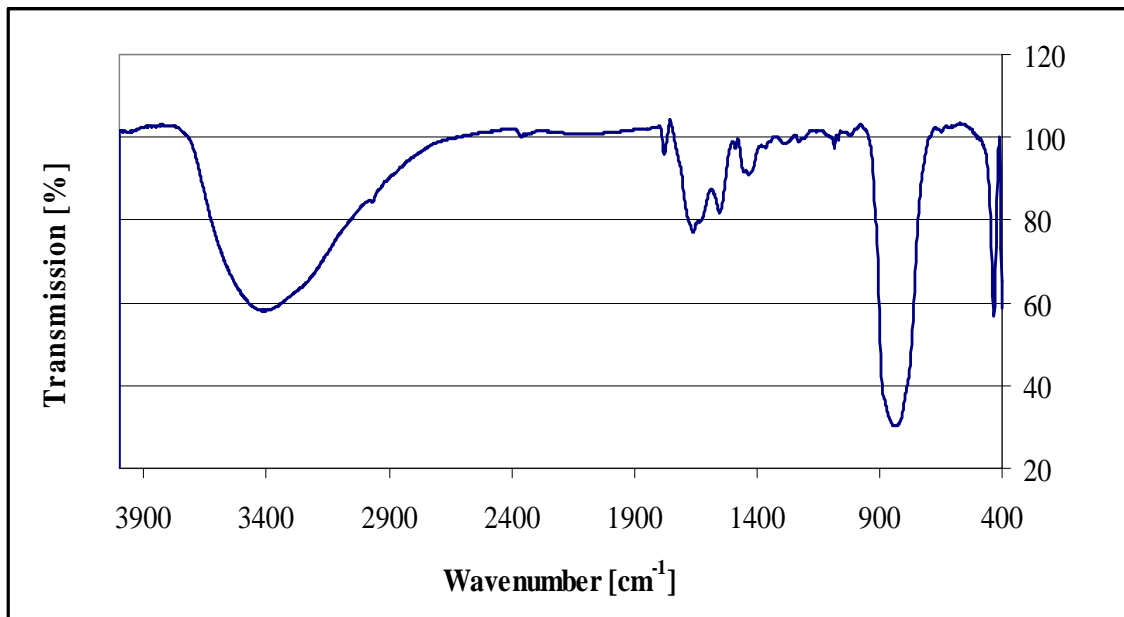


**Figure 5.3.** Infrared spectrum of the product from calcium acetate and  $\text{MoO}_3$ .

In contrast, when calcium nitrate or calcium chloride were used as the calcium source to react with  $\text{MoO}_3$ , the formation of calcium molybdate did not occur. Instead only peaks from  $\text{MoO}_3$  starting material were seen in the X-ray powder diffraction (ICDD #: 05-0508). The pH at the start of the reaction was 3.15 when calcium nitrate was used and 3.50 when calcium chloride was used. After completion of the reaction, the pH of the solution was 1.58 when calcium nitrate was used and 1.02 when calcium chloride was used. Large decreases in pH to very low values occurred. This suggests that the reaction occurs in the forward direction but halts when the pH becomes too low.

To test this theory, the reaction with calcium nitrate and  $\text{MoO}_3$  was carried out using a solution buffered by 2,2-bis-(hydroxymethyl)-2,2'2''-nitrilotriethanol and HCl with a pH to near that of the reaction between calcium acetate and  $\text{MoO}_3$ . The reaction started at pH of 6.27 and ended at pH of 2.34. The X-ray powder diffraction pattern of

the white solid produced showed the formation of calcium molybdate (tetragonal phase) (ICDD # 29-0351, Figure 5.4). The infrared spectrum of the white solid was very similar to the product gained from the reaction of calcium acetate and  $\text{MoO}_3$  (Figure 5.5). The weight of the white solid produced after reflux for 72 hours was 1.62 grams corresponding to a yield of 80.1% based on  $\text{MoO}_3$ . The low yield may be due to the formation of a soluble complex of the molybdate with the buffer. The fact that calcium nitrate can form calcium molybdate at higher pH showed that the precipitation of the desired product is primarily pH dependent and not ligand dependent.

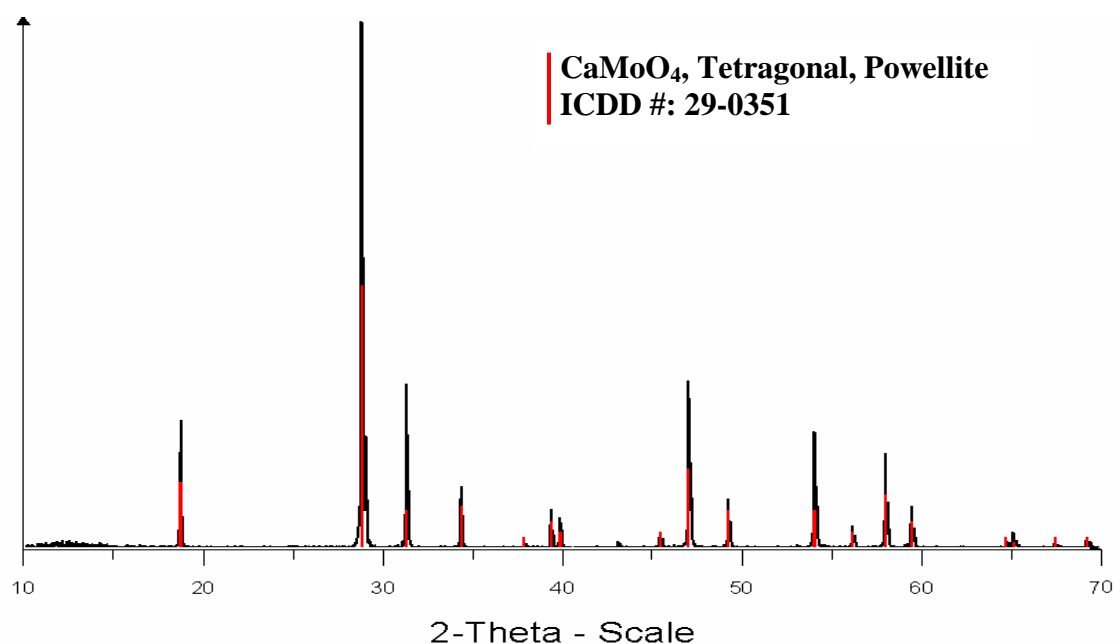


**Figure 5.4.** The XRD pattern of the product from calcium nitrate and  $\text{MoO}_3$  in  $\text{C}_8\text{H}_{19}\text{NO}_5$  buffer solution.



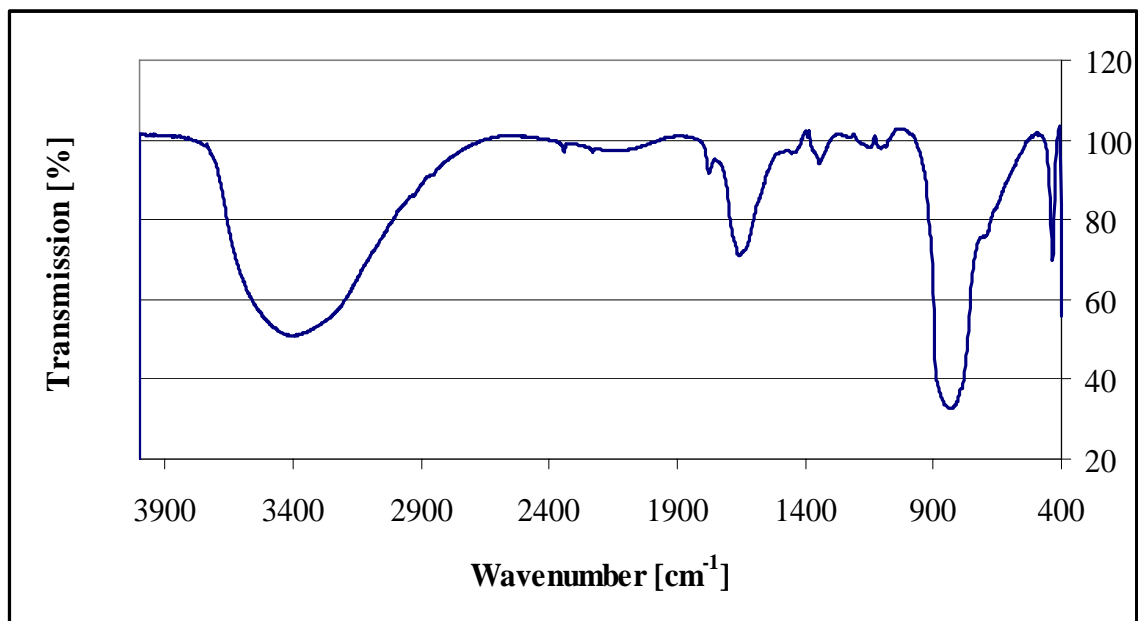


**Figure 5.5.** Infrared spectrum of the product from calcium nitrate and  $\text{MoO}_3$  in  $\text{C}_8\text{H}_{19}\text{NO}_5\text{-HCl}$  buffer solution after 72 hours at reflux.

For more confirmation, the reaction with calcium nitrate and  $\text{MoO}_3$  was carried out using sodium acetate-acetic acid buffer. The pH of the reaction at the start was 4.60 and was constant during the whole process. The white product produced at reflux for 72 hours, characterized using X-ray powder diffraction, showed the formation of calcium molybdate phase (Figure 5.6). The infrared spectrum of the product showed similarities to the products from Figures 5.3, and 5.5. Nevertheless, the yield of the product was 2.21 g, corresponding to a yield of 110%. The high yield is probably due to the formation of something else besides the powellite, which is in the amorphous form.

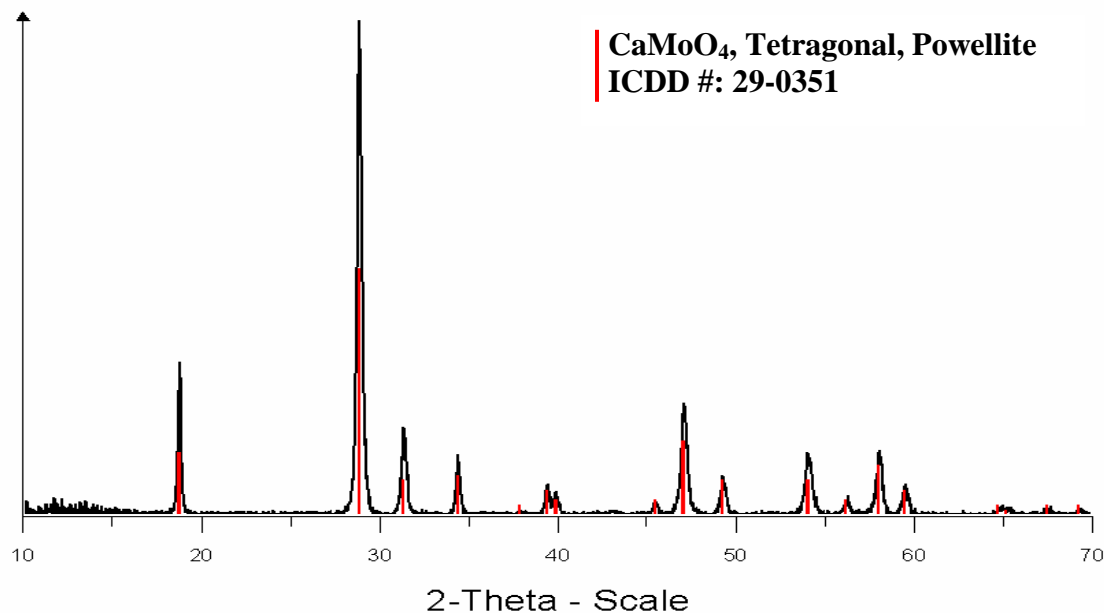


**Figure 5.6.** The XRD pattern of the product from calcium nitrate and  $\text{MoO}_3$  in sodium acetate-acetic acid buffer solution.

As expected, the reaction of strontium acetate and barium acetate with  $\text{MoO}_3$  at reflux for 72 hours produced phase pure strontium molybdenum oxide and barium molybdenum oxide, respectively (Figure 5.7 and 5.9). Both infrared spectra of the products displayed an adsorption band around  $880\text{ cm}^{-1}$ , which corresponded to the Mo-O stretching vibration in the  $\text{MoO}_4^{2-}$  (tetrahedron) (Figure 5.8 for the reaction with strontium acetate). The yield of both products was 98.6 %. In addition, the pH of both reactions at the start was around 5.8. Nonetheless, at low pH ( $\sim 3.50$ ) the reactions from strontium nitrate and barium nitrate with  $\text{MoO}_3$  did not produce the desired metal molybdates. Thus, an increase in the pH was required for the synthesis to occur. The results are in agreement with the literature displaying that the tetrahedral monomeric molybdate ion  $\text{MoO}_4^{2-}$  is stable at pH higher than 4.0.<sup>24</sup>

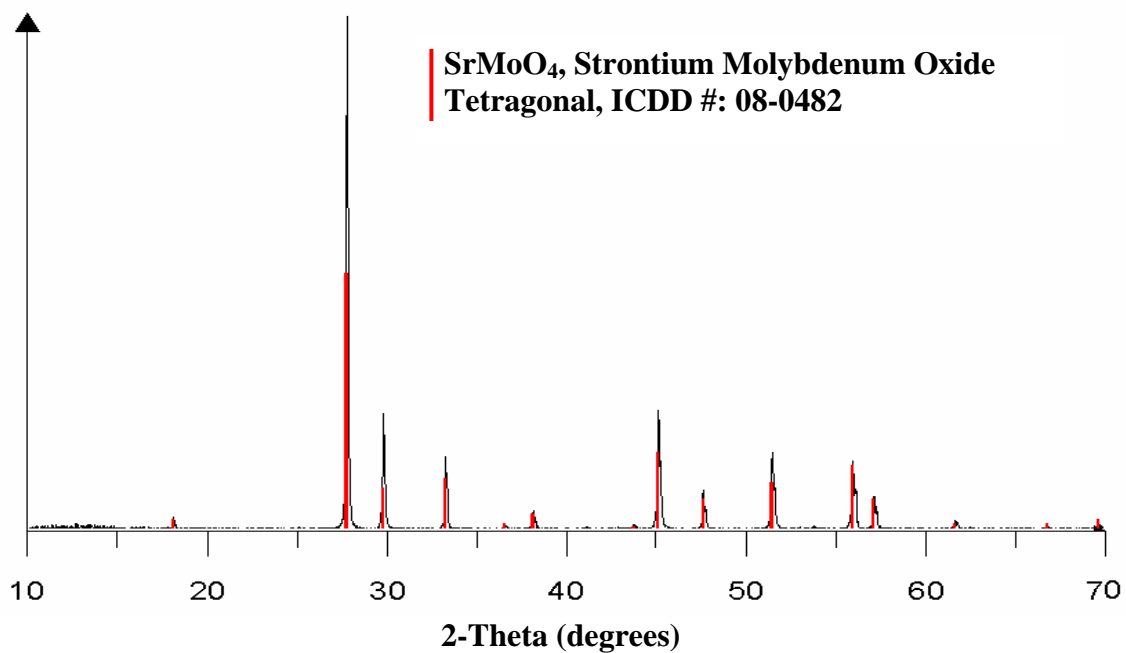


**Figure 5.7.** The XRD pattern of the product from strontium acetate and MoO<sub>3</sub>.

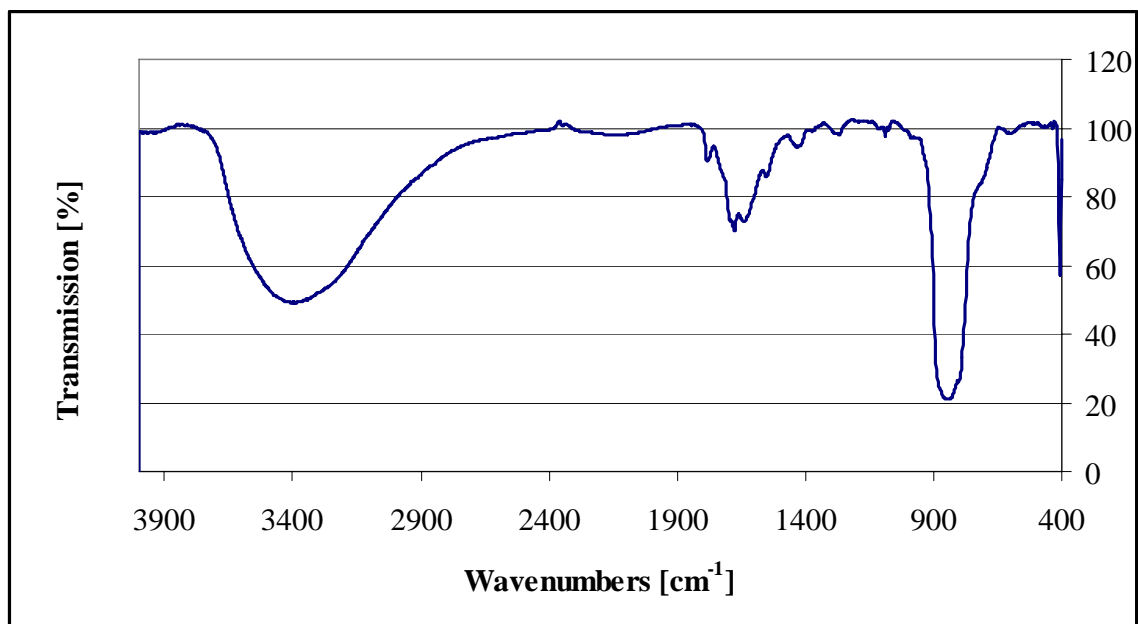


**Figure 5.8.** Infrared spectrum of the product from strontium acetate and MoO<sub>3</sub>.

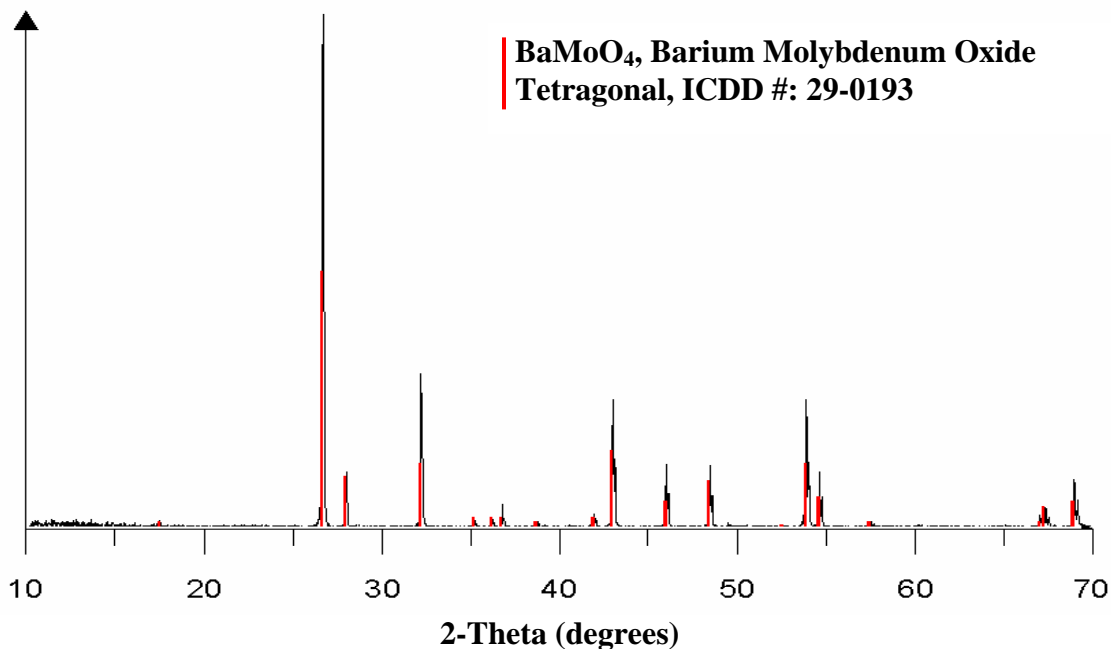


**Figure 5.9.** The XRD pattern of the product from barium acetate and  $\text{MoO}_3$ .

## CONCLUSIONS

A simple method to prepare scheelite-type materials with the general formula  $\text{AMoO}_4$  ( $A = \text{Ca}, \text{Sr}, \text{Ba}$ ) from the direct synthesis of alkaline earth salts and  $\text{MoO}_3$  was accomplished. It was found that the alkaline earth metal acetates formed the alkaline earth molybdates when reacted with  $\text{MoO}_3$  at reflux. In addition, two different solutions [2,2-bis(hydroxymethyl) -2,2'2''-nitrilotriethanol ( $\text{C}_8\text{H}_{19}\text{NO}_5$ )-HCl], and [sodium acetate (2M)-acetic acid ( $\text{CH}_3\text{CO}_2\text{Na}-\text{CH}_3\text{CO}_2\text{H}$ )] were successfully tested for the reaction of calcium nitrate with  $\text{MoO}_3$ . It was demonstrated that for the alkaline earth molybdates to form, the pH of the reaction should be above 4.0. The method used is environmentally friendly since water is used as a solvent, cost effective compared to the traditional techniques used, and gains a high yield of product.

## REFERENCES

- [1] Dinesh, R.; Fujiwara, T.; Watanabe, T.; Byrappa, K.; Yoshimura, M. *Journal of Materials Science* **2006**, *41*, 1541-1546.
- [2] Zhang, Y.; Holzwarth, N. A. W.; Williams, R. T. *Physical Review B: Condensed Matter and Materials Physics* **1998**, *57*, 12738-12750.
- [3] Romanyuk, Y. E.; Ehrentraut, D.; Pollnau, M.; Garcia-Revilla, S.; Valiente, R. *Applied Physics A: Materials Science & Processing* **2004**, *79*, 613-618.
- [4] Achary, S. N.; Patwe, S. J.; Mathews, M. D.; Tyagi, A. K. *Journal of Physics and Chemistry of Solids* **2006**, *67*, 774-781.
- [5] Kay, M. I.; Frazer, B. C.; Almodovar, I. *Journal of Chemical Physics* **1964**, *40*, 504-6.
- [6] Sleight, A. W. *Acta Crystallographica, Section B: Structural Crystallography and Crystal Chemistry* **1972**, *28*, 2899-902.
- [7] Zalkin, A.; Templeton, D. H. *Journal of Chemical Physics* **1964**, *40*, 501-4.
- [8] Abdel-Rehim, A. M. *Journal of Thermal Analysis and Calorimetry* **2004**, *76*, 557-569.
- [9] Abdel-Rehim, A. M. *Journal of Thermal Analysis* **1997**, *48*, 177-202.
- [10] Abdel-Rehim, A. M. *Journal of Thermal Analysis and Calorimetry* **1999**, *57*, 415-431.
- [11] Cho, W.-S.; Yashima, M.; Kakihana, M.; Kudo, A.; Sakata, T.; Yoshimura, M. *Journal of the American Ceramic Society* **1997**, *80*, 765-769.

- [12] Yang, P.; Yao, G.-Q.; Lin, J.-H. *Inorganic Chemistry Communications* **2004**, *7*, 389-391.
- [13] Barbosa, L. B.; Ardila, D. R.; Cusatis, C.; Andreeta, J. P. *Journal of Crystal Growth* **2002**, *235*, 327-332.
- [14] Petrov, A.; Kofstad, P. *Journal of Solid State Chemistry* **1979**, *30*, 83-8.
- [15] Vukasovich, M. S.; Farr, J. P. G. *Polyhedron* **1986**, *5*, 551-9.
- [16] Klopogge, J. T.; Weier, M. L.; Duong, L. V.; Frost, R. L. *Materials Chemistry and Physics* **2004**, *88*, 438-443.
- [17] Blistanov, A. A.; Galagan, B. I.; Denker, B. I.; Ivleva, L. I.; Osiko, V. V.; Polozkov, N. M.; Sverchkov, Y. E. *Kvantovaya Elektronika (Moscow)* **1989**, *16*, 1152-4.
- [18] Flournoy, P. A.; Brixner, L. H. *Journal of the Electrochemical Society* **1965**, *112*, 779-81.
- [19] Corbet, F.; Eyraud, C. *Bulletin de la Societe Chimique de France* **1961**, 571-4.
- [20] Rao, C. N. R.; Gopalakrishnan, J. *New Directions in Solid State Chemistry*; 2nd ed.; Cambridge University Press: Cambridge ; New York, 1997.
- [21] Thangadurai, V.; Knittlmayer, C.; Weppner, W. *Materials Science & Engineering, B: Solid-State Materials for Advanced Technology* **2004**, *B106*, 228-233.
- [22] Marques, A. P. d. A.; De Melo, D. M. A.; Paskocimas, C. A.; Pizani, P. S.; Joya, M. R.; Leite, E. R.; Longo, E. *Journal of Solid State Chemistry* **2006**, *179*, 671-678.
- [23] Nakamoto, K. *Infrared and Raman Spectra of Inorganic and Coordination Compounds*; 4th ed.; Wiley: New York, 1986.

[24] Baes, C. F.; Mesmer, R. E. *The Hydrolysis of Cations*; Wiley: New York, 1976.

## **CHAPTER VI**

### **REMOVAL OF LEAD FROM WATER USING MOLYBDENUM AND TUNGSTEN OXIDES**

#### **INTRODUCTION**

There have been increasing concern about the effect of lead and other heavy metals on humans and aquatic ecosystems.<sup>1</sup> It has been found that lead is both a cancer-causing agent and a reproductive toxin.<sup>2</sup> In the state of California, the non significant risk level for lead established by the office of Environmental Health Hazard Assessment is 0.5 µg/day.<sup>2</sup> However, the maximum value is so small that people who routinely use calcium-containing dietary supplements and antacids may exceed this limit.<sup>2</sup> Lead can produce toxic effects involving largely the hematopoietic system, nervous system, and kidney.<sup>3</sup> Since children have a greater rate of intestinal absorption and retention of lead, they are more vulnerable to lead exposure.<sup>4</sup> In 1991, the Centers for Disease Control and Prevention (CDC) had estimated that 2.2 % of American children aged 1-5 years, which corresponds to 434,000 children, have blood lead level higher than 10 µg/dL which is defined as the health concern level for young children.<sup>5</sup>

Remediation of lead impacted media from waste management can be a challenge. Moreover, lead has always been a politically sensitive issue to address since there are no local or federal clean-up standards for total lead concentrations in soils.<sup>6</sup>



Current metal removal technologies have progressed from the need by the industry to achieve acceptable limits. Using permeable reactive barriers is a common method for ground water remediation.<sup>7</sup> Permeable reactive barriers are placed inside a migrating plume of contaminated groundwater.

Metal ions are important raw materials for technical applications. Consequently, complexation of metal ions is a critical technique for recovering metals from various sources and for their removal from municipal and industrial waste.<sup>8</sup> Hence, complexation, separation and removal of metal ions have received increasing attention as a new area of research and led to new technological developments such as recovery of rare metal ions from seawater and removal of traces of radioactive metal ions from wastes.

Lead molybdate compounds ( $\text{PbMoO}_4$ ) have received growing attention due to their significant applications as optic modulators, deflectors, and ionic conductors.<sup>9-11</sup> Recently,  $\text{PbMoO}_4$  crystals have been considered to have a great potential for use in efficient low-temperature scintillators for nuclear instrumental applications.<sup>12</sup> Single crystals of lead molybdate are traditionally grown from a high temperature melt by the Czochralski method, whereby a single-crystal rod is rotated and gradually pulled from the melt.<sup>13,14</sup> However, the quality of  $\text{PbMoO}_4$  single crystals depends on the stoichiometry of the Czochralski melt, which in turn relies mainly on the powder-processing techniques used for the preparation of lead molybdate. The solid state reaction from  $\text{PbO}$  and  $\text{MoO}_3$  is another alternative for the synthesis of  $\text{PbMoO}_4$ . Unfortunately, the drawback of this technique is that some side reactions take place unless the conditions for  $\text{PbMoO}_4$  synthesis are precisely controlled.<sup>15</sup> Consequently, the formation of some unwanted

phases such as  $\text{Pb}_2\text{MoO}_5$  and other lead polymolybdates may occur.<sup>16,17</sup> In addition, even by carefully maintaining the  $\text{PbO}:\text{MoO}_3$  stoichiometry during the high temperature treatment, the difference in original particle sizes and inhomogeneity of the mixing of the powders cause the localized nonstoichiometry to exist.<sup>18</sup>

Tungsten oxide ( $\text{WO}_3$ ) has been intensively studied due to its attractive physical and chemical properties. It is well known that  $\text{WO}_3$  is a good photochromic, electrochromic, thermochromic, and gas sensor material.<sup>19-22</sup> The major natural tungsten ores are scheelite mineral ( $\text{CaWO}_4$ ) and wolframite ( $\text{Fe, Mn} \text{ } \text{WO}_4$ ). Depending on the size of the cation, divalent metal tungstates can adopt either the scheelite or the wolframite structure. Large bivalent cations, such as Ca, Ba, Pb, and Sr prefer the scheelite structure with the tungsten in tetrahedral coordination. On the other hand, smaller bivalent cations, such as Fe, Mn, Co, Ni, Mg, and Zn prefer the wulfenite structure where the tungsten is in octahedral coordination.<sup>23</sup> Stolzite ( $\text{PbWO}_4$ ), named after J. Stolz from the Czech Republic, has a crystal structure similar to that of the scheelite with the  $\text{Pb}^{2+}$  in 8-coordination and tetrahedral  $(\text{WO}_4)^{2-}$  groups. As a consequence, stolzite can be a good oxide ion conductor, especially when doped with rare earth elements.<sup>24</sup> In addition, lead tungstate has attracted intense interest for the scintillator applications in high-energy physics and can also be used as an oscillator for nanosecond Raman lasing, which in turn is useful for applications, such as the generation of a wavelength in the UV range for ozone differential absorption lidar.<sup>25-27</sup> Moreover,  $\text{PbWO}_4$  has an optical transparency from 0.33 to 5.5  $\mu\text{m}$ , which has a potential use for trace gas detection in the IR.<sup>23</sup> Lead tungstate has traditionally been synthesized using

the Czochralski and the Bridgeman methods, while the hydrothermal route usually results in  $\text{PbWO}_4$  crystals with poorly defined shaped.<sup>27-29</sup>

There have been numerous methods to remediate lead from water. The main challenge, after successfully removing lead, is what to do with the precipitate formed? We are proposing a new technique to remove lead from contaminated water using a variety of transition metal oxides, and the precipitate obtained, after simple filtration of water, can have different applications, such as in optic modulators, deflectors, and ionic conductors etc...

## **EXPERIMENTAL**

All reagents were commercial products (ACS Reagent grade or higher) and were used without further purification. Bulk pyrolyses at various temperatures were performed in air in a digitally-controlled muffle furnace using approximately 1 g samples, a ramp of 10 °C/min, and a hold time for 4 hours. The X-ray powder diffraction (XRD) patterns were recorded on a Bruker AXS D-8 Advance X-ray powder diffractometer using copper  $\text{K}_\alpha$  radiation. Crystalline phases were identified using a search/match program and the PDF-2 database of the International Center for Diffraction Data. Lead concentrations were determined by voltametric stripping using Hach-HSA 1000 Scanning Lead Analyzer. Lead standard solutions were prepared from lead acetate or lead nitrate solutions. All the glassware used were treated with a 10% nitric acid solution for several hours.

### Reaction of MoO<sub>3</sub> with lead acetate

MoO<sub>3</sub> (1.43 g, 10.0 mmol) was added to a solution of lead acetate (4.55 g, 12.0 mmol) in water (100 ml). The mixture was refluxed for 7 days. Upon cooling, a white solid was isolated by filtration through a fine sintered glass filter and dried in vacuum at room temperature over night. The yield of the yellow product was 3.39 g. Powder X-ray diffraction of the product indicated the formation of wulfenite [PbMoO<sub>4</sub>, ICDD # 44-1486]. There were also several peaks due to unreacted MoO<sub>3</sub> (Figure 6.1) at  $2\theta = 14, 26,$  and 39 degrees.

In order to test the MoO<sub>3</sub> as a potential reagent for removal of lead from contaminated water and to study the effect of the temperature on yield of the product, the same reaction was performed with continuous stirring at room temperature for 7 days. The X-ray powder diffraction of the solid showed a more limited formation of the mineral wulfenite than the higher temperature reaction (Figure 6.2). Infrared spectrum (DRIFTS, solid diluted in KBr, cm<sup>-1</sup>) of the product was taken at room temperature (Figure 6.3). The spectrum showed a broad peak at 880 cm<sup>-1</sup>, two sharp peaks at 500cm<sup>-1</sup> and 1000 cm<sup>-1</sup> and two small peaks at 1400 cm<sup>-1</sup> and 1500 cm<sup>-1</sup>. The infrared spectrum was compared to one of a commercial lead molybdate purchased from Aldrich (Figure 6.4). The latter showed one broad peak at 880 cm<sup>-1</sup>, and two small peaks at 1400 cm<sup>-1</sup> and 1500 cm<sup>-1</sup>.

### Reaction of lead acetate with tungsten trioxide

To compare the effectiveness of  $\text{MoO}_3$  with other transition metal oxides, the reactions of lead acetate with tungsten oxide ( $\text{WO}_3$ ) were performed using the same stoichiometry as in the case of molybdenum trioxide.

The reaction was carried out for 72 hours at reflux and with continuous stirring at room temperature, and both results were compared. The weight of the light green product obtained after 72 hours at reflux with lead acetate in water was 3.86 g, while the weight of the solid at room temperature was 2.83 g. The X-ray powder diffraction of the product from reflux indicated the formation of the mineral stolzite [ $\text{PbWO}_4$ , ICDD # 19-0708] with a small amount of the  $\text{WO}_3$  remaining (Figure 6.5). On the other hand, the three peaks of the  $\text{WO}_3$  were very intense in the product obtained when the reaction was conducted with stirring at room temperature (Figure 6.6).

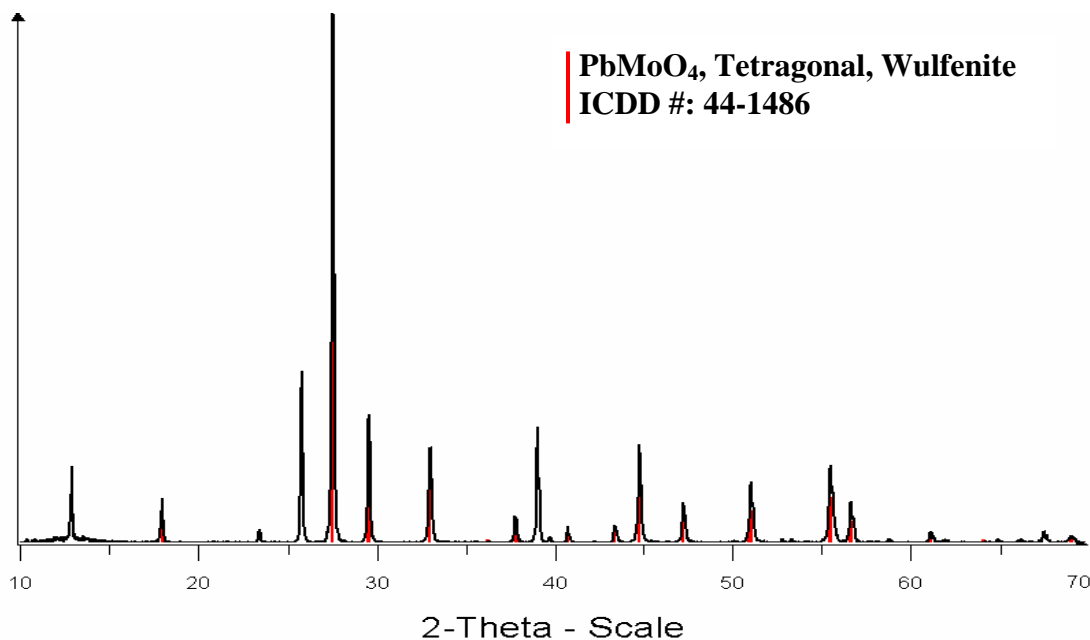


**Figure 6.1.** The XRD pattern of the product from lead acetate and  $\text{MoO}_3$  after reflux.

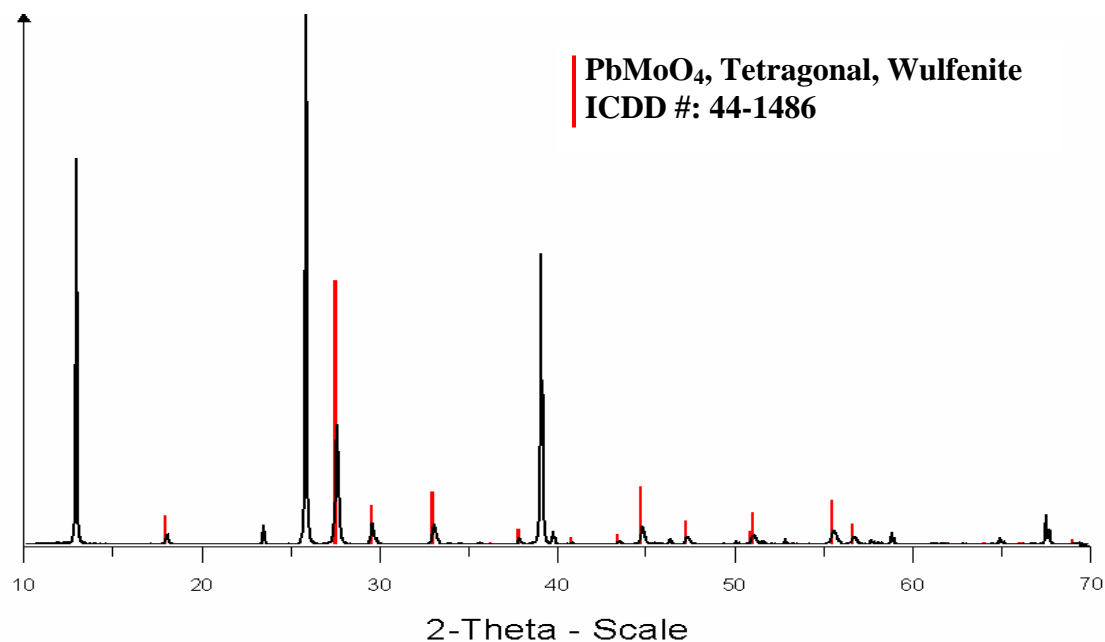


**Figure 6.2.** The XRD pattern of the product from lead acetate and MoO<sub>3</sub> after stirring at room temperature.

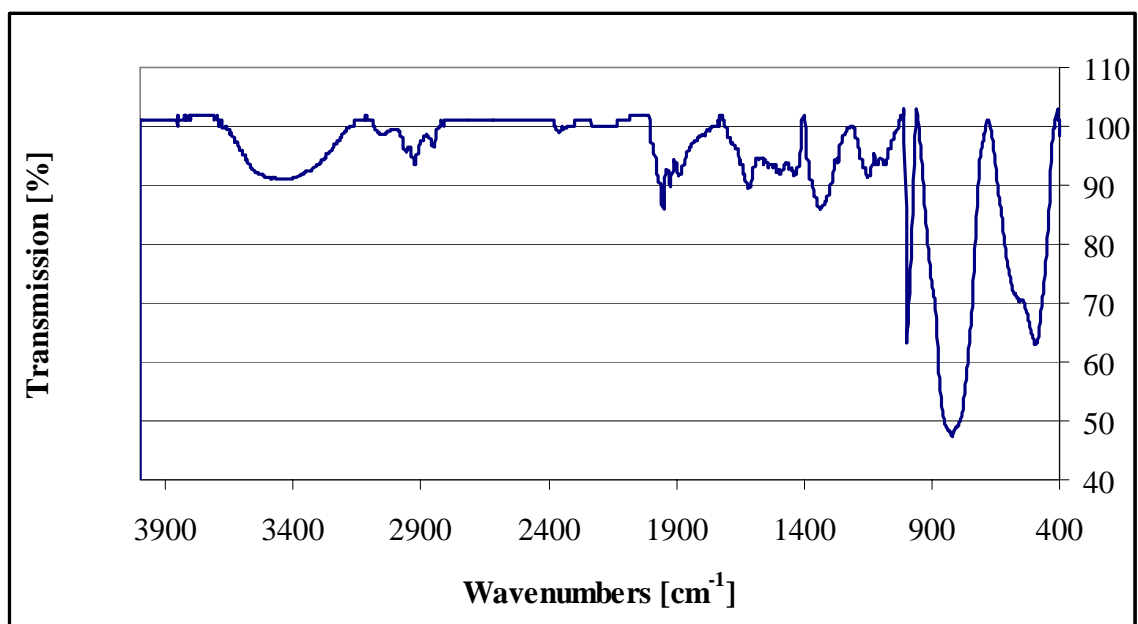


**Figure 6.3.** Infrared spectrum of the product from lead acetate and MoO<sub>3</sub> after stirring at room temperature.

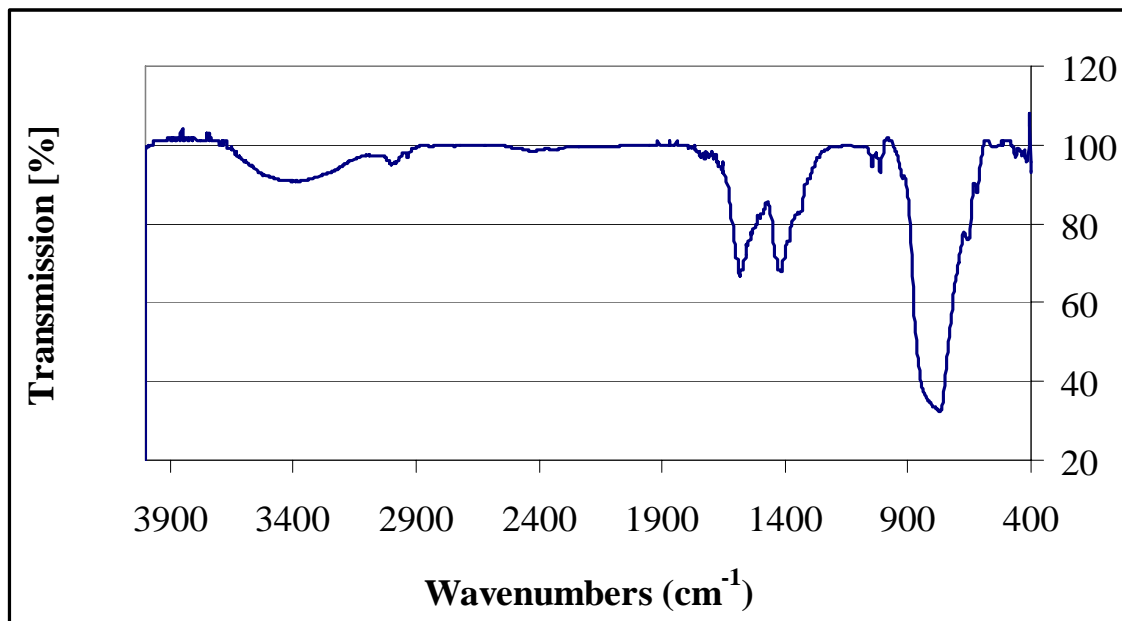


**Figure 6.4.** Infrared spectrum of the lead molybdate from Aldrich

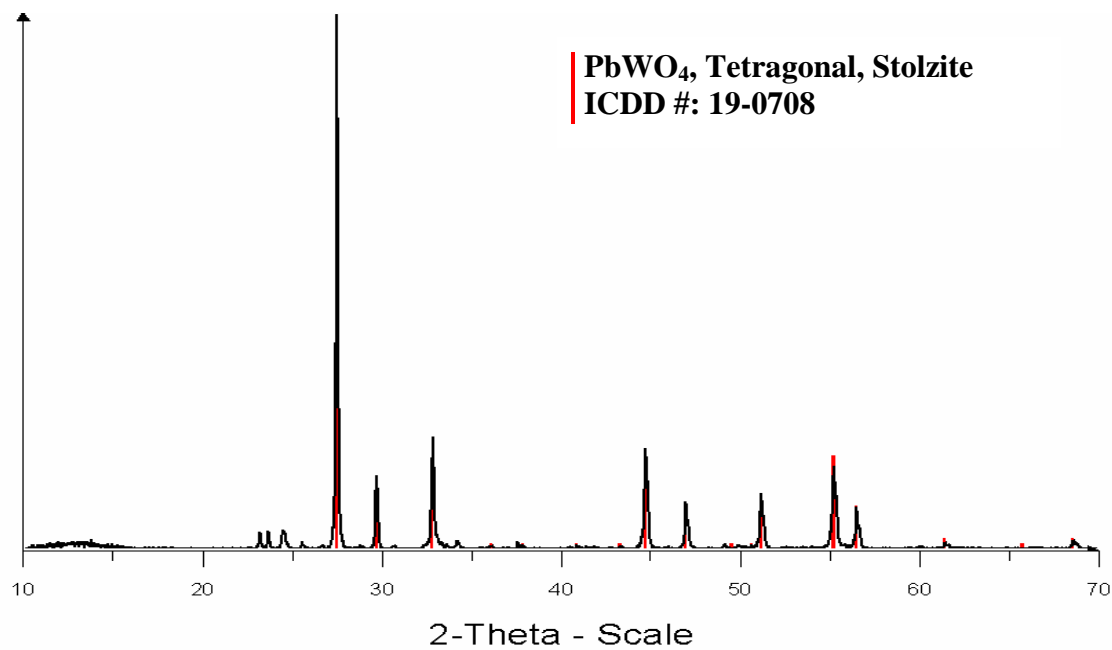


**Figure 6.5.** The XRD pattern of the product from lead acetate and WO<sub>3</sub> after heating at reflux.

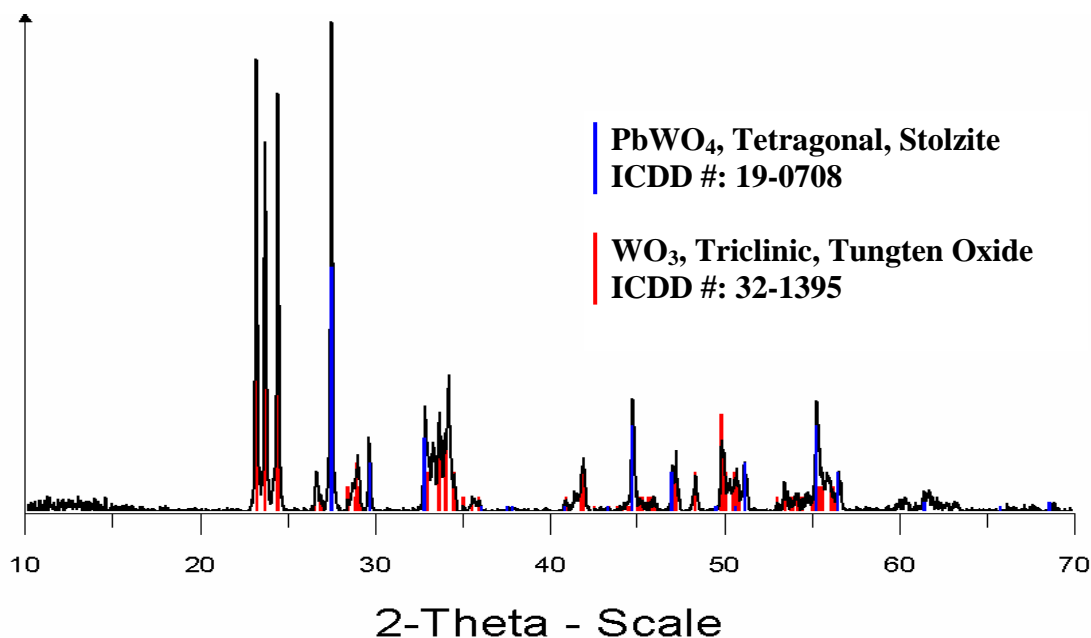


**Figure 6.6.** The XRD pattern of the product from lead acetate and  $\text{WO}_3$  after continuously stirring at room temperature.

### Determination of lead uptake

An aqueous solution of 500.0 ppm lead was prepared, and the reactions of the lead solution with different amounts of  $\text{WO}_3$  ( $m = 0.5, 1.0$  and  $1.5$  g) were monitored for an extended period of time. The maximum uptake was calculated and the kinetics of lead uptake was monitored.

## RESULTS AND DISCUSSION

### Reaction of $\text{MoO}_3$ with lead acetate

It has been discovered that molybdenum trioxide can react directly with metal salts to form mixed metal molybdates. Moreover,  $\text{MoO}_3$  was successfully used to remove uranium from water and form uranium molybdenum oxide (Chapter 2). For further investigation, the reaction of lead acetate with  $\text{MoO}_3$  in water was carried out as a



potential route to synthesize lead molybdate and as a tool to remediate lead from aqueous solutions. The solid product isolated by filtration and dried in vacuum over night at room temperature was identified by the powder X-ray diffraction as the mineral wulfenite (Figure 6.2). There were three additional small peaks of  $\text{MoO}_3$  at  $2\theta = 14, 26$  and  $39$  degrees, implying that the reaction did not go to completion. The weight of yellow product recovered from the reflux reaction was  $3.32\text{ g}$  which corresponded to a yield of  $92.3\%$  based on  $\text{MoO}_3$ . On the other hand, the weight gained of the product from the reaction of lead acetate with  $\text{MoO}_3$  after stirring the mixture at room temperature was  $1.73\text{ g}$ , corresponding to a yield of  $47.1\%$  based on  $\text{MoO}_3$ . Furthermore, the X-ray powder diffraction pattern of the latter showed the formation of wulfenite and three intense peaks at  $2\theta = 14, 26$  and  $39$  degrees (Figure 6.3). Both XRD patterns demonstrated the successful uptake of lead by  $\text{MoO}_3$  through the formation of a new product, lead molybdate. However, more time was needed for the reactions to go to completion, particularly when the mixture was stirred at room temperature. This was also confirmed by the high intensity of the peaks of the extractant,  $\text{MoO}_3$ , in Figure 6.3 and the low yield realized in the reaction performed at room temperature. A comparison of the infrared spectra between the product from the reaction of lead acetate and  $\text{MoO}_3$  and the commercial lead molybdate showed that both spectra displayed one strong peak around  $800\text{ cm}^{-1}$  which can be assigned to the asymmetric vibration mode of  $\text{MoO}_4^{2-}$  anion.<sup>17,18</sup> The absorption peak at  $500\text{ cm}^{-1}$  in Figure 6.4 can be attributed to Mo-O stretching frequency in  $\text{MoO}_3$ .<sup>30</sup> In addition, asymmetric stretch of Mo-O in  $\text{MoO}_3$  can be identified at  $1000\text{ cm}^{-1}$ .<sup>18</sup>

### **Reaction of lead acetate with tungsten trioxide**

Since tungsten trioxide is chemically very similar to  $\text{MoO}_3$ , the idea was to apply the knowledge and technique gained from molybdenum trioxide in the use of  $\text{WO}_3$  as potential lead remediation tool. In this regard, the reaction of lead acetate with  $\text{WO}_3$  was investigated.  $\text{WO}_3$  (10.0 mmol) was added to a solution of lead acetate (12.0 mmol) in water (100 ml). The mixture was heated at reflux for 72 hours. The green product produced was isolated by filtration through a fine sintered glass filter and dried in vacuum at room temperature over night. The weight of the solid was 3.86 g and corresponded to a yield of 84.8% based on  $\text{WO}_3$ . The X-ray powder diffraction pattern of the product showed the formation of the mineral stolzite [ $\text{PbWO}_4$ , ICDD # 19-0708] (Figure 6.6). In addition, a small amount of unreacted tungsten oxide was detected by the appearance of three very small adjacent peaks of  $\text{WO}_3$  at  $2\theta$  between 24 and 25 degrees (Figure 6.5). The yield gained when the reaction was carried out at room temperature was 62.2% based on  $\text{WO}_3$ . The X-ray powder diffraction pattern of the solid product showed the formation of the tetragonal phase of stolzite and three intense peaks of  $\text{WO}_3$ , implying that the reaction at room temperature did not go to completion. The difference in the yields showed that more time was needed for tungsten oxide to remove all the lead present in the solution.

### **Kinetics of lead uptake**

The  $\text{WO}_3$  (1.5 g) was reacted with 20.0 ml of a 500.0 ppm lead solution. The reaction was monitored for an extended period of time. The result from the reaction is shown in Figure 6.7. Under the reaction conditions, the lead uptake is pseudo first order.

The reaction was repeated 4 times to check the reproducibility. The average rate constant was determined to be  $0.63 \pm 0.05 \text{ h}^{-1}$ . At the completion of the reaction, the lead concentration was 38 ppm.

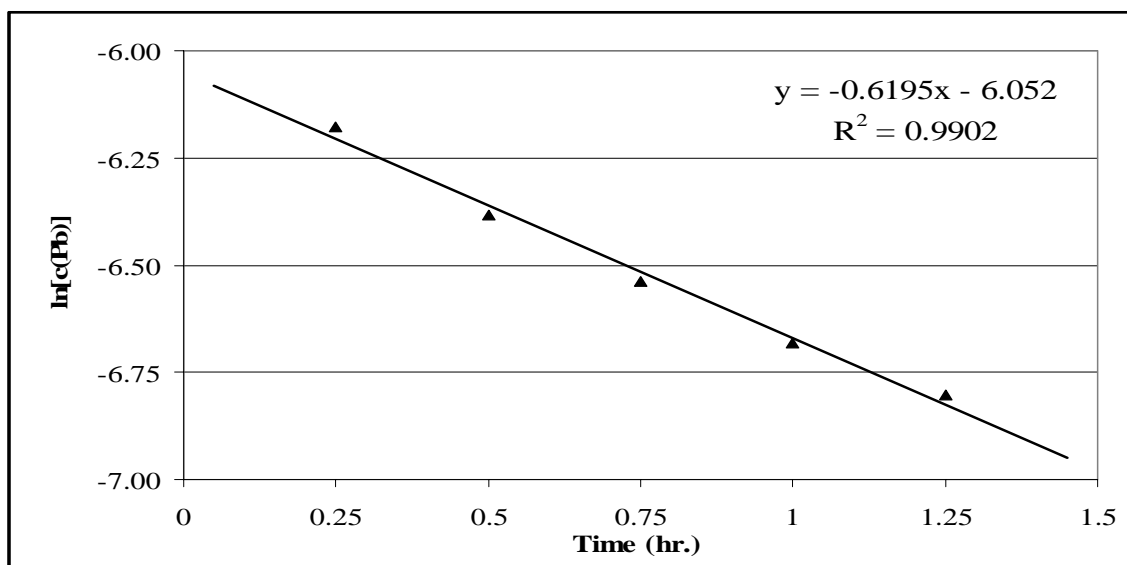


**Figure 6.7.** Plot of  $\ln[\text{Pb}]$  versus time.

For further investigation, various amounts of  $\text{WO}_3$  (0.5, 1.0 and 1.5 g) were used to treat 20 ml of 500.0 ppm lead solution. Figure 6.8 demonstrates the relationship between the rate constant and the amount of extractant.

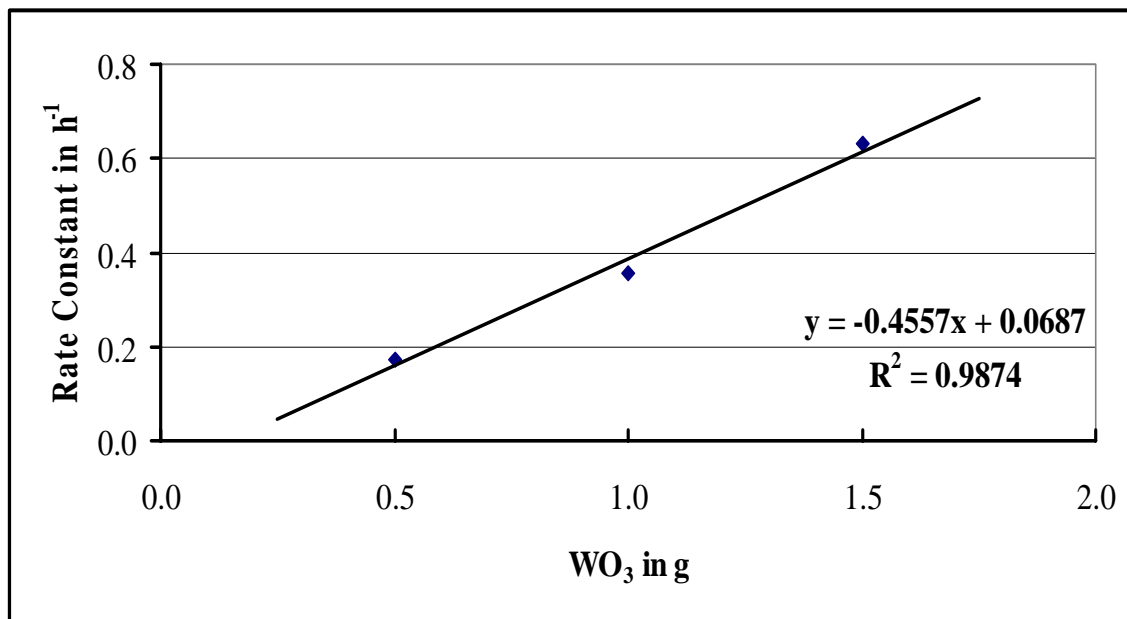


**Figure 6.8.** Plot of the rate constant versus mass of WO<sub>3</sub>.

The linear fit of pseudo first order rate constants shows that the overall reaction is second order with  $\text{Rate} = K [\text{Pb}] [\text{WO}_3]$ . Of course in this term, the concentration of the WO<sub>3</sub> cannot be represented by molarity but by the surface area of the solid. This gives a rate constant of 0.21 hr<sup>-1</sup> per m<sup>2</sup> of WO<sub>3</sub>.

## CONCLUSIONS

It had been demonstrated that molybdenum oxide, and tungsten oxide can not only absorb lead from water but also form useful lead-molybdate, and tungstate products respectively even at ambient temperature. To the best of our knowledge, this is the first time that such products can be formed at room temperature. No regeneration of the starting material is necessary since the solids gained can have various applications. The effect of the temperature on the products was investigated, and it was concluded that the

yield of the products from lead acetate and  $\text{WO}_3$  was higher when heat was applied. In addition, the kinetics of lead uptake by  $\text{WO}_3$  was studied, and it was found that the overall reaction was second order.

## REFERENCES

- [1] Brown, P. A.; Gill, S. A.; Allen, S. J. *Water Research* **2000**, *34*, 3907-3916.
- [2] Wolf, R. E. *Atomic Spectroscopy* **1997**, *18*, 169-174.
- [3] Stark, A. D.; Meigs, J. W.; Fitch, R. A. *Archives of Environmental Health* **1978**, *33*, 222-6.
- [4] Ziegler, E. E.; Edwards, B. B.; Jensen, R. L.; Mahaffey, K. R.; Fomon, S. J. *Pediatric Research* **1978**, *12*, 29-34.
- [5] Clark, S.; Grote, J.; Wilson, J.; Succop, P.; Chen, M.; Galke, W.; McLaine, P. *Environmental Research* **2004**, *96*, 196-205.
- [6] Carey, M. J.; Nagelski, S. D. *Waste Management (Oxford)* **1996**, *16*, 263-270.
- [7] Blowes, D. W.; Ptacek, C. J.; Benner, S. G.; McRae, C. W. T.; Bennett, T. A.; Puls, R. W. *Journal of Contaminant Hydrology* **2000**, *45*, 123-137.
- [8] Kavakli, P. A.; Gueven, O. *Journal of Applied Polymer Science* **2004**, *93*, 1705-1710.

- [9] Bonner, W. A.; Zydzik, G. J. *Journal of Crystal Growth* **1970**, 7, 65-8.
- [10] Satoh, T.; Ohhara, A.; Fujii, N.; Namikata, T. *Journal of Crystal Growth* **1974**, 24-25, 441-4.
- [11] Takano, S.; Esashi, S.; Mori, K.; Namikata, T. *Journal of Crystal Growth* **1974**, 24-25, 437-40.
- [12] Minowa, M.; Itakura, K.; Moriyama, S.; Ootani, W. *Nuclear Instruments & Methods in Physics Research, Section A: Accelerators, Spectrometers, Detectors, and Associated Equipment* **1992**, A320, 500-3.
- [13] Brown, S.; Marshall, A.; Hirst, P. *Materials Science & Engineering, A: Structural Materials: Properties, Microstructure and Processing* **1993**, A173, 23-7.
- [14] Laudise, R. A. *The Growth of Single Crystals*; Englewood Cliffs: N.J., 1970.
- [15] He, C.; Lin, Y.; Su, W.; Shen, B.; Li, Z.; Gu, W.; Rong, X. *Guisuanyan Xuebao* **1981**, 9, 285-94.
- [16] Machida, N.; Chusho, M.; Minami, T. *Journal of Non-Crystalline Solids* **1988**, 101, 70-4.
- [17] Znasik, P.; Jamnicky, M. *Journal of Non-Crystalline Solids* **1992**, 146, 74-80.
- [18] Zeng, H. C. *Journal of Materials Research* **1996**, 11, 703-15.

- [19] Antonelli, D. M.; Ying, J. Y. *Chemistry of Materials* **1996**, 8, 874-81.
- [20] Franke, E. B.; Trimble, C. L.; Hale, J. S.; Schubert, M.; Woollam, J. A. *Journal of Applied Physics* **2000**, 88, 5777-5784.
- [21] Ozkan, E.; Lee, S.-H.; Liu, P.; Tracy, C. E.; Tepehan, F. Z.; Pitts, J. R.; Deb, S. K. *Solid State Ionics* **2002**, 149, 139-146.
- [22] Teoh, L. G.; Shieh, J.; Lai, W. H.; Hung, I. M.; Hon, M. H. *Journal of Alloys and Compounds* **2005**, 396, 251-254.
- [23] Klopogge, J. T.; Weier, M. L.; Duong, L. V.; Frost, R. L. *Materials Chemistry and Physics* **2004**, 88, 438-443.
- [24] Ihn, G. S.; Lee, J. H.; Buck, R. P. *Taehan Hwahakhoe Chi* **1983**, 27, 111-16.
- [25] Kaminskii, A. A.; McCray, C. L.; Lee, H. R.; Lee, S. W.; Temple, D. A.; Chyba, T. H.; Marsh, W. D.; Barnes, J. C.; Annanenko, A. N.; Legun, V. D.; Eichler, H. J.; Gad, G. M. A.; Ueda, K. *Optics Communications* **2000**, 183, 277-287.
- [26] Liu, B.; Yu, S.-H.; Li, L.; Zhang, Q.; Zhang, F.; Jiang, K. *Angewandte Chemie, International Edition* **2004**, 43, 4745-4750.
- [27] Nitsch, K.; Nikl, M.; Ganschow, S.; Reiche, P.; Uecker, R. *Journal of Crystal Growth* **1996**, 165, 163-165.

- [28] An, C.; Tang, K.; Shen, G.; Wang, C.; Qian, Y. *Materials Letters* **2002**, 57, 565-568.
- [29] Tanji, K.; Ishii, M.; Usuki, Y.; Kobayashi, M.; Hara, K.; Takano, H.; Senguttuvan, N. *Journal of Crystal Growth* **1999**, 204, 505-511.
- [30] Eda, K. *Journal of Solid State Chemistry* **1991**, 95, 64-73.



## CHAPTER VII

### CONCLUSIONS AND FUTURE DIRECTIONS

#### CONCLUSIONS

The work in this thesis demonstrates the ability of molybdenum trioxide not only to remove heavy metals from water, but also to form useful metal molybdates. The removal and the synthesis occur via the direct reaction of molybdenum trioxide with heavy metals in water and the formation of insoluble metal molybdenum oxide. The reflux method can be used for the synthesis of a family of metal molybdate compounds. However, the reaction can also take place by stirring at room temperature. High yield was obtained during the process.

In the case of uranium,  $\text{MoO}_3$  could absorb up to 165 % by weight of uranium producing uranium molybdenum oxide mineral called umohoite. Moreover, a regeneration method was developed in which first  $\text{MoO}_3$  adsorbed uranium from water, then the uranium and the molybdenum trioxide were separated by treating the umohoite product with aqueous ammonia. The recovery of uranium from the separation was 98.9 %. The rate of the uptake of  $\text{MoO}_3$  was studied. The effect of the nature of salt, the pH of the solution and the temperature on the formation of the metal molybdate were investigated.

The reaction of gadolinium acetate with molybdenum trioxide produced the ferroelectric orthorhombic  $\text{Gd}_2(\text{MoO}_4)_3$  after heating the insoluble hydrated salt formed to 1000 °C. The latter has significant applications due to its electronic and optical properties. On the other hand, the reaction with lanthanum acetate with  $\text{MoO}_3$  yielded mixed metal molybdate acetate that was converted to the cubic form of  $\text{La}_2\text{Mo}_2\text{O}_9$  upon heating to 550 °C. The lanthanum molybdate exhibits good ionic conductivity and hence is of interest as a solid electrolyte material for numerous electrochemical applications.

## **FUTURE DIRECTIONS**

The research covered in this thesis has raised many interesting questions on why the reaction of  $\text{MoO}_3$  with a number of metal salts yielded directly anhydrous metal molybdates, while with other metal salts hydrated form of the metal molybdates was formed. A fundamental understanding of the mechanism of the formation of metal molybdate from molybdenum trioxide and metal salts is one area of research awaiting further exploration. In addition, further development of the method using competing reactions could be useful for application in environmental remediation and for construction of reactive barriers for the prevention of the spread of contaminant plumes.

VITA  
Mohamed Chehbouni  
Candidate for the Degree of  
Doctor of Philosophy

Thesis: ENVIRONMENTAL, SYNTHETIC, AND MATERIALS  
APPLICATIONS OF MOLYBDENUM TRIOXIDE

Major Field: Chemistry

Biographical:

Education:

Received his chemical engineering diploma from the University of Applied Sciences, Aachen, Germany, in 1999.

Completed the requirements for the Doctor of Philosophy degree in Chemistry at Oklahoma State University in July, 2006.

Publications:

The author published several research papers and presented his work in numerous regional, national and international conferences.

Professional Membership:

American Chemical Society (ACS).

Phi Lambda Upsilon (PLU): National Honorary Chemical Society.